

ANSEL C. UGURAL ■ SAUL K. FENSTER

Advanced Mechanics of Materials and Applied Elasticity

SIXTH EDITION



FREE SAMPLE CHAPTER

SHARE WITH OTHERS



*Advanced Mechanics of
Materials and
Applied Elasticity*

Sixth Edition

This page intentionally left blank

*Advanced Mechanics of
Materials and
Applied Elasticity*

Sixth Edition

ANSEL C. UGURAL

SAUL K. FENSTER



Pearson

Boston • Columbus • New York • San Francisco • Amsterdam • Cape Town
Dubai • London • Madrid • Milan • Munich • Paris • Montreal • Toronto • Delhi • Mexico City
São Paulo • Sydney • Hong Kong • Seoul • Singapore • Taipei • Tokyo

Many of the designations used by manufacturers and sellers to distinguish their products are claimed as trademarks. Where those designations appear in this book, and the publisher was aware of a trademark claim, the designations have been printed with initial capital letters or in all capitals.

The authors and publisher have taken care in the preparation of this book, but make no expressed or implied warranty of any kind and assume no responsibility for errors or omissions. No liability is assumed for incidental or consequential damages in connection with or arising out of the use of the information or programs contained herein.

For information about buying this title in bulk quantities, or for special sales opportunities (which may include electronic versions; custom cover designs; and content particular to your business, training goals, marketing focus, or branding interests), please contact our corporate sales department at corpsales@pearsoned.com or (800) 382-3419.

For government sales inquiries, please contact governmentsales@pearsoned.com.

For questions about sales outside the U.S., please contact intlcs@pearson.com.

Visit us on the Web: informit.com

Library of Congress Control Number: 2019932748

Copyright © 2020 Pearson Education, Inc.

Cover illustration: Yulia Grigoryeva/Shutterstock

All rights reserved. This publication is protected by copyright, and permission must be obtained from the publisher prior to any prohibited reproduction, storage in a retrieval system, or transmission in any form or by any means, electronic, mechanical, photocopying, recording, or likewise. For information regarding permissions, request forms and the appropriate contacts within the Pearson Education Global Rights & Permissions Department, please visit www.pearsoned.com/permissions/.

ISBN-13: 978-0-13-485928-6

ISBN-10: 0-13-485928-6

ScoutAutomatedPrintCode

Contents

Preface	xvii
Acknowledgments	xx
About the Authors	xxi
List of Symbols	xxii
<i>Chapter 1</i> Analysis of Stress	1
1.1 Introduction	1
1.1.1 Mechanics of Materials and Theory of Elasticity	1
1.1.2 Historical Development	2
1.2 Scope of the Book	3
1.3 Analysis and Design	4
1.3.1 Role of Analysis in Design	6
1.3.2 Selection of Factor of Safety	6
1.3.3 Case Studies	7
1.4 Conditions of Equilibrium	8
1.5 Definition and Components of Stress	9
1.5.1 Sign Convention	11
1.5.2 Equality of Shearing Stresses	12
1.5.3 Some Special Cases of Stress	12
1.6 Internal Force Resultant and Stress Relations	13
1.6.1 Basic Formulas for Stress	15
1.6.2 Combined Stresses	17
1.7 Stresses on Inclined Sections	17
1.7.1 Axially Loaded Members	18
1.8 Variation of Stress within a Body	20
1.8.1 Equations of Equilibrium	20
1.9 Plane-Stress Transformation	23
1.9.1 Stress Tensor	25
1.9.2 Polar Representations of State of Plane Stress	25
1.9.3 Cartesian Representation of State of Plane Stress	25

1.10	Principal Stresses and Maximum In-Plane Shear Stress	26
1.11	Mohr's Circle for Two-Dimensional Stress	28
1.12	Three-Dimensional Stress Transformation	35
1.13	Principal Stresses in Three Dimensions	38
1.13.1	Invariants for Three-Dimensional Stress	40
1.14	Normal and Shear Stresses on an Oblique Plane	42
1.14.1	Octahedral Stresses	44
1.15	Mohr's Circles in Three Dimensions	45
1.15.1	Absolute Maximum Shear Stress	46
1.15.2	Equations of Three Mohr's Circles for Stress	47
1.16	Boundary Conditions in Terms of Surface Forces	49
1.17	Indicial Notation	50
	References	51
	Problems	51
 <i>Chapter 2 Strain and Material Properties</i>		68
2.1	Introduction	68
2.2	Deformation	69
2.2.1	Superposition	69
2.3	Strain Defined	70
2.3.1	Plane Strain	70
2.3.2	Three-Dimensional Strain	72
2.3.3	Eulerian and Lagrangian Coordinates	73
2.3.4	Large Strains	74
2.4	Equations of Compatibility	75
2.5	State of Strain at a Point	76
2.5.1	Transformation of Two-Dimensional Strain	76
2.5.2	Transformation of Three-Dimensional Strain	78
2.5.3	Invariants in Three-Dimensional Strain	79
2.5.4	Mohr's Circle for Plane Strain	80
2.6	Engineering Materials	83
2.6.1	General Properties of Some Common Materials	84
2.7	Stress-Strain Diagrams	86
2.7.1	Ductile Materials in Tension	86
2.7.2	Geometry Change of Specimen	87
2.7.3	True Stress and True Strain	88
2.7.4	Brittle Materials in Tension	89
2.7.5	Materials in Compression	89
2.7.6	Materials in Shear	90
2.7.7	Short-Time Effects of Temperature on Stress-Strain Properties	90
2.8	Elastic versus Plastic Behavior	91
2.9	Hooke's Law and Poisson's Ratio	92
2.9.1	Volume Change	93
2.9.2	Deflection of Axially Loaded Members	93

2.10	Generalized Hooke's Law	96
2.11	Orthotropic Materials	101
	2.11.1 Generalized Hook's Law for Orthotropic Material	102
2.12	Measurement of Strain: Strain Gage	103
	2.12.1 Strain Rosette of Three Gages	104
	2.12.2 Rectangular and Delta Strain Rosettes	106
2.13	Strain Energy	107
	2.13.1 Strain Energy Density for Normal and Shear Stresses	108
	2.13.2 Strain Energy Density for Three-Dimensional Stresses	110
2.14	Strain Energy in Common Structural Members	111
	2.14.1 Strain Energy for Axially Loaded Bars	111
	2.14.2 Strain Energy of Circular Bars in Torsion	112
	2.14.3 Strain Energy for Beams in Bending	113
2.15	Components of Strain Energy	113
2.16	Saint-Venant's Principle	115
	2.16.1 Confirmation of Saint-Venant's Rule	116
	References	117
	Problems	118
 <i>Chapter 3 Problems in Elasticity</i>		133
3.1	Introduction	133
3.2	Fundamental Principles of Analysis	134
	3.2.1 Three-Dimensional Problems	134
	3.2.2 Two-Dimensional Problems	134
Part A: Formulation and Methods of Solution		135
3.3	Plane Strain Problems	135
3.4	Plane Stress Problems	138
	3.4.1 Stress–Strain Relations for Orthotropic Materials	139
3.5	Comparison of Two-Dimensional Isotropic Problems	140
3.6	Airy's Stress Function	141
	3.6.1 Generalized Plane Strain Problems	142
	3.6.2 Antiplane Shear Deformations	142
3.7	Solution of Elasticity Problems	143
	3.7.1 Polynomial Solutions	144
3.8	Thermal Stresses	149
	3.8.1 Equations of Thermoelasticity	149
3.9	Basic Relations in Polar Coordinates	152
	3.9.1 Equations of Equilibrium	153
	3.9.2 Stress Function	153
	3.9.3 Strain-Displacement Relations	154
	3.9.4 Hooke's Law	155
	3.9.5 Transformation Equations	155
	3.9.6 Compatibility Equation	156

Part B: Stress Concentrations	157
3.10 Stresses Due to Concentrated Loads	157
3.10.1 Compression of a Wedge (Fig. 3.10a)	157
3.10.2 Bending of a Wedge (Fig. 3.10b)	159
3.10.3 Concentrated Load on a Straight Boundary (Fig. 3.11a)	160
3.11 Stress Distribution Near a Concentrated Load Acting on a Beam	161
3.11.1 Accuracy of Results	163
3.12 Stress Concentration Factors	163
3.12.1 Circular Hole in a Large Plate in Simple Tension	165
3.12.2 Circular Hole in a Large Plate in Biaxial Tension	167
3.12.3 Elliptic Hole in a Large Plate in Tension	167
3.12.4 Graphs for Stress Concentration Factors	168
Part C: Contact Mechanics	169
3.13 Contact Stresses and Deflections	169
3.13.1 Hertz Theory	170
3.13.2 Johnson–Kendall–Roberts Theory	170
3.14 Spherical and Cylindrical Contacts	171
3.14.1 Two Spheres in Contact	171
3.14.2 Two Parallel Cylinders in Contact	173
3.15 Contact Stress Distribution	174
3.15.1 Two Spheres in Contact (Figure 3.18a)	174
3.15.2 Two Parallel Cylinders in Contact (Figure 3.20a)	174
3.16 General Contact	178
References	181
Problems	182
 <i>Chapter 4 Failure Criteria</i>	 192
4.1 Introduction	192
4.1.1 Failure	192
Part A: Static Loading	193
4.2 Failure by Yielding	193
4.2.1 Creep: Time-Dependent Deformation	194
4.3 Failure by Fracture	195
4.3.1 Types of Fracture in Tension	196
4.4 Yield and Fracture Criteria	197
4.5 Maximum Shearing Stress Theory	198
4.6 Maximum Distortion Energy Theory	199
4.6.1 Yield Surfaces for Triaxial Stress	200
4.7 Octahedral Shearing Stress Theory	200
4.8 Comparison of the Yielding Theories	204
4.9 Maximum Principal Stress Theory	205
4.10 Mohr’s Theory	206
4.11 Coulomb–Mohr Theory	207
4.12 Introduction to Fracture Mechanics	210
4.12.1 Stress-Intensity Factors	211

4.13	Fracture Toughness	213
Part B: Repeated and Dynamic Loadings		216
4.14	Fatigue: Progressive Fracture	216
4.14.1	Fatigue Tests	216
4.14.2	Estimating the Endurance Limit and Fatigue Strength	217
4.15	Failure Criteria for Metal Fatigue	217
4.15.1	Uniaxial State of Stress	218
4.15.2	Comparison of Fatigue Failure Criteria	219
4.15.3	Design for Uniaxial Stress	219
4.15.4	Combined State of Stress	221
4.16	Fatigue Life	223
4.17	Impact Loads	225
4.17.1	Strain Rate	226
4.17.2	Basic Assumptions of Impact Analysis	227
4.18	Longitudinal and Bending Impact	227
4.18.1	Freely Falling Weight	227
4.18.2	Horizontally Moving Weight	228
4.19	Ductile–Brittle Transition	230
	References	232
	Problems	233
 <i>Chapter 5 Bending of Beams</i>		242
5.1	Introduction	242
Part A: Exact Solutions		243
5.2	Pure Bending of Beams of Symmetrical Cross Section	243
5.2.1	Kinematic Relationships	244
5.2.2	Timoshenko Beam Theory	246
5.3	Pure Bending of Beams of Asymmetrical Cross Section	246
5.3.1	Stress Distribution	248
5.3.2	Transformation of Inertia Moments	248
5.4	Bending of a Cantilever of Narrow Section	251
5.4.1	Comparison of the Results with the Elementary Theory Results	253
5.5	Bending of a Simply Supported Narrow Beam	254
5.5.1	Use of Stress Functions	255
5.5.2	Comparison of the Results with the Elementary Theory Results	256
Part B: Approximate Solutions		256
5.6	Elementary Theory of Bending	256
5.6.1	Assumptions of Elementary Theory	257
5.6.2	Method of Integration	258
5.7	Normal and Shear Stresses	260
5.7.1	Rectangular Cross Section	262
5.7.2	Various Cross Sections	262
5.7.3	Beam of Constant Strength	267
5.8	Effect of Transverse Normal Stress	268

5.9	Composite Beams	270
5.9.1	Transformed Section Method	270
5.9.2	Equation of Neutral Axis	271
5.9.3	Stresses in the Transformed Beam	272
5.9.4	Composite Beams of Multi Materials	272
5.10	Shear Center	276
5.10.1	Thin-Walled Open Cross Sections	277
5.10.2	Arbitrary Solid Cross Sections	281
5.11	Statically Indeterminate Systems	281
5.11.1	The Method of Superposition	282
5.12	Energy Method for Deflections	284
5.12.1	Form Factor for Shear	285
	Part C: Curved Beams	286
5.13	Elasticity Theory	286
5.13.1	Equations of Equilibrium and Compatibility	286
5.13.2	Boundary Conditions	287
5.13.3	Stress Distribution	288
5.13.4	Deflections	289
5.14	Curved Beam Formula	289
5.14.1	Basic Assumptions	289
5.14.2	Location of the Neutral Axis	290
5.14.3	Tangential Stress	291
5.14.4	Winkler's Formula	293
5.15	Comparison of the Results of Various Theories	293
5.15.1	Correction of σ_θ for Beams with Thin-Walled Cross Sections	294
5.16	Combined Tangential and Normal Stresses	296
	References	300
	Problems	300
	 <i>Chapter 6 Torsion of Prismatic Bars</i>	 315
6.1	Introduction	315
6.2	Elementary Theory of Torsion of Circular Bars	316
6.2.1	Shearing Stress	317
6.2.2	Angle of Twist	317
6.2.3	Axial and Transverse Shear Stresses	320
6.3	Stresses on Inclined Planes	321
6.3.1	Stress Transformation	321
6.3.2	Transmission of Power by Shafts	323
6.4	General Solution of the Torsion Problem	324
6.4.1	Geometry of Deformation	324
6.4.2	Equations of Equilibrium	325
6.4.3	Equations of Compatibility	325
6.5	Prandtl's Stress Function	326
6.5.1	Boundary Conditions	326

6.5.2	Force and Moments over the Ends	327
6.5.3	Circular Cross Section	331
6.6	Prandtl's Membrane Analogy	333
6.6.1	Equation of Equilibrium	333
6.6.2	Shearing Stress and Angle of Twist	335
6.7	Torsion of Narrow Rectangular Cross Section	338
6.7.1	Thin-Walled Open Cross Sections	339
6.8	Torsion of Multiply Connected Thin-Walled Sections	340
6.8.1	Shearing Stress	340
6.8.2	Angle of Twist	341
6.9	Fluid Flow Analogy and Stress Concentration	344
6.10	Torsion of Restrained Thin-Walled Members of Open Cross Section	346
6.10.1	Torsional and Lateral Shears	347
6.10.2	Boundary Conditions	348
6.10.3	Long Beams Under Torsion	348
6.10.4	Angle of Twist	348
6.11	Torsion Bar Springs	350
6.12	Curved Circular Bars	351
6.12.1	Helical Springs	352
	References	354
	Problems	355
 <i>Chapter 7 Numerical Methods</i>		364
7.1	Introduction	364
Part A: Finite Difference Analysis		365
7.2	Finite Differences	365
7.2.1	Central Differences	366
7.3	Finite Difference Equations	368
7.4	Curved Boundaries	370
7.5	Boundary Conditions	373
Part B: Finite Element Analysis		377
7.6	Fundamentals	377
7.7	The Bar Element	379
7.7.1	Equilibrium Method	379
7.7.2	Energy Method	379
7.8	Arbitrarily Oriented Bar Element	380
7.8.1	Coordinate Transformation	380
7.8.2	Force Transformation	381
7.8.3	Displacement Transformation	383
7.8.4	Governing Equations	383
7.9	Axial Force Equation	384
7.10	Force-Displacement Relations for a Truss	386
7.10.1	The Assembly Process	386
7.11	Beam Element	393

7.12	Properties of Two-Dimensional Elements	399
7.12.1	Displacement Matrix	399
7.12.2	Strain, Stress, and Elasticity Matrices	401
7.13	General Formulation of the Finite Element Method	402
7.13.1	Outline of General Finite Element Analysis	403
7.14	Triangular Finite Element	407
7.14.1	Element Nodal Forces	410
7.15	Case Studies in Plane Stress	414
7.16	Computational Tools	423
	References	423
	Problems	424
 <i>Chapter 8 Thick-Walled Cylinders and Rotating Disks</i>		434
8.1	Introduction	434
8.1.1	Basic Relations	434
8.2	Thick-Walled Cylinders Under Pressure	435
8.2.1	Special Cases	438
8.2.2	Closed-Ended Cylinder	440
8.3	Maximum Tangential Stress	441
8.4	Application of Failure Theories	442
8.5	Compound Cylinders: Press or Shrink Fits	443
8.6	Rotating Disks of Constant Thickness	446
8.6.1	Annular Disk	447
8.6.2	Solid Disk	448
8.7	Disk Flywheels	449
8.7.1	Design Factors	450
8.7.2	Stresses and Displacement	450
8.8	Rotating Disks of Variable Thickness	453
8.9	Rotating Disks of Uniform Stress	456
8.10	Thermal Stresses in Thin Disks	458
8.10.1	Annular Disk	459
8.10.2	Solid Disk	459
8.11	Thermal Stress in Long Circular Cylinders	460
8.11.1	Solid Cylinder	460
8.11.2	Cylinder with a Central Circular Hole	461
8.11.3	Special Case	464
8.12	Finite Element Solution	464
8.12.1	Axisymmetric Element	464
	References	466
	Problems	466
 <i>Chapter 9 Beams on Elastic Foundations</i>		473
9.1	Introduction	473
9.2	General Theory	473

9.3	Infinite Beams	475
9.4	Semi-Infinite Beams	480
9.5	Finite Beams	483
9.6	Classification of Beams	484
9.7	Beams Supported by Equally Spaced Elastic Elements	485
9.8	Simplified Solutions for Relatively Stiff Beams	486
9.9	Solution by Finite Differences	488
9.10	Applications	490
	9.10.1 Grid Configurations of Beams	490
	References	492
	Problems	493
 <i>Chapter 10 Applications of Energy Methods</i>		496
10.1	Introduction	496
Part A: Energy Principles		497
10.2	Work Done in Deformation	497
10.3	Reciprocity Theorem	498
10.4	Castigliano's Theorem	499
	10.4.1 Application to Bars and Beams	500
	10.4.2 Application to Trusses	500
	10.4.3 Use of a Fictitious Load	501
10.5	Unit- or Dummy-Load Method	506
10.6	Crotti–Engesser Theorem	508
10.7	Statically Indeterminate Systems	510
Part B: Variational Methods		514
10.8	Principle of Virtual Work	514
	10.8.1 Variation in Strain Energy	514
	10.8.2 Virtual Work Done by Forces	515
10.9	Principle of Minimum Potential Energy	515
10.10	Deflections by Trigonometric Series	517
	10.10.1 Strain Energy	518
	10.10.2 Virtual Work	518
10.11	Rayleigh–Ritz Method	522
	References	524
	Problems	525
 <i>Chapter 11 Stability of Columns</i>		534
11.1	Introduction	534
11.2	Critical Load	534
	11.2.1 Equilibrium Method	535
	11.2.2 Energy Method	536
11.3	Buckling of Pin-Ended Columns	536
	11.3.1 Modes of Buckling	538
11.4	Deflection Response of Columns	539

11.4.1	Effects of Large Deflections	539
11.4.2	Effects of Imperfections	540
11.4.3	Effects of Inelastic Behavior	540
11.5	Columns with Different End Conditions	540
11.6	Critical Stress: Classification of Columns	543
11.6.1	Long Columns	543
11.6.2	Short Columns	544
11.6.3	Intermediate Columns: Inelastic Buckling	544
11.7	Design Formulas for Columns	548
11.8	Imperfections in Columns	550
11.9	Local Buckling of Columns	552
11.10	Eccentrically Loaded Columns: Secant Formula	552
11.10.1	Simplified Formula for Short Columns	554
11.11	Energy Methods Applied to Buckling	554
11.12	Solution by Finite Differences	562
11.13	Finite Difference Solution for Unevenly Spaced Nodes	567
	References	568
	Problems	569
 <i>Chapter 12</i> Plastic Behavior of Materials		578
12.1	Introduction	578
12.2	Plastic Deformation	579
12.2.1	Slip Action: Dislocation	579
12.3	Idealized Stress–Strain Diagrams	580
12.3.1	True Stress–True Strain Relationships	580
12.4	Instability in Simple Tension	582
12.5	Plastic Axial Deformation and Residual Stress	585
12.6	Plastic Deflection of Beams	588
12.7	Analysis of Perfectly Plastic Beams	590
12.7.1	Shape Factor	593
12.7.2	Plastic Hinge	593
12.8	Collapse Load of Structures: Limit Design	600
12.8.1	Collapse Mechanism	600
12.8.2	Ultimate Load by the Energy Method	601
12.9	Elastic–Plastic Torsion of Circular Shafts	605
12.9.1	Yield Torque	606
12.9.2	Elastic–Plastic Torque	606
12.9.3	Ultimate Torque	607
12.9.4	Residual Rotation and Stress	608
12.10	Plastic Torsion: Membrane Analogy	610
12.10.1	Membrane–Roof Analogy	610
12.10.2	Sand Hill Analogy	611
12.11	Elastic–Plastic Stresses in Rotating Disks	612
12.11.1	Initial Yielding	612

12.11.2	Partial Yielding	612
12.11.3	Complete Yielding	614
12.12	Plastic Stress–Strain Relations	614
12.13	Plastic Stress–Strain Increment Relations	620
12.14	Stresses in Perfectly Plastic Thick-Walled Cylinders	623
12.14.1	Complete Yielding	624
12.14.2	Partial Yielding	626
	References	627
	Problems	628
 <i>Chapter 13 Stresses in Plates and Shells</i>		635
13.1	Introduction	635
Part A: Bending of Thin Plates		635
13.2	Basic Assumptions	635
13.3	Strain–Curvature Relations	636
13.4	Stress, Curvature, and Moment Relations	638
13.5	Governing Equations of Plate Deflection	640
13.6	Boundary Conditions	642
13.7	Simply Supported Rectangular Plates	644
13.8	Axisymmetrically Loaded Circular Plates	648
13.9	Deflections of Rectangular Plates by the Strain-Energy Method	650
13.10	Sandwich Plates	652
13.10.1	Design of Sandwich Beams and Plates	653
13.11	Finite Element Solution	654
13.11.1	Strain, Stress, and Elasticity Matrices	655
13.11.2	Displacement Function	655
13.11.3	Stiffness Matrix	657
13.11.4	External Nodal Forces	657
Part B: Membrane Stresses in Thin Shells		657
13.12	Theories and Behavior of Shells	657
13.13	Simple Membrane Action	658
13.14	Symmetrically Loaded Shells of Revolution	660
13.14.1	Equations of Equilibrium	661
13.14.2	Conditions of Compatibility	662
13.15	Some Typical Cases of Shells of Revolution	662
13.15.1	Spherical Shell	662
13.15.2	Conical Shell	663
13.15.3	Circular Cylindrical Shell	664
13.16	Thermal Stresses in Compound Cylinders	668
13.17	Cylindrical Shells of General Shape	670
	References	673
	Problems	673

<i>Appendix A</i>	Problem Formulation and Solution	679
A.1	Basic Method	679
	A.1.1 Numerical Accuracy	680
	A.1.2 Daily Planning	680
<i>Appendix B</i>	Solution of the Stress Cubic Equation	682
B.1	Principal Stresses	682
	B.1.1 Direction Cosines	683
<i>Appendix C</i>	Moments of Composite Areas	687
C.1	Centroid	687
C.2	Moments of Inertia	690
	C.2.1 Parallel Axis Theorem	690
	C.2.2 Principal Moments of Inertia	692
<i>Appendix D</i>	Tables and Charts	699
D.1	Charts of Stress Concentration Factors	705
<i>Appendix E</i>	Introduction to MATLAB	710
	Answers to Selected Problems	713
	Index	722

Preface

INTRODUCTION

Advanced Mechanics of Materials and Applied Elasticity, Sixth Edition, is an outgrowth of classroom notes prepared in connection with advanced undergraduate and first-year graduate courses in the mechanics of solids and elasticity. It is designed to satisfy the requirements of courses subsequent to an elementary treatment of the strength of materials. In addition to its applicability to aeronautical, civil, and mechanical engineering and to engineering mechanics curricula, the text is useful to practicing engineers. Emphasis is given to *numerical techniques* (which lend themselves to computerization) in the solution of problems resisting *analytical treatment*. The attention devoted to numerical solutions is not intended to deny the value of classical analysis, which is given a rather full treatment. Instead, the coverage provided here seeks to fill what we believe to be a void in the world of textbooks.

We have attempted to present a balance between the theory necessary to gain insight into the mechanics, but which can often offer no more than crude approximations to real problems because of simplifications related to geometry and conditions of loading, and numerical solutions, which are so useful in presenting stress analysis in a more realistic setting. This text emphasizes those aspects of theory and application that prepare a student for more advanced study or for professional practice in design and analysis.

The theory of elasticity plays three important roles in the text. First, it provides exact solutions where the configurations of loading and boundary are relatively simple. Second, it provides a check on the limitations of the mechanics of materials approach. Third, it serves as the basis of approximate solutions employing numerical analysis.

To make the text as clear as possible, the fundamentals of the mechanics of materials are addressed as necessary. The physical significance of the solutions and practical applications are also emphasized. In addition, we have made a special effort to illustrate important principles and applications with numerical examples. Consistent with announced national policy, problems are included in the text in which the physical quantities are expressed in the International System of Units (SI). All important quantities are defined in both SI and U.S. Customary System (USCS) of units. A sign convention, consistent with vector mechanics, is employed throughout for loads, internal forces, and stresses. This convention conforms to that used in most classical strength of materials and

elasticity texts, as well as to that most often employed in the numerical analysis of complex structures.

ORGANIZATION OF THE TEXT

Because of its extensive subdivision into a variety of topics and use of alternative methods of analysis, this text provides great flexibility for instructors when choosing assignments to cover courses of varying length and content. Most chapters are substantially self-contained, so the order of presentation can be smoothly altered to meet an instructor's preference. Ideally, Chapters 1 and 2, which address the analysis of basic concepts, should be studied first. The emphasis placed on the treatment of two-dimensional problems in elasticity (Chapter 3) may then differ according to the scope of the course.

This sixth edition of *Advanced Mechanics of Materials and Applied Elasticity* seeks to preserve the objectives and emphases of the previous editions. Every effort has been made to provide a more complete and current text through the inclusion of new material dealing with the fundamental principles of stress analysis and design: stress concentrations, contact stresses, failure criteria, fracture mechanics, compound cylinders, finite element analysis (FEA), energy and variational methods, buckling of stepped columns, common shell types, case studies in analysis and design, and MATLAB solutions. The entire text has been reexamined, and many improvements have been made throughout by a process of elimination and rearrangement. Some sections have been expanded to improve on previous expositions.

The references (identified in *brackets*), which are provided as an aid to those students who wish to pursue certain aspects of a subject in further depth, have been updated and listed at the end of each chapter. We have resisted the temptation to increase the material covered except where absolutely necessary. Nevertheless, we have added a number of illustrative examples and problems important in engineering practice and design. Extra care has been taken in the presentation and solution of the sample problems. All the problem sets have been reviewed and checked to ensure both their clarity and their numerical accuracy. Most changes in subject-matter coverage were prompted by the suggestions of faculty familiar with earlier editions.

In this sixth edition, we have maintained the previous editions' clarity of presentation, simplicity as the subject permits, unpretentious depth, an effort to encourage intuitive understanding, and a shunning of the irrelevant. In this context, as throughout, emphasis is placed on the use of fundamentals to help build students' understanding and ability to solve the more complex problems.

SUPPLEMENTS

The book is accompanied by a comprehensive instructor's *Solutions Manual*. Written and class tested, it features complete solutions to all problems in the text. Answers to selected problems are given at the end of the book. The password-protected Solutions Manual is available for adopters at the Pearson Instructor Resource Center, pearsonhighered.com/irc.

Optional Material is also available from the Pearson Resource Center, pearsonhighered.com/irc. This material includes PowerPoint slides of figures and tables, and solutions using MATLAB for a variety of sample problems of practical importance. The book, however, is independent of any software package.

Register your copy of *Advanced Mechanics of Materials and Applied Elasticity, Sixth Edition*, on the InformIT site for convenient access to updates and corrections as they become available. To start the registration process, go to informit.com/register and log in or create an account. Enter the product ISBN (9780134859286) and click Submit. Look on the Registered Products tab for an Access Bonus Content link next to this product, and follow that link to access any available bonus materials. If you would like to be notified of exclusive offers on new editions and updates, please check the box to receive email from us.

Acknowledgments

It is a particular pleasure to acknowledge the contributions of those who assisted in the evolution of the text. Thanks, of course, are due to the many readers who have contributed general ideas and to reviewers who have made detailed comments on previous editions. These notably include the following: F. Freudenstein, Columbia University; R. A. Scott, University of Michigan; M. W. Wilcox and Y. Chan Jian, Southern Methodist University; C. T. Sun, University of Florida; B. Koplik, H. Kountouras, K. A. Narh, R. Sodhi, and C. E. Wilson, New Jersey Institute of Technology; H. Smith, Jr., South Dakota School of Mines and Technology; B. P. Gupta, Gannon University; S. Bang, University of Notre Dame; B. Koo, University of Toledo; J. T. Easley, University of Kansas; J. A. Bailey, North Carolina State University; W. F. Wright, Vanderbilt University; R. Burks, SUNY Maritime College; G. E. O. Widera, University of Illinois; R. H. Koebke, University of South Carolina; B. M. Kwak, University of Iowa; G. Nadig, Widener University; R. L. Brown, Montana State University; S. H. Advani, West Virginia University; E. Nassat, Illinois Institute of Technology; R. I. Sann, Stevens Institute of Technology; C. O. Smith, University of Nebraska; J. Kempner, Polytechnic University of New York; and P. C. Prister, North Dakota State University; R. Wetherhold, University of Buffalo, SUNY; and Shaofan Li, University of California at Berkeley.

Accuracy checking of the problems, proofreading, and typing of the *Solutions Manual* were done expertly by my former student, Dr. Youngjin Chung. Also contributing considerably to this volume with typing new inserts, scanning some figures, limited proofreading, and cover design was Errol A. Ugural. Their hard work is much appreciated. I am deeply indebted to my colleagues who have found the text useful through the years, as well as to Laura Lewin, executive editor at Pearson, who encouraged development of this edition. Lastly, I am very thankful for the support and understanding of my wife Nora, daughter Aileen, and son Errol during preparation of this book.

*Ansel C. Ugural
Holmdel, New Jersey*

About the Authors

Ansel C. Ugural, Ph.D., has been a research and visiting professor of mechanical and civil engineering at the New Jersey Institute of Technology. He has taught in the engineering mechanics department at the University of Wisconsin. Dr. Ugural also served as chairman and tenured professor of mechanical engineering at Fairleigh Dickinson University for twenty years. He has considerable and diverse industrial experience in both full-time and consulting capacities as a design, development, and research engineer.

Professor Ugural earned his MS in mechanical engineering and PhD in engineering mechanics from the University of Wisconsin–Madison. Dr. Ugural was a National Science Foundation (NSF) fellow. He has been a member of several professional societies, including the American Society of Mechanical Engineers and the American Society of Engineering Education. He is also listed in *Who's Who in Engineering*.

Dr. Ugural is the author of several books, including *Mechanics of Materials*; *Mechanical Design: An Integrated Approach*; *Mechanical Design of Machine Components*; *Stresses in Beams, Plates, and Shells*; and *Plates and Shells: Theory and Analysis*. Most of these texts have been translated into Korean, Chinese, and Portuguese. In addition, Professor Ugural has published numerous articles in trade and professional journals.

Saul K. Fenster, Ph.D., served as president and tenured professor at New Jersey Institute of Technology for more than two decades. In addition, he has held varied positions at Fairleigh Dickinson University and taught at the City University of New York. His experience includes membership on a number of corporate boards and economic development commissions. Fenster is a fellow of the American Society of Mechanical Engineers, the American Society for Engineering Education, and the American Society for Manufacturing Engineers. He is coauthor of a text on mechanics.

Symbols

Roman Letters

A	area
B	width
C	carryover factor, torsional rigidity
c	distance from neutral axis to outer fiber
D	distribution factor, flexural rigidity of plate
$[D]$	elasticity matrix
d	diameter, distance
E	modulus of elasticity in tension or compression
E_s	modulus of plasticity or secant modulus
E_t	tangent modulus
e	dilatation, distance, eccentricity
$\{F\}$	nodal force matrix of bar and beam finite elements
F	body force per unit volume, concentrated force
f	coefficient of friction
$\{f\}$	displacement function of finite element
G	modulus of elasticity in shear or modulus of rigidity
g	acceleration of gravity ($\approx 9.81 \text{ m/s}^2$)
h	depth of beam, height, membrane deflection, mesh width
I	moment of inertia of area, stress invariant
J	polar moment of inertia of area, strain invariant
K	bulk modulus, spring constant of an elastic support, stiffness factor, thermal conductivity, fatigue factor, strength coefficient, stress concentration factor
$[K]$	stiffness matrix of whole structure
k	constant, modulus of elastic foundation, spring constant
$[k]$	stiffness matrix of finite element
L	length, span
l, m, n	direction cosines
M	moment
M_{xy}	twisting moment in plates
m	moment caused by unit load

N	fatigue life (cycles), force
n	factor of safety, number, strain hardening index
P	concentrated force
p	distributed load per unit length or area, pressure, stress resultant
Q	first moment of area, heat flow per unit length, shearing force
$\{Q\}$	nodal force matrix of two-dimensional finite element
R	radius, reaction
r	radius, radius of gyration
r, θ	polar coordinates
S	elastic section modulus, shear center
s	distance along a line or a curve
T	temperature, twisting couple or torque
t	thickness
U	strain energy
U_o	strain energy per unit volume
U^*	complementary energy
u, v, w	components of displacement
V	shearing force, volume
v	velocity
W	weight, work
x, y, z	rectangular coordinates
Z	plastic section modulus

Greek Letters

α	angle, coefficient of thermal expansion, form factor for shear
β	numerical factor, angle
γ	shear strain, weight per unit volume or specific weight, angle
δ	deflection, finite difference operator, variational symbol, displacement
$\{\delta\}$	nodal displacement matrix of finite element
Δ	change of a function
ε	normal strain
θ	angle, angle of twist per unit length, slope
ν	Poisson's ratio
λ	axial load factor, Lamé constant
Π	potential energy
ρ	density (mass per unit volume), radius
σ	normal stress
τ	shear stress
ϕ	total angle of twist
Φ	stress function
ω	angular velocity
ψ	stream function

This page intentionally left blank

5.1 INTRODUCTION

In this chapter we are concerned with the bending of straight as well as curved *beams*—that is, structural elements possessing one dimension significantly greater than the other two, usually loaded in a direction normal to the longitudinal axis. We first examine the elasticity or “exact” solutions of beams that are straight and made of homogeneous, linearly elastic materials. Then, we consider solutions for straight beams using mechanics of materials or elementary theory, special cases involving members made of composite materials, and the shear center. The deflections and stresses in beams caused by pure bending as well as those due to lateral loading are discussed. We analyze stresses in curved beams using both exact and elementary methods, and compare the results of the various theories.

Except in the case of very simple shapes and loading systems, the theory of elasticity yields beam solutions only with considerable difficulty. Practical considerations often lead to assumptions about stress and deformation that result in mechanics of materials or elementary theory solutions. The theory of elasticity can sometimes be applied to test the validity of such assumptions. This theory has three roles in these problems: It can serve to place limitations on the use of the elementary theory, it can be used as the basis of approximate solutions through numerical analysis, and it can provide exact solutions for simple configurations of loading and shape.

Part A: Exact Solutions

5.2 PURE BENDING OF BEAMS OF SYMMETRICAL CROSS SECTION

The simplest case of *pure bending* is that of a beam possessing a vertical axis of symmetry, subjected to equal and opposite end couples (Fig. 5.1a). The semi-inverse method is now applied to analyze this problem. The *moment* M_z shown in Fig. 5.1a is defined as *positive*, because it acts on a positive (negative) face with its vector in the positive (negative) coordinate direction. This *sign convention* agrees with that of stress (Section 1.5). We will assume that the normal stress over the cross section varies linearly with y and that the remaining stress components are zero:

$$\sigma_x = ky, \quad \sigma_y = \sigma_z = \tau_{xy} = \tau_{xz} = \tau_{yz} = 0 \quad (5.1)$$

Here k is a constant, and $y = 0$ contains the *neutral surface*—that is, the surface along which $\sigma_x = 0$. The intersection of the neutral surface and the cross section locates the neutral axis (abbreviated NA). Figure 5.1b shows the linear stress field in a section located an arbitrary distance a from the left end.

Since Eqs. (5.1) indicate that the lateral surfaces are free of stress, we need only be assured that the stresses are consistent with the boundary conditions at the ends. These *conditions of equilibrium* require that the resultant of the internal forces be zero and that the moments of the internal forces about the neutral axis equal the applied moment

$$\int_A \sigma_x dA = 0, \quad - \int_A y \sigma_x dA = M_z \quad (5.2)$$

where A is the cross-sectional area. Note that the zero stress components τ_{xy}, τ_{xz} in Eqs. (5.1) satisfy the conditions that no y - and z -directed forces exist at the end faces. Moreover, because of the y symmetry of the section, $\sigma_x = ky$ produces no moment about the y axis. The negative sign in the second expression implies that a *positive* moment M_z is one that results in *compressive* (negative) stress at points of *positive* y . Substituting Eqs. (5.1) into Eqs. (5.2) yields

$$k \int_A y dA = 0, \quad -k \int_A y^2 dA = M_z \quad (5.3a, b)$$

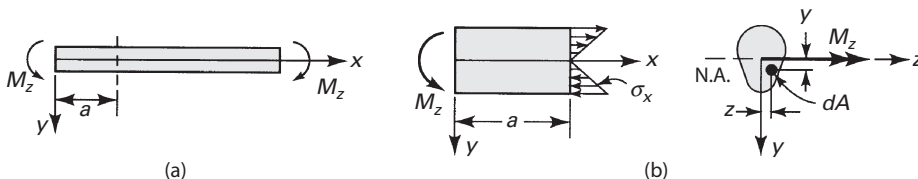


FIGURE 5.1. (a) Beam of singly symmetric cross section in pure bending; (b) stress distribution across cross section of the beam.

Since $k \neq 0$, Eq. (5.3a) indicates that the first moment of cross-sectional area about the neutral axis is zero. This requires that *the neutral and centroidal axes of the cross section coincide*. Neglecting body forces, it is clear that the equations of equilibrium (3.4), are satisfied by Eqs. (5.1). It can also readily be verified that Eqs. (5.1) together with Hooke's law fulfill the compatibility conditions, Eq. (2.12). Thus, Eqs. (5.1) represent an exact solution.

The integral in Eq. (5.3b) defines the moment of inertia I_z of the cross section about the z axis of the beam cross section (Appendix C); therefore,

$$k = -\frac{M_z}{I_z} \quad (\text{a})$$

An expression for normal stress can now be written by combining Eqs. (5.1) and (a):

$$\sigma_x = -\frac{M_z y}{I_z} \quad (\text{5.4})$$

This is the familiar elastic *flexure formula* applicable to straight beams.

Since, at a given section, M and I are constant, the maximum stress is obtained from Eq. (5.4) by taking $|y|_{\max} = c$:

$$\sigma_{\max} = \frac{Mc}{I} = \frac{M}{I/c} = \frac{M}{S} \quad (\text{5.5})$$

where S is the *elastic section modulus*. Equation (5.5) is widely employed in practice because of its simplicity. To facilitate its use, section moduli for numerous common sections are tabulated in various handbooks. A fictitious stress in extreme fibers, computed from Eq. (5.5) for the experimentally obtained *ultimate* bending moment (Section 12.7), is termed the *modulus of rupture* of the material in bending. This quantity, $\sigma_{\max} = M_u/S$, is frequently used as a *measure of the bending strength* of materials.

5.2.1 Kinematic Relationships

To gain further insight into the beam problem, we now consider the *geometry of deformation*—that is, beam kinematics. Fundamental to this discussion is the hypothesis that sections originally plane remain so subsequent to bending. For a beam of symmetrical cross section, *Hooke's law* and Eq. (5.4) lead to

$$\begin{aligned} \epsilon_x &= -\frac{M_z y}{EI_z}, & \epsilon_y &= \epsilon_z = \nu \frac{M_z y}{EI_z} \\ \gamma_{xy} &= \gamma_{xz} = \gamma_{yz} = 0 \end{aligned} \quad (\text{5.6})$$

where EI_z is the *flexural rigidity*.

Let us examine the deflection of the beam axis, whose axial deformation is zero. Figure 5.2a shows an element of an initially straight beam, now in a deformed state. Because the beam is subjected to pure bending, uniform throughout, each element of

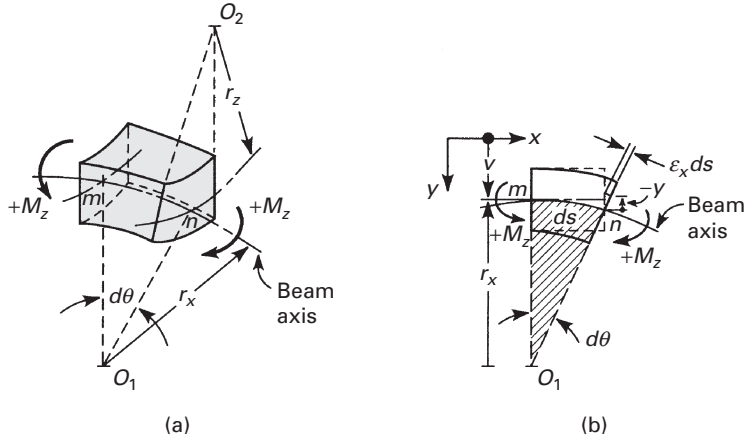


FIGURE 5.2. (a) Segment of a bent beam; (b) geometry of deformation.

infinitesimal length experiences identical deformation, with the result that the beam curvature is everywhere the same. The deflected axis of the beam or the deflection curve is thus shown deformed, with *radius of curvature* r_x . The *curvature of the beam axis* in the xy plane in terms of the y deflection v is

$$\frac{1}{r_x} = \frac{d^2v/dx^2}{[1 + (dv/dx)^2]^{3/2}} \approx \frac{d^2v}{dx^2} \quad (5.7)$$

where the approximate form is valid for small deformations ($dv/dx \ll 1$). The sign convention for curvature of the beam axis is such that this sign is *positive* when the beam is bent concave *downward*, as shown in the figure.

As shown by the geometry in Fig. 5.2b, the shaded sectors are similar. Hence, the radius of curvature and the strain are related as follows:

$$d\theta = \frac{ds}{r_x} = -\frac{\epsilon_x ds}{y} \quad (5.8)$$

where ds is the arc length mn along the longitudinal axis of the beam. For a small displacement, $ds \approx dx$ and θ represents the slope dv/dx of the beam axis. Clearly, for the positive curvature shown in Fig. 5.2a, θ increases as we move from left to right along the beam axis. On the basis of Eqs. (5.6) and (5.8),

$$\frac{1}{r_x} = -\frac{\epsilon_x}{y} = \frac{M_z}{EI_z} \quad (5.9a)$$

Following a similar procedure and noting that $\epsilon_z \approx -v\epsilon_x$, we may also obtain the curvature in the yz plane as

$$\frac{1}{r_z} = -\frac{\epsilon_z}{y} = -\frac{vM_z}{EI_z} \quad (5.9b)$$

The basic *equation of the deflection curve* of a beam is obtained by combining Eqs. (5.7) and (5.9a) as follows:

$$\frac{d^2v}{dx^2} = \frac{M_z}{EI_z} \quad (5.10)$$

This expression, relating the beam curvature to the bending moment, is known as the Bernoulli–Euler law of *elementary bending theory*. It is observed from Fig. 5.2 and Eq. (5.10) that a positive moment produces a positive curvature. If the sign convention adopted in this section for either moment or deflection (and curvature) is reversed, the plus sign in Eq. (5.10) should likewise be reversed.

Reference to Fig. 5.2a reveals that the top and bottom lateral surfaces have been deformed into saddle-shaped or *anticlastic* surfaces of curvature $1/r_z$. The vertical sides have been simultaneously rotated as a result of bending. Examining Eq. (5.9b) suggests a method for *determining Poisson's ratio* [Ref. 5.1]. For a given beam and bending moment, a measurement of $1/r_z$ leads directly to v . The effect of anticlastic curvature is small when the beam depth is comparable to its width.

5.2.2 Timoshenko Beam Theory

The Timoshenko theory of beams, developed by S. P. Timoshenko at the beginning of the twentieth century, constitutes an improvement over the Euler–Bernoulli theory. In the *static* case, the difference between the two hypotheses is that the former includes the effect of shear stresses on the deformation by assuming a constant shear over the beam height, whereas the latter ignores the influence of transverse shear on beam deformation. The Timoshenko theory is also said to be an extension of the ordinary beam theory that allows for the effect of the transverse *shear deformation* while relaxing the assumption that plane sections remain plane and normal to the deformed beam axis.

The Timoshenko beam theory is well suited to describing the behavior of short beams and sandwich composite beams. In the *dynamic* case, the theory incorporates *shear deformation* as well as *rotational inertia* effects, and it will be more accurate for not very slender beams. By effectively taking into account the mechanism of deformation, Timoshenko's theory lowers the stiffness of the beam, with the result being a larger deflection under static load and lower predicted fundamental frequencies of vibration for a prescribed set of boundary conditions.

5.3 PURE BENDING OF BEAMS OF ASYMMETRICAL CROSS SECTION

In this section, we extend the discussion in Section 5.2 to the more general case in which a beam of arbitrary cross section is subjected to end couples M_y and M_z about the y and z axes, respectively (Fig. 5.3). Following a procedure similar to that described in Section 5.2, plane sections are again taken to remain plane. Assume that the normal stress σ_x

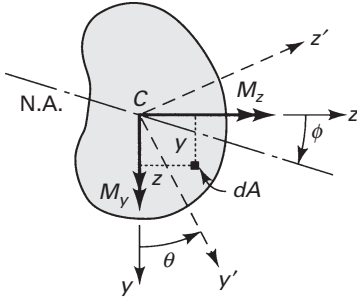


FIGURE 5.3. *Pure bending of beams of asymmetrical cross section.*

acting at a point within dA is a linear function of the y and z coordinates of the point; assume further that the remaining stresses are zero. Then the stress field is

$$\begin{aligned}\sigma_x &= c_1 + c_2 y + c_3 z & (5.11) \\ \sigma_y &= \sigma_z = \tau_{xy} = \tau_{xz} = \tau_{yz} = 0\end{aligned}$$

where c_1, c_2, c_3 are constants to be evaluated.

The *equilibrium conditions* at the beam ends, as before, relate to the force and bending moment:

$$\int_A \sigma_x dA = 0 \quad (a)$$

$$\int_A z \sigma_x dA = M_y, \quad - \int_A y \sigma_x dA = M_z \quad (b, c)$$

Carrying σ_x , as given by Eq. (5.11), into Eqs. (a), (b), and (c) results in the following expressions:

$$c_1 \int_A dA + c_2 \int_A y dA + c_3 \int_A z dA = 0 \quad (d)$$

$$c_1 \int_A z dA + c_2 \int_A yz dA + c_3 \int_A z^2 dA = M_y \quad (e)$$

$$c_1 \int_A y dA + c_2 \int_A y^2 dA + c_3 \int_A yz dA = -M_z \quad (f)$$

For the origin of the y and z axes to be coincident with the centroid of the section, it is required that

$$\int_A y dA = \int_A z dA = 0 \quad (g)$$

Based on Eq. (d), we conclude that $c_1 = 0$; based on Eqs. (5.11), we conclude that $\sigma_x = 0$ at the origin. Thus, the neutral axis passes through the centroid, as in the beam of symmetrical section. In addition, the field of stress described by Eqs. (5.11) satisfies the equations of *equilibrium* and *compatibility* and the lateral surfaces are free of stress. Now consider the defining relationships

$$I_y = \int_A z^2 dA, \quad I_z = \int_A y^2 dA, \quad I_{yz} = \int_A yz dA \quad (5.12)$$

The quantities I_y and I_z are the moments of inertia about the y and z axes, respectively, and I_{yz} is the product of inertia about the y and z axes. From Eqs. (e) and (f), together with Eqs. (5.12), we obtain expressions for c_2 and c_3 .

5.3.1 Stress Distribution

Substitution of the constants into Eqs. (5.11) results in the following *generalized flexure formula*:

$$\sigma_x = \frac{(M_y I_z + M_z I_{yz})z - (M_y I_{yz} + M_z I_y)y}{I_y I_z - I_{yz}^2} \quad (5.13)$$

The *equation of the neutral axis* is found by equating this expression to zero:

$$(M_y I_z + M_z I_{yz})z - (M_y I_{yz} + M_z I_y)y = 0 \quad (5.14)$$

This is an inclined line through the centroid C . The *angle* ϕ between the neutral axis and the z axis is determined as follows:

$$\tan \theta = \frac{y}{z} = \frac{M_y I_z + M_z I_{yz}}{M_y I_{yz} + M_z I_y} \quad (5.15)$$

The angle ϕ (measured from the z axis) is positive in the *clockwise* direction, as shown in Fig. 5.3. The highest bending stress occurs at a point located *farthest* from the neutral axis.

There is a specific orientation of the y and z axes for which the product of inertia I_{yz} vanishes. Labeling the axes so oriented as y' and z' , we have $I_{y'z'} = 0$. The flexure formula under these circumstances becomes

$$\sigma_x = \frac{M_{y'} z'}{I_{y'}} - \frac{M_{z'} y'}{I_{z'}} \quad (5.16)$$

The y' and z' axes now coincide with the *principal* axes of inertia of the cross section, and we can find the stresses at any point by applying Eq. (5.13) or Eq. (5.16).

The kinematic relationships discussed in Section 5.2 are valid for beams of asymmetrical section provided that y and z represent the principal axes.

5.3.2 Transformation of Inertia Moments

Recall that the two-dimensional stress (or strain) and the moment of inertia of an area are second-order tensors (Section 1.17). Thus, *the transformation equations for stress and moment of inertia are analogous* (Section C.2.2). In turn, the Mohr's circle analysis and all conclusions drawn for stress apply to the moment of inertia. With reference to the coordinate axes shown in Fig. 5.3, applying Eq. (C.12a), the moment of inertia about the y' axis is

$$I_{y'} = \frac{I_y + I_z}{2} + \frac{I_y - I_z}{2} \cos 2\theta - I_{yz} \sin 2\theta \quad (5.17)$$

From Eq. (C.13), the orientation of the principal axes is given by

$$\tan 2\theta_p = -\frac{2I_{yz}}{I_y - I_z} \quad (5.18)$$

The principal moments of inertia, I_1 and I_2 , from Eq. (C.14) are

$$I_{1,2} = \frac{I_x + I_y}{2} \pm \sqrt{\left(\frac{I_x - I_y}{2}\right)^2 + I_{xy}^2} \quad (5.19)$$

where the subscripts 1 and 2 refer to the maximum and minimum values, respectively.

Determination of the moments of inertia and stresses in an asymmetrical section is illustrated in Example 5.1.

EXAMPLE 5.1 Analysis of an Angle in Pure Bending

A 150- by 150-mm slender angle of 20-mm thickness is subjected to oppositely directed end couples $M_z = 11 \text{ kN} \cdot \text{m}$ at the centroid of the cross section. What bending stresses exist at points A and B on a section away from the ends (Fig. 5.4a)? Determine the orientation of the neutral axis.

Solution Equations (5.13) and (5.16) are applied to obtain the normal stress. This requires first determining a number of section properties through the use of familiar expressions of mechanics given in Appendix C. The computer program presented in Table C.2 provides a check of the numerical values obtained here for the area characteristics and may be extended to compute the stresses.

Location of the Centroid C . Let \bar{y} and \bar{z} represent the distances from C to arbitrary reference lines (denoted as Z and Y):

$$\bar{z} = \frac{\Sigma A_i \bar{z}_i}{\Sigma A_i} = \frac{A_1 \bar{z}_1 + A_2 \bar{z}_2}{A_1 + A_2} = \frac{130 \times 20 \times 10 + 150 \times 20 \times 75}{130 \times 20 + 150 \times 20} = 45 \text{ mm}$$

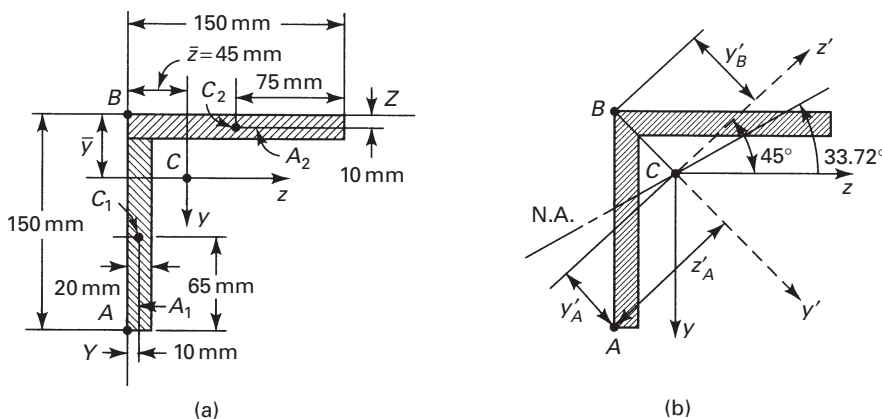


FIGURE 5.4. Example 5.1. An equal-leg-angle cross section of beam.

where \bar{z}_i represents the z distance from the Y reference line to the centroid of each subarea (A_1 and A_2) composing the total cross section. Since the section is symmetrical, $\bar{z} = \bar{y}$.

Moments and Products of Inertia. For a rectangular section of depth h and width b , the moment of inertia about the neutral \bar{z} axis is $I_{\bar{z}} = bh^3/12$ (Table C.1). We now use the yz axes as reference axes through C . Representing the distances from C to the centroids of each subarea by d_{y_1} , d_{y_2} , d_{z_1} , and d_{z_2} we obtain the moments of inertia with respect to these axes using the parallel-axis theorem. Applying Eq. (C.9),

$$I_z = \sum (I_{\bar{z}} + Ad_y^2) = I_{\bar{z}_1} + A_1 d_{y_1}^2 + I_{\bar{z}_2} + A_2 d_{y_2}^2$$

Thus, referring to Fig. 5.4a,

$$\begin{aligned} I_z = I_y &= \frac{1}{12} \times 20 \times (130)^3 + 130 \times 20 \times (40)^2 \\ &\quad + \frac{1}{12} \times 150 \times (20)^3 + 150 \times 20 \times (35)^2 \\ &= 11.596 \times 10^6 \text{ mm}^4 \end{aligned}$$

The transfer formula, Eq. (C.11), for a product of inertia yields

$$\begin{aligned} I_{yz} &= \sum (I_{\bar{y}\bar{z}} + Ad_y d_z) \\ &= 0 + 130 \times 20 \times 40 \times (-35) + 0 + 150 \times 20 \times (-35) \times 30 \\ &= -6.79 \times 10^6 \text{ mm}^4 \end{aligned}$$

Stresses Using Eq. (5.13). We have $y_A = 0.105$ m, $y_B = -0.045$ m, $z_A = -0.045$ m, $z_B = -0.045$ m, and $M_y = 0$. Hence,

$$\begin{aligned} (\sigma_x)_A &= \frac{M_z (I_{yz} z_A - I_y y_A)}{I_y I_z - I_{yz}^2} \\ &= \frac{11(10^3) [(-6.79)(-0.045) - (11.596)(0.105)]}{[(11.596)^2 - (-6.79)^2] 10^{-6}} = -114 \text{ MPa} \quad \text{(h)} \end{aligned}$$

Similarly,

$$(\sigma_x)_B = \frac{11(10^3) [(-6.79)(-0.045) - (11.596)(-0.045)]}{[(11.596)^2 - (-6.79)^2] 10^{-6}} = 103 \text{ MPa}$$

Alternatively, these stresses may be calculated as described next.

Directions of the Principal Axes and the Principal Moments of Inertia.

Employing Eq. (5.18), we have

$$\tan 2\theta_p = \frac{-2(-6.79)}{11.596 - 11.596} = \infty, \quad 2\theta_p = 90^\circ \text{ or } 270^\circ$$

Therefore, the two values of θ_p are 45° and 135° . Substituting the first of these values into Eq. (5.17), we obtain $I_{y'} = [11.596 + 6.79 \sin 90^\circ]$. Since the principal moments of inertia are, by application of Eq. (5.19),

$$I_{1,2} = [11.596 \pm \sqrt{0 + 6.79^2}]10^6 = [11.596 \pm 6.79]10^6$$

we see that $I_1 = I_{y'} = 18.386 \times 10^6 \text{ mm}^4$ and $I_2 = I_{z'} = 4.806 \times 10^6 \text{ mm}^4$. The principal axes are indicated in Fig. 5.4b as the $y'z'$ axes.

Stresses Using Eq. (5.16). The components of bending moment about the principal axes are

$$M_{y'} = 11(10^3) \sin 45^\circ = 7778 \text{ N} \cdot \text{m}$$

$$M_{z'} = 11(10^3) \cos 45^\circ = 7778 \text{ N} \cdot \text{m}$$

Equation (5.16) is now applied, referring to Fig 5.4b, with $y'_A = 0.043 \text{ m}$, $z'_A = -0.106 \text{ m}$, $y'_B = -0.0636 \text{ m}$, and $z'_B = 0$ determined from geometric considerations:

$$(\sigma_x)_A = \frac{7778(-0.106)}{18.386 \times 10^{-6}} - \frac{7778(0.043)}{4806 \times 10^{-6}} = -114 \text{ MPa}$$

$$(\sigma_x)_B = 0 - \frac{7778(-0.0636)}{4.806 \times 10^{-6}} = 103 \text{ MPa}$$

as before.

Direction of the Neutral Axis. From Eq. (5.15), with $M_y = 0$,

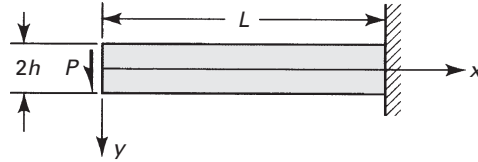
$$\tan \phi = \frac{I_{yz}}{I_y} \quad \text{or} \quad \phi = \arctan \frac{-6.79}{11.596} = -30.4^\circ$$

The negative sign indicates that the neutral is located counterclockwise from the z axis (Fig. 5.4b).

5.4 BENDING OF A CANTILEVER OF NARROW SECTION

Consider a narrow cantilever beam of rectangular cross section, loaded at its free end by a concentrated force of magnitude such that the beam weight may be neglected (Fig. 5.5). This situation may be regarded as a case of plane stress provided that the beam thickness t

FIGURE 5.5. Deflections of an end-loaded cantilever beam.



is small relative to the beam depth $2h$. The distribution of stress in the beam, as we found in Example 3.1, is given by

$$\sigma_x = -\left(\frac{Px}{I}\right)y, \quad \sigma_y = 0, \quad \tau_{xy} = -\frac{P}{2I}(h^2 - y^2) \quad (3.21)$$

To derive expressions for the beam displacement, we must relate stress, described by Eq. (3.21), to strain. This is accomplished through the use of the strain-displacement relations and Hooke's law:

$$\frac{\partial u}{\partial x} = -\frac{Pxy}{EI}, \quad \frac{\partial v}{\partial y} = \frac{vPxy}{EI} \quad (\text{a, b})$$

$$\frac{\partial u}{\partial y} + \frac{\partial v}{\partial x} = \frac{2(1+\nu)\tau_{xy}}{E} = -\frac{(1+\nu)P}{EI}(h^2 - y^2) \quad (\text{c})$$

Integration of Eqs. (a) and (b) yields

$$u = -\frac{Px^2y}{2EI} + u_1(y) \quad (\text{d})$$

$$v = \frac{vPxy^2}{2EI} + v_1(x) \quad (\text{e})$$

Differentiating Eqs. (d) and (e) with respect to y and x , respectively, and substituting into Eq. (c), we have

$$\frac{du_1}{dy} - \frac{P}{2EI}(2+\nu)y^2 = -\frac{dv_1}{dx} + \frac{P}{2EI}x^2 - \frac{(1+\nu)Ph^2}{EI}$$

In this expression, note that the left and right sides depend only on y and x , respectively. These variables are independent of each other, so we conclude that the equation can be valid only if each side is equal to the same constant:

$$\frac{du_1}{dy} - \frac{P}{2EI}(2+\nu)y^2 = a_1, \quad \frac{dv_1}{dx} - \frac{Px^2}{2EI} + \frac{(1+\nu)Ph^2}{EI} = -a_1$$

These are integrated to yield

$$u_1(y) = \frac{P}{6EI}(2+\nu)y^3 + a_1y + a_2$$

$$v_1(x) = \frac{Px^3}{6EI} - \frac{(1+\nu)Pxh^2}{EI} - a_1x + a_3$$

in which a_2 and a_3 are constants of integration. The displacements may now be written

$$u = -\frac{Px^2y}{2EI} + \frac{P}{6EI}(2+\nu)y^3 + a_1y + a_2 \quad (5.20a)$$

$$v = \frac{\nu Pxy^2}{2EI} + \frac{Px^3}{6EI} - \frac{(1+\nu)Pxh^2}{EI} - a_1x + a_2 \quad (5.20b)$$

The constants a_1 , a_2 , and a_3 depend on known conditions. If, for example, the situation at the fixed end is such that

$$\frac{\partial u}{\partial x} = 0, \quad v = u = 0 \quad \text{at } x = L, y = 0$$

then, from Eqs. (5.20),

$$a_1 = \frac{PL^2}{2EI}, \quad a_2 = 0, \quad a_3 = \frac{PL^3}{3EI} + \frac{PLh^2(1+\nu)}{EI}$$

The beam displacement is therefore

$$u = \frac{P}{2EI}(L^2 - x^2)y + \frac{(2+\nu)Py^3}{6EI} \quad (5.21)$$

$$v = \frac{P}{EI} \left[\frac{x^3}{6} + \frac{L^3}{3} + \frac{x}{2}(\nu y^2 - L^2) + h^2(1+\nu)(L-x) \right] \quad (5.22)$$

On examining these equations, it becomes that u and v do not obey a simple linear relationship with y and x . We conclude that plane sections do not, as assumed in elementary theory, remain plane subsequent to bending.

5.4.1 Comparison of the Results with the Elementary Theory Results

The vertical displacement of the beam axis is obtained by substituting $y = 0$ into Eq. (5.22):

$$(v)_{y=0} = \frac{Px^3}{6EI} - \frac{PL^2x}{2EI} + \frac{PL^3}{3EI} + \frac{Ph^2(1+\nu)}{EI}(L-x) \quad (5.23)$$

Introducing this relation into Eq. (5.7), the radius of curvature is given by

$$\frac{1}{r_x} \approx \frac{Px}{EI} = \frac{M}{EI}$$

provided that dv/dx is a small quantity. Once again, we obtain Eq. (5.9a), the beam curvature–moment relationship of elementary bending theory.

It is also a simple matter to compare the total vertical deflection at the free end ($x = 0$) with the deflection derived in elementary theory. Substituting $x = 0$ into Eq. (5.23), the total deflection is

$$(v)_{x=y=0} = \frac{PL^3}{3EI} + \frac{Ph^2(1+\nu)L}{EI} = \frac{PL^3}{3EI} + \frac{Ph^2L}{2GI} \quad (5.24)$$

where the deflection associated with shear is clearly $Ph^2L/2GI = 3PL/2GA$. The ratio of the shear deflection to the bending deflection at $x = 0$ provides a measure of beam slenderness:

$$\frac{Ph^2L/2GI}{PL^3/3EI} = \frac{3}{2} \frac{h^2E}{L^2G} = \frac{3}{4}(1+\nu) \left(\frac{2h}{L}\right)^2 \approx \left(\frac{2h}{L}\right)^2$$

If, for example, $L = 10(2h)$, the preceding quotient is only $\frac{1}{100}$. For a slender beam, $2h \ll L$ and the deflection is mainly due to bending. In contrast, in cases involving vibration at higher modes, and in wave propagation, the effect of shear is of great importance in slender as well as in other beams.

In the case of *wide beams* ($t \gg 2h$), Eq. (5.24) must be modified by replacing E and ν as indicated in Table 3.1.

5.5 BENDING OF A SIMPLY SUPPORTED NARROW BEAM

In this section, we consider the stress distribution in a narrow beam of thickness t and depth $2h$ subjected to a uniformly distributed loading (Fig. 5.6). The situation described here is one of plane stress, subject to the following boundary conditions, consistent with the origin of an x, y coordinate system located at midspan and midheight of the beam, as shown:

$$(\tau_{xy})_{y=\pm h} = 0, \quad (\sigma_y)_{y=+h} = 0, \quad (\sigma_y)_{y=-h} = -p/t \quad (\text{a})$$

Since no longitudinal load is applied at the ends, it would appear reasonable to state that $\sigma_x = 0$ at $x = \pm L$. However, this boundary condition leads to a complicated solution, and a less severe statement is used instead:

$$\int_{-h}^h \sigma_x t dy = 0 \quad (\text{b})$$

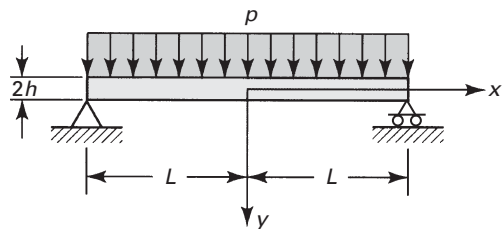
The corresponding condition for bending couples at $x = \pm L$ is

$$\int_{-h}^h \sigma_x ty dy = 0 \quad (\text{c})$$

For y equilibrium, it is required that

$$\int_{-h}^h \tau_{xy} t dy = \pm pL \quad x = \pm L \quad (\text{d})$$

FIGURE 5.6. *Bending of a simply supported beam with a uniform load.*



5.5.1 Use of Stress Functions

The problem is treated by superimposing the solutions Φ_2 , Φ_3 , and Φ_5 (Section 3.6) with

$$c_2 = b_2 = a_3 = c_3 = a_5 = b_5 = c_5 = e_5 = 0$$

We then have

$$\Phi = \Phi_2 + \Phi_3 + \Phi_5 = \frac{a_2}{2}x^2 + \frac{b_3}{2}x^2y + \frac{d_3}{6}y^3 + \frac{d_5}{6}x^2y^3 - \frac{2d_5}{60}y^5$$

The stresses are

$$\begin{aligned}\sigma_x &= d_3y + d_5\left(x^2y - \frac{2}{3}y^3\right) \\ \sigma_y &= a_2 + b_3y + \frac{d_5}{3}y^3 \\ \tau_{xy} &= -b_3x - d_5xy^2\end{aligned}\tag{e}$$

The conditions (a) are

$$\begin{aligned}-b_3 - d_5h^2 &= 0 \\ a_2 + b_3h + \frac{d_5}{3}h^3 &= 0 \\ a_2 - b_3h - \frac{d_5}{3}h^3 &= -\frac{p}{t}\end{aligned}$$

and the solution is

$$a_2 = -\frac{p}{2t}, \quad b_3 = \frac{3p}{4th}, \quad d_5 = -\frac{3p}{4th^3}$$

The constant d_3 is obtained from condition (c) as follows:

$$\int_{-h}^h \left[d_3y + d_5\left(L^2y - \frac{2}{3}y^3\right) \right] yt \, dy = 0$$

or

$$d_3 = -d_5\left(L^2 - \frac{2}{5}h^2\right) = \frac{3p}{4th}\left(\frac{L^2}{h^2} - \frac{2}{5}\right)$$

Expressions (e), together with the values obtained for the constants, also fulfill conditions (b) and (d).

The state of stress is thus represented by

$$\sigma_x = \frac{py}{2I}(L^2 - x^2) + \frac{py}{I}\left(\frac{y^2}{3} - \frac{h^2}{5}\right)\tag{5.25a}$$

$$\sigma_y = \frac{-p}{2I}\left(\frac{y^3}{3} - h^2y + \frac{2h^3}{3}\right)\tag{5.25b}$$

$$\tau_{xy} = \frac{-px}{2I}(h^2 - y^2)\tag{5.25c}$$

where $I = \frac{2}{3}th^3$ is the area moment of inertia taken about a line through the centroid, parallel to the z axis. Although the solutions given by Eqs. (5.25) satisfy the equations of elasticity and the boundary conditions, they are not exact. We can see this by substituting $x = \pm L$ into Eq. (5.25a) to obtain the following expression for the normal distributed forces per unit area at the ends:

$$p_x = \frac{py}{I} \left(\frac{y^2}{3} - \frac{h^2}{5} \right)$$

This state cannot exist, as no forces act at the ends. From Saint-Venant's principle, however, we may conclude that the solutions do predict the correct stresses throughout the beam, except near the supports.

5.5.2 Comparison of the Results with the Elementary Theory Results

Recall that the longitudinal normal stress derived from elementary beam theory is $\sigma_x = -My/I$; this is equivalent to the first term of Eq. (5.25a). The second term is then the difference between the longitudinal stress results given by the two approaches. To gauge the magnitude of the deviation, consider the ratio of the second term of Eq. (5.25a) to the result of elementary theory at $x = 0$. At this point, the bending moment is a maximum. Substituting $y = h$ for the condition of maximum stress, we obtain

$$\frac{\Delta\sigma_x}{(\sigma_x)_{\text{elem. theory}}} = \frac{(ph/I)(h^2/3 - h^2/5)}{phL^2/2I} = \frac{4}{15} \left(\frac{h}{L} \right)^2$$

For a beam of length 10 times its depth, this ratio is small, $\frac{1}{1500}$. For beams of ordinary proportions, we can conclude that elementary theory provides a result of sufficient accuracy for σ_x . On the one hand, for σ_y , this stress is not found in the elementary theory. On the other hand, the result for τ_{xy} is the same as that yielded by elementary beam theory.

The displacement of the beam may be determined in a manner similar to that described for a cantilever beam (Section 5.4).

Part B: Approximate Solutions

5.6 ELEMENTARY THEORY OF BENDING

We may conclude, on the basis of the previous sections, that exact solutions are difficult to obtain. We also observed that for a slender beam, the results of the exact theory do not differ markedly from those found with the mechanics of materials or elementary approach provided that solutions close to the ends are not required. The bending deflection is very much larger than the shear deflection, so the stress associated with the former predominates. As a consequence, the normal strain ϵ_y resulting from transverse loading may be neglected.

Because it is more easily applied, the elementary approach is usually preferred in engineering practice. The exact and elementary theories should be regarded as complementary—rather than competitive—approaches, enabling the analyst to obtain the degree of accuracy required in the context of the specific problem at hand.

5.6.1 Assumptions of Elementary Theory

The basic presuppositions of the elementary theory [Ref. 5.2], for a slender beam whose cross section is symmetrical about the vertical plane of loading, are

$$\varepsilon_y = \frac{\partial v}{\partial y} = 0, \quad \gamma_{xy} = \frac{\partial u}{\partial y} + \frac{\partial v}{\partial x} = 0 \quad (5.26)$$

$$\varepsilon_x = \frac{\sigma_x}{E} \quad (\text{independent of } z)$$

$$\varepsilon_z = 0, \quad \gamma_{yz} = \gamma_{xz} = 0 \quad (5.27)$$

The first equation of Eqs. (5.26) is equivalent to the assertion $v = v(x)$. Thus, all points in a beam at a given longitudinal location x experience identical deformation. The second equation of Eqs. (5.26), together with $v = v(x)$, yields, after integration,

$$u = -y \frac{dv}{dx} + u_0(x) \quad (\text{a})$$

The third equation of Eqs. (5.26) and Eqs. (5.27) imply that the beam is considered *narrow*, and we have a case of *plane stress*.

At $y = 0$, the bending deformation should vanish. Referring to Eq. (a), it is clear that $u_0(x)$ must represent axial deformation. The term dv/dx is the *slope* θ of the beam axis, as shown in Fig. 5.7a, and is very much smaller than unity. Therefore,

$$u = -y \frac{dv}{dx} = -y\theta$$

The slope is *positive* when *clockwise*, provided that the x and y axes have the directions shown. Since u is a linear function of y , this equation restates the kinematic hypothesis of the elementary theory of bending: *Plane sections perpendicular to the longitudinal axis of the beam remain plane subsequent to bending*. This assumption is confirmed by the exact theory *only* in the case of *pure bending*.

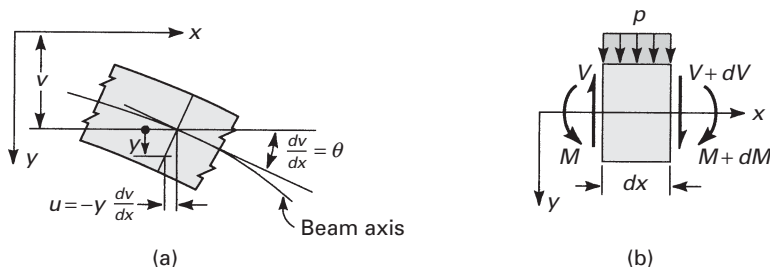


FIGURE 5.7. (a) Longitudinal displacements in a beam due to rotation of a plane section; (b) element between adjoining sections of a beam.

5.6.2 Method of Integration

In the next section, we obtain the stress distribution in a beam according to the elementary theory. We now derive some useful relations involving the shear force V , the bending moment M , the load per unit length p , the slope θ , and the *deflection*. Consider a beam element of length dx subjected to a distributed loading (Fig. 5.7b). Since dx is small, we omit the variation in the load per unit length p . In the free-body diagram, all the forces and the moments are positive. The shear force obeys the sign convention discussed in Section 1.4, while the bending moment is in agreement with the convention adopted in Section 5.2.

In general, the shear force and bending moment vary with the distance x , such that these quantities will have different values on each face of the element. The increments in shear force and bending moment are denoted by dV and dM , respectively. The equilibrium of forces in the vertical direction is governed by $V - (V + dV) - p dx = 0$ or

$$\frac{dV}{dx} = -p \quad (5.28)$$

That is, the rate of change of shear force with respect to x is equal to the algebraic value of the distributed loading. Equilibrium of the moments about a z axis through the left end of the element, neglecting the higher-order infinitesimals, leads to

$$\frac{dM}{dx} = -V \quad (5.29)$$

This relation states that the rate of change of bending moment is equal to the algebraic value of the shear force—a relation that is valid only if a distributed load or no load acts on the beam segment. Combining Eqs. (5.28) and (5.29), we have

$$\frac{d^2M}{dx^2} = p \quad (5.30)$$

The basic equation of bending of a beam, Eq. (5.10), combined with Eq. (5.30), may now be written as

$$\frac{d^2}{dx^2} \left(EI \frac{d^2v}{dx^2} \right) = p \quad (5.31)$$

For a beam of *constant* flexural rigidity EI , the beam equations derived here may be expressed as

$$\begin{aligned} EI \frac{d^4v}{dx^4} &= EIv^{IV} = p \\ EI \frac{d^3v}{dx^3} &= EIv''' = -V \\ EI \frac{d^2v}{dx^2} &= EIv'' = M \\ EI \frac{dv}{dx} &= EIv' = \int M dx \end{aligned} \quad (5.32)$$

These relationships also apply to *wide beams* provided that we substitute $E/(1-\nu^2)$ for E (Table 3.1).

In many problems of practical importance, the deflection due to transverse loading of a beam may be obtained through successive integration of the beam equation:

$$\begin{aligned}
 EIv^{IV} &= p \\
 EIv''' &= \int_0^x p \, dx + c_1 \\
 EIv'' &= \int_0^x dx \int_0^x p \, dx + c_1x + c_2 \\
 EIv' &= \int_0^x dx \int_0^x dx \int_0^x p \, dx + \frac{1}{2}c_1x^2 + c_2x + c_3 \\
 EIv &= \int_0^x dx \int_0^x dx \int_0^x dx \int_0^x p \, dx + \frac{1}{6}c_1x^3 + \frac{1}{2}c_2x^2 + c_3x + c_4
 \end{aligned}
 \tag{5.33}$$

Alternatively, we could begin with $EIv'' = M(x)$ and integrate twice to obtain

$$EIv = \int_0^x dx \int_0^x M \, dx + c_3x + c_4 \tag{5.34}$$

In either case, the constants c_1 , c_2 , c_3 and c_4 , which correspond to the homogeneous solution of the differential equations, may be evaluated from the boundary conditions. The constants c_1 , c_2 , c_3/EI , and c_4/EI represent the values at the origin of V , M , θ , and v , respectively. In the method of successive integration, there is no need to distinguish between statically determinate and statically indeterminate systems (Section 5.11), because the equilibrium equations represent only two of the boundary conditions (on the first two integrals), and because the *total* number of boundary conditions is always equal to the total number of unknowns.

EXAMPLE 5.2 Displacements of a Cantilever Beam

A cantilever beam AB of length L and constant flexural rigidity EI carries a moment M_o at its free end A (Fig. 5.8a). Derive the equation of the deflection curve and determine the slope and deflection at A .

Solution From the free-body diagram of Fig. 5.8b, observe that the bending moment is $+M_o$ throughout the beam. Thus, the third of Eqs. (5.32) becomes

$$EIv'' = M_o$$

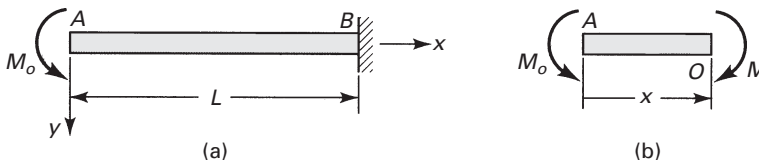


FIGURE 5.8. Example 5.2. (a) A cantilever beam is subjected to moment at its free end; (b) free-body diagram of part AO .

Integration yields

$$EIv' = M_o x + c_1$$

The constant of integration c_1 can be found from the condition that the slope is zero at the support; therefore, we have $v'(L) = 0$ from which $c_1 = -M_o L$. The slope is then

$$v' = \frac{M_o}{EI}(x - L) \quad (5.35)$$

Integrating, we obtain

$$v = \frac{M_o}{2EI}(x^2 - 2Lx) + c_2$$

The boundary condition on the deflection at the support is $v(L) = 0$, which yields $c_2 = M_o L^2 / 2EI$. The equation of the deflection curve is thus a parabola:

$$v = \frac{M_o}{2EI}(L^2 + x^2 - 2Lx) \quad (5.36)$$

However, every element of the beam experiences the same moments and deformation. The deflection curve should, therefore, be part of a circle. This inconsistency results from the use of an approximation for the curvature, Eq. (5.7). The error is very small, however, when the deformation v is small [Ref. 5.1].

The slope and deflection at A are readily found by letting $x = 0$ in Eqs. (5.35) and (5.36):

$$\theta_A = -\frac{M_o L}{EI}, \quad v_A = \frac{M_o L^2}{2EI} \quad (5.37)$$

The minus sign indicates that the angle of rotation is counterclockwise (Fig. 5.8a).

5.7 NORMAL AND SHEAR STRESSES

When a beam is bent by transverse loads, usually both a bending moment M and a shear force V act on each cross section. The distribution of the normal stress associated with the bending moment is given by the *flexure formula*, Eq. (5.4):

$$\sigma_x = -\frac{My}{I} \quad (5.38)$$

where M and I are taken with respect to the z axis (Fig. 5.7).

In accordance with the assumptions of elementary bending, Eqs. (5.26) and (5.27), we omit the contribution of the shear strains to beam deformation in these calculations. However, shear stresses do exist, and the shearing forces are the resultant of the stresses.

The shearing stress τ_{xy} acting at section mn , which is assumed to be uniformly distributed over the area $b \cdot dx$, can be determined on the basis of equilibrium of forces acting on the shaded part of the beam element (Fig. 5.9). Here b is the width of the beam a distance y_1 from the neutral axis, and dx is the length of the element. The distribution of normal stresses produced by M and $M + dM$ is indicated in the figure. The normal force distributed over the left face mr on the shaded area A^* is equal to

$$\int_{-b/2}^{b/2} \int_{y_1}^{h_1} \sigma_x dy dz = \int_{A^*} -\frac{My}{I} dA$$

Similarly, an expression for the normal force on the right face ns may be written in terms of $M + dM$. The equilibrium of x -directed forces acting on the beam element is governed by

$$-\int_{A^*} \frac{(M + dM)y}{I} dA - \int_{A^*} -\frac{My}{I} dA = \tau_{xy} b dx$$

from which we have

$$\tau_{xy} = -\frac{1}{Ib} \int_{A^*} \frac{dM}{dx} y dA$$

After substituting in Eq. (5.29), we obtain the *shear formula* (also called the *shear stress formula*) for beams:

$$\tau_{xy} = \frac{V}{Ib} \int_{A^*} y dA = \frac{VQ}{Ib} \quad (5.39)$$

The integral represented by Q is the *first moment of the shaded area A^** with respect to the neutral axis z :

$$Q = \int_{A^*} y dA = A^* \bar{y} \quad (5.40)$$

By definition, \bar{y} is the distance from the neutral axis to the centroid of A^* . In the case of sections of regular geometry, $A^* \bar{y}$ provides a convenient means of calculating Q . The shear force acting across the width of the beam per unit length

$$q = \tau_{xy} b = \frac{VQ}{I} \quad (a)$$

is called the *shear flow*.

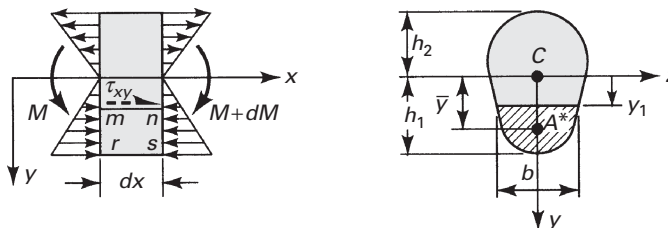


FIGURE 5.9. (a) Beam segment for analyzing shear stress; (b) cross section of beam.

5.7.1 Rectangular Cross Section

In the case of a *rectangular cross section* of width b and depth $2h$, the shear stress at y_1 is

$$\tau_{xy} = \frac{V}{Ib} \int_{-b/2}^{b/2} \int_{y_1}^h y \, dy \, dz = \frac{V}{2I} (h^2 - y_1^2) \quad (5.41)$$

This equation shows that the shear stress varies parabolically with y_1 . It is zero when $y_1 = \pm h$, and has its maximum value at the neutral axis:

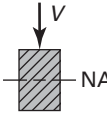
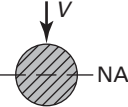
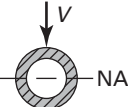
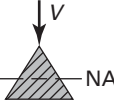
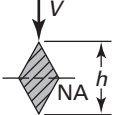
$$\tau_{\max} = \frac{Vh^2}{2I} = \frac{3V}{2A} \quad (5.42)$$

where $A = 2bh$ is the area of the rectangular cross section. Note that the maximum shear stress (either horizontal or vertical: $\tau_{xy} = \tau_{yx}$) is 1.5 times larger than the average shear stress V/A . As observed in Section 5.4, for a *thin* rectangular beam, Eq. (5.42) is the exact distribution of shear stress. More generally, for wide rectangular sections and for other sections, Eq. (5.39) yields only approximate values of the shearing stress.

5.7.2 Various Cross Sections

Because the shear formula for beams is based on the flexure formula, the limitations of the bending formula apply when it is used. Problems involving various types of cross sections can be solved by following procedures identical to that for rectangular sections. Table 5.1

TABLE 5.1. *Maximum Shearing Stress for Some Typical Beam Cross-Sectional Forms*

Cross Section	Maximum Shearing Stress	Location
Rectangle 	$\tau_{\max} = \frac{3V}{2A}$	NA
Circle 	$\tau_{\max} = \frac{4V}{3A}$	NA
Hollow Circle 	$\tau_{\max} = 2\frac{V}{A}$	NA
Triangle 	$\tau_{\max} = \frac{3V}{2A}$	Halfway between top and bottom
Diamond 	$\tau_{\max} = \frac{9V}{8A}$	At $h/8$ above and below the NA

Notes: A , cross-sectional area; V , transverse shear force; NA, the neutral axis.

shows some typical cases. Observe that shear stress can always be expressed as a constant times the average shear stress (P/A), where the constant is a function of the cross-sectional form. Nevertheless, the maximum shear stress does not always occur at the neutral axis. For instance, in the case of a cross section having nonparallel sides, such as a triangular section, the maximum value of Q/b (and thus τ_{xy}) occurs at midheight, $h/2$, while the neutral axis is located at a distance $h/3$ from the base.

The following examples illustrate the application of the normal and shear stress formulas.

EXAMPLE 5.3 Stresses in a Beam of T-Shaped Cross Section

A simply supported beam of length L carries a concentrated load P (Fig. 5.10a). *Find:* (a) The maximum shear stress, the shear flow q_j , and the shear stress T_j in the joint between the flange and the web; (b) the maximum bending stress. *Given:* $P = 5$ kN and $L = 4$ m.

Solution The distance \bar{y} from the Z axis to the centroid is obtained as follows (Fig. 5.10a):

$$\bar{y} = \frac{A_1\bar{y}_1 + A_2\bar{y}_2}{A_1 + A_2} = \frac{20(60)70 + 60(20)30}{20(60) + 60(20)} = 50 \text{ mm}$$

The moment of inertia I about the NA is determined by the parallel axis theorem:

$$I = \frac{1}{12}(60)(20)^3 + 20(60)(20)^2 + \frac{1}{12}(20)(60)^3 + 20(60)(20)^2 = 136 \times 10^4 \text{ mm}^4$$

The shear and moment diagrams (Figs. 5.10b and c) are sketched by applying the method of sections.

- a. The maximum shearing stress in the beam takes place at the NA on the cross section supporting the largest shear force V . Consequently, $Q_{\text{NA}} = 50(20)25 = 25 \times 10^3 \text{ mm}^3$. The shear force equals 2.5 kN on all cross sections of the beam (Fig. 5.10b). Thus,

$$\tau_{\text{max}} = \frac{V_{\text{max}} Q_{\text{NA}}}{Ib} = \frac{2.5 \times 10^3 (25 \times 10^{-6})}{136 \times 10^{-8} (0.02)} = 2.3 \text{ MPa}$$

The first moment of the area of the flange about the NA is

$$Q_f = 20(60)20 = 24 \times 10^3 \text{ mm}^3.$$

Shear flow and shear stress in the joint are

$$q_j = \frac{VQ_f}{I} = \frac{2.5 \times 10^3 (24 \times 10^{-6})}{136 \times 10^{-8}} = 44.1 \text{ kN/m}$$

and $\tau_j = q_j/b = 44.1/0.02 = 2.205 \text{ MPa}$.

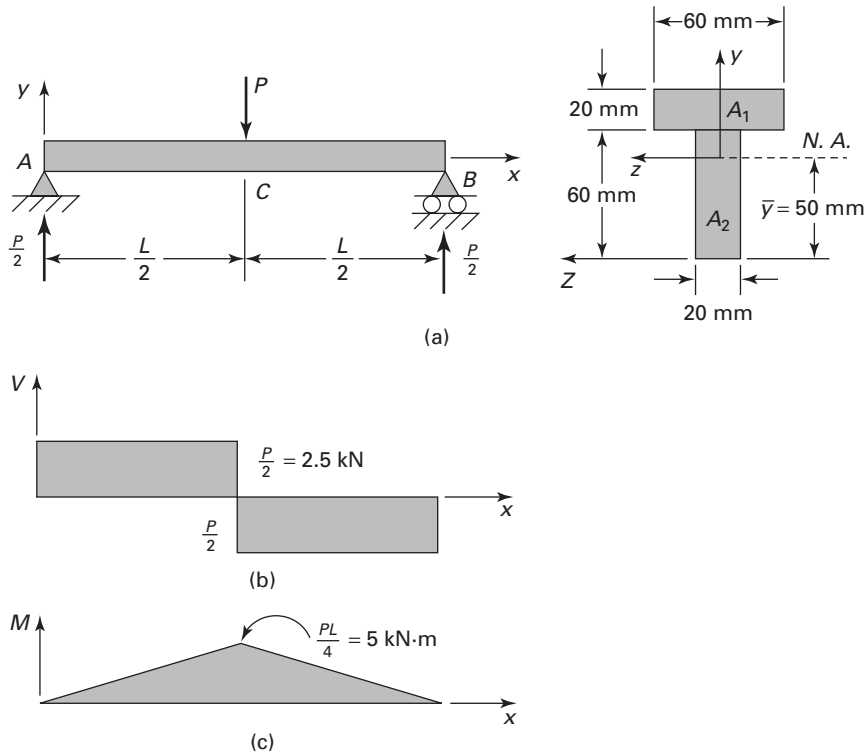


FIGURE 5.10. Example 5.3. (a) Load diagram and beam cross section; (b) shear diagram; (c) moment diagram.

b. The largest moment takes place at midspan (Fig. 5.10c). Equation (5.39) is therefore

$$\sigma_{\max} = \frac{Mc}{I} = \frac{5 \times 10^3 (0.05)}{136 \times 10^{-8}} = 183.8 \text{ MPa}$$

EXAMPLE 5.4 Shear Stresses in a Flanged Beam

A cantilever wide-flange beam is loaded by a force P at the free end acting through the centroid of the section. The beam is of constant thickness t (Fig. 5.11a). Determine the shear stress distribution in the section.

Solution The vertical shear force at every section is P . It is assumed that the shear stress τ_{xy} is uniformly distributed over the web thickness. Then, in the web, for $0 \leq y_1 \leq h_1$ and applying Eq. (5.39),

$$\tau_{xy} = \frac{V}{Ib} A^* \bar{y} = \frac{P}{I} \left[b(h - h_1) \left(h_1 + \frac{h - h_1}{2} \right) + t(h_1 - y_1) \left(y_1 + \frac{h_1 - y_1}{2} \right) \right]$$

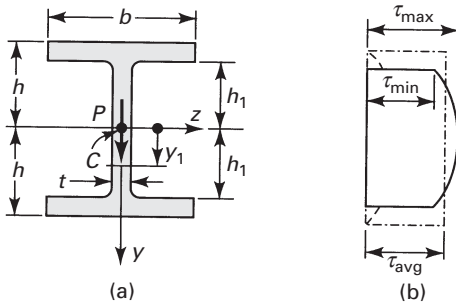


FIGURE 5.11. Example 5.4. (a) Cross section of a wide-flange beam; (b) shearing stress distribution.

This equation may be written as

$$\tau_{xy} = \frac{P}{2It} \left[b(h^2 - h_1^2) + t(h_1^2 - y_1^2) \right] \quad (b)$$

The shearing stress thus varies parabolically in the web (Fig. 5.11b). The extreme values of τ_{xy} found at $y_1 = 0$ and $y_1 = \pm h_1$ are, from Eq. (b), as follows:

$$\tau_{\max} = \frac{P}{2It} (bh^2 - bh_1^2 + th_1^2), \quad \tau_{\min} = \frac{Pb}{2It} (h^2 - h_1^2)$$

Usually $t \gg b$ so that the maximum and minimum stresses do not differ appreciably, as is seen in the figure. Similarly, the shear stress in the flange, for $h_1 < y_1 \leq h$, is

$$\tau_{xz} = \frac{P}{Ib} \left[b(h - y_1) \left(y_1 + \frac{h - y_1}{2} \right) \right] = \frac{P}{2I} (h^2 - y_1^2) \quad (c)$$

This is the parabolic equation for the variation of stress in the flange, shown by the dashed lines in Fig. 5.11b.

Comments Clearly, for a *thin* flange, the shear stress is very small as compared with the shear stress in the web. As a consequence, the approximate *average* value of *shear stress* in the beam may be found by dividing P by the web cross section, with the web height assumed to be equal to the beam's overall height: $\tau_{\text{avg}} = P/2$. This result is indicated by the dotted lines in Fig. 5.11b.

The distribution of stress given by Eq. (c) is *fictional*, because the inner planes of the flanges must be free of shearing stress, as they are load-free boundaries of the beam. This contradiction cannot be resolved by the elementary theory; instead, the theory of elasticity must be applied to obtain the correct solution. Fortunately, this defect of the shearing stress formula does not lead to serious error since, as pointed out previously, the web carries almost all the shear force. To reduce the stress concentration at the juncture of the web and the flange, the sharp corners should be rounded.

EXAMPLE 5.5 Beam of Circular Cross Section

A cantilever beam of circular cross section supports a concentrated load P at its free end (Fig. 5.12a). The shear force V in this beam is constant and equal to the magnitude of the load $P = V$. Find the maximum shearing stresses (a) in a solid cross section and (b) in a hollow cross section.

Assumptions: All shear stresses do not act parallel to the y axis. At a point such as a or b on the boundary of the cross section, the shear stress τ must act parallel to the boundary. The shear stresses at line ab across the cross section are not parallel to the y axis and cannot be determined by the shear formula, $\tau = VQ/Ib$. The maximum shear stresses occur along the neutral axis z , are uniformly distributed, and act parallel to the y axis. These stresses are within approximately 5% of their true value [Ref. 5.1].

Solution

a. Solid Cross Section (Fig. 5.12b). The shear formula may be used to calculate, with reasonable accuracy, the shear stresses at the neutral axis. The area properties for a circular cross section of radius c (see Table C.1) are

$$I = \frac{\pi c^4}{4} \quad Q = A^* \bar{y} = \frac{\pi c^2}{2} \left(\frac{4c}{3\pi} \right) = \frac{2c^2}{3} \quad (d)$$

and $b = 2c$. The maximum shear stress is thus

$$\tau_{\max} = \frac{VQ}{Ib} = \frac{4V}{3\pi c^2} = \frac{4V}{3A} \quad (e)$$

where A is the cross-sectional area of the beam.

Comment This result shows that the largest shear stress in a circular beam is $4/3$ times the average shear stress $\tau_{\text{avg}} = V/A$.

b. Hollow Circular Cross Section (Fig. 5.11c). Equation (5.43) applies with equal rigor to circular tubes, since the same assumptions stated in the foregoing are valid. But in this case, by Eq. (C.3), we have

$$Q = \frac{2}{3}(c_2^3 - c_1^3), \quad b = 2(c_2 - c_1), \quad A = \pi(c_2^2 - c_1^2)$$

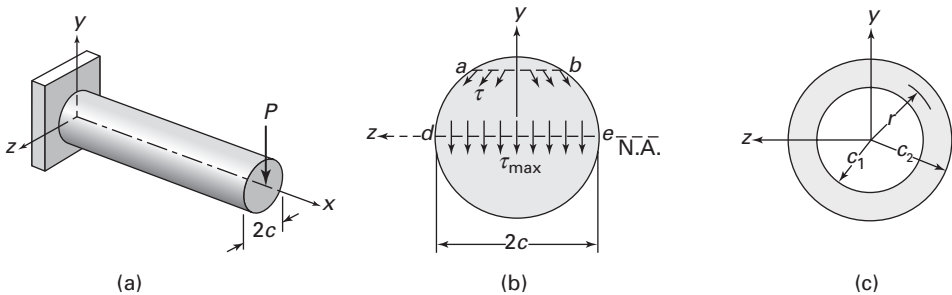


FIGURE 5.12. Example 5.5. (a) A cantilever beam under a load P ; (b) shear stress distribution on a circular cross section; (c) hollow circular cross section.

and

$$I = \frac{\pi}{4}(c_2^4 - c_1^4)$$

So, the maximum shear stress may be written in the following form:

$$\tau_{\max} = \frac{VQ}{Ib} = \frac{4V}{3A} \frac{c_2^2 + c_2c_1 + c_1^2}{c_2^2 + c_1^2} \quad (\text{f})$$

Comment Note that for $c_1 = 0$, Eq. (e) reduces to Eq. (5.43) for a solid circular beam, as expected. In the special case of a *thin-walled tube*, we have $r/t > 10$, where r and t represent the mean radius and thickness, respectively. As a theoretical limiting case, setting $c_2 = c_1 = r$ means that Eq. (e) results in $\tau_{\max} = 2V/A$.

5.7.3 Beam of Constant Strength

When a beam is stressed to a constant permissible stress, σ_{all} throughout, then clearly the beam material is used to its greatest capacity. For a given material, such a design is of minimum weight. At any cross section, the required section modulus S is defined as

$$s = \frac{M}{\sigma_{\text{all}}} \quad (5.43)$$

where M presents the bending moment on an arbitrary section. Tapered beams designed in this way are called *beams of constant strength*. Ultimately, the shear stress at those beam locations where the moment is small controls the design.

Examples of beams with uniform strength include leaf springs and certain cast machine elements. For a structural member, fabrication and design constraints make it impractical to produce a beam of constant stress. Hence, welded cover plates are often used for parts of prismatic beams where the moment is large—for instance, in a bridge girder. When the angle between the sides of a tapered beam is small, the flexure formula allows for little error. On the contrary, the results found by applying the shear stress formula may not be accurate enough for nonprismatic beams. Often, a modified form of this formula is used for design purposes. The exact distribution in a rectangular wedge is found by applying the theory of elasticity (Section 3.10).

EXAMPLE 5.6 Design of a Uniform Strength Beam

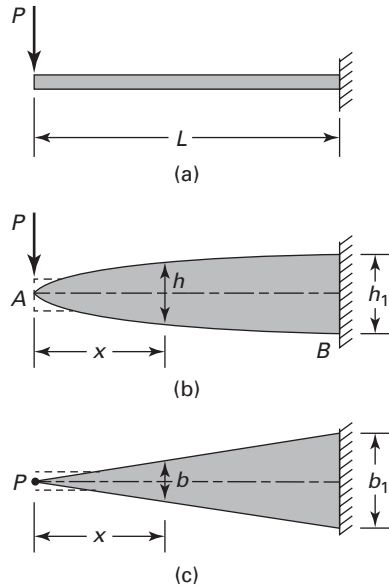
A cantilever beam of constant strength and rectangular cross section is to carry a concentrated load P at the free end (Fig. 5.13a). Find the required cross-sectional area for two cases: (a) the width b is constant; (b) the height h is constant.

Solution

a. At a distance x from A , $M = Px$ and $S = bh^2/6$. By applying Eq. (5.43), we have

$$\frac{bh^2}{6} = \frac{Px}{\sigma_{\text{all}}} \quad (\text{g})$$

FIGURE 5.13. Example 5.6. (a) Constant-strength cantilever; (b) side view; (c) top view.



Likewise, at a fixed end ($x = L$ and $h = h_1$),

$$\frac{bh_1^2}{6} = \frac{PL}{\sigma_{\text{all}}}$$

Dividing Eq. (g) by the preceding relationship leads to

$$h = h_1 \sqrt{\frac{x}{L}} \quad (\text{h})$$

Thus, the depth of the beam varies parabolically from the free end (Fig. 5.13b).

b. Equation (g) now gives

$$b = \left(\frac{6P}{h^2 \sigma_{\text{all}}} \right) x = \frac{b_1}{L} x \quad (\text{i})$$

Comments In Eq. (i), the term in parentheses represents a constant and is set equal to b_1/L ; hence, when $x = L$, the width is b_1 (Fig. 5.13c). Clearly, the cross section of the beam near end A must be designed to resist the shear force, as depicted by the dashed lines in the figure.

5.8 EFFECT OF TRANSVERSE NORMAL STRESS

When a beam is subjected to a transverse load, a *transverse normal stress* is created. According to Eq. (5.26), this stress is not related to the normal strain ϵ_y , so it cannot be determined using Hooke's law. However, an expression for the average transverse normal stress can be obtained from the *equilibrium requirement* of force balance along the axis of

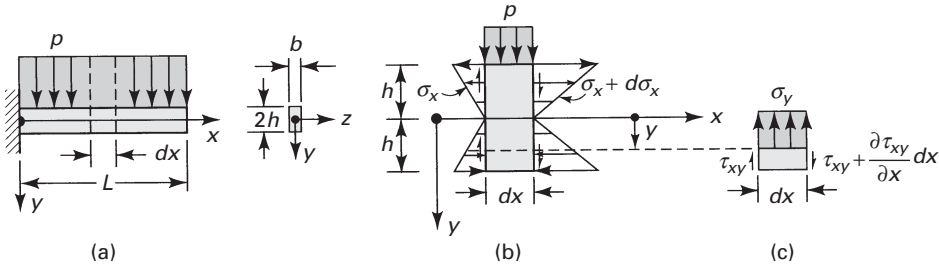


FIGURE 5.14. (a) Uniformly loaded cantilever beam of rectangular cross section; (b) free-body diagram of a segment; (c) stresses in a beam element.

the beam. For this purpose, a procedure is used similar to that employed for determining the shear stress in Section 5.7.

Consider, for example, a rectangular cantilever beam of width b and depth $2h$ subject to a uniform load of intensity p (Fig. 5.14a). The free-body diagram of an isolated beam segment of length dx is shown in Fig. 5.14b. Passing a horizontal plane through this segment results in the free-body diagram of Fig. 5.14c, for which the condition of statics $\Sigma F_y = 0$ yields

$$\sigma_y \cdot b dx = \int_{-b/2}^{b/2} \int_y^h \frac{\partial \tau_{xy}}{\partial x} dx \cdot dy dz = b \int_y^h \frac{\partial \tau_{xy}}{\partial x} dx dy \quad (a)$$

Here, the shear stress is defined by Eq. (5.41) as

$$\tau_{xy} = \frac{V}{2I} (h^2 - y^2) = \frac{3V}{4bh} \left[1 - \left(\frac{y}{h} \right)^2 \right] \quad (b)$$

After substituting Eqs. (5.28) and (b) into Eq. (a), we have

$$\sigma_y = \int_y^h -\frac{3p}{4bh} \left[1 - \left(\frac{y}{h} \right)^2 \right] dy$$

Integration yields the transverse normal stress in the form

$$\sigma_y = -\frac{p}{b} \left[\frac{1}{2} - \frac{3}{4} \left(\frac{y}{h} \right) + \frac{1}{4} \left(\frac{y}{h} \right)^3 \right] \quad (5.44a)$$

This stress varies as a *cubic parabola*, ranging from $-plb$ at the surface ($y = -h$) where the load acts, to zero at the opposite surface ($y = h$).

The distribution of the bending and the shear stresses in a uniformly loaded cantilever beam (Fig. 5.12a) is determined from Eqs. (5.38) and (b):

$$\begin{aligned} \sigma_x &= -\frac{My}{I} = -\frac{3p}{4bh^3} (L-x)^2 y \\ \tau_{xy} &= \frac{3p}{4bh} (L-x) \left[1 - \left(\frac{y}{h} \right)^2 \right] \end{aligned} \quad (5.44b)$$

The largest values of σ_x , τ_{xy} , and σ_y given by Eqs. (5.44) are

$$\sigma_{x,\max} = \pm \frac{3pL^2}{4bh^2}, \quad \tau_{\max} = \frac{3pL}{4bh}, \quad \sigma_{y,\max} = -\frac{p}{b} \quad (\text{c})$$

To compare the magnitudes of the maximum stresses, consider the following ratios:

$$\frac{\tau_{\max}}{\sigma_{x,\max}} = \frac{h}{L}, \quad \frac{\sigma_{y,\max}}{\sigma_{x,\max}} = \frac{4}{3} \left(\frac{h}{L} \right)^2 \quad (\text{d, e})$$

Because L is much greater than h in most beams ($L \geq 20h$), the shear and the transverse normal stresses will usually be orders of magnitude smaller than the bending stresses. This justification is the rationale for assuming $\gamma_{xy} = 0$ and $\varepsilon_y = 0$ in the technical theory of bending. Note that Eq. (e) results in even smaller values than Eq. (d). Therefore, in practice, it is reasonable to neglect σ_y .

The foregoing conclusion applies, in most cases, to beams of a variety of cross-sectional shapes and under various load configurations. Clearly, the factor of proportionality in Eqs. (d) and (e) will differ for beams of different sectional forms and for different loadings of a given beam.

5.9 COMPOSITE BEAMS

Beams constructed of two or more materials having different moduli of elasticity are referred to as *composite beams*. Examples include multilayer beams made by bonding together multiple sheets, sandwich beams consisting of high-strength material faces separated by a relatively thick layer of low-strength material such as plastic foam, and reinforced concrete beams. The assumptions of the technical theory for a homogeneous beam (Section 5.6) are valid for a beam composed of more than one material.

5.9.1 Transformed Section Method

To analyze composite beams, we will use the common *transformed-section method*. In this technique, the cross sections of several materials are transformed into an *equivalent* cross section of one material on which the resisting forces and the neutral axis are the same as on the original section. The usual flexure formula is then applied to the new section. To illustrate this method, we will use a frequently encountered example: a beam with a symmetrical cross section built of two different materials (Fig. 5.15a).

The *cross sections of the beam remain plane* during bending. Hence, the condition of *geometric compatibility of deformation* is satisfied. It follows that the normal strain ε_x varies linearly with the distance y from the neutral axis of the section; that is, $\varepsilon_x = ky$ (Figs. 5.15a and b). The location of the neutral axis is yet to be determined. Both materials composing the beam are assumed to obey Hooke's law, and their moduli of elasticity are designated as E_1 and E_2 . Then, the *stress-strain relation* gives

$$\sigma_{x1} = E_1 \varepsilon_x = E_1 ky, \quad \sigma_{x2} = E_2 \varepsilon_2 = E_2 ky \quad (\text{5.45a, b})$$

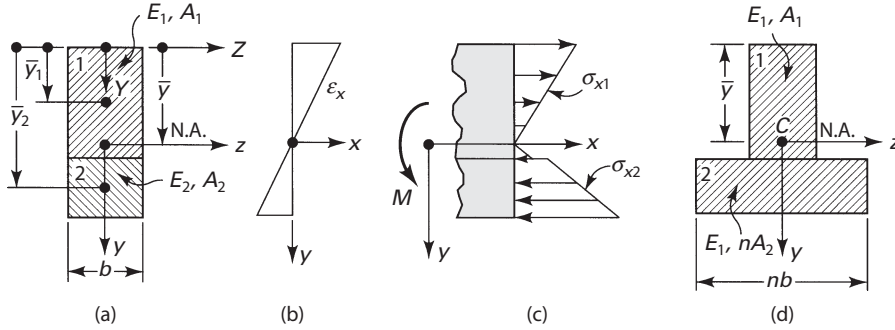


FIGURE 5.15. *Beam composed of two materials: (a) composite cross section; (b) strain distribution; (d) transformed cross section.*

This result is sketched in Fig. 5.13c for the assumption that $E_2 > E_1$. We introduce the notation

$$n = \frac{E_2}{E_1} \quad (5.46)$$

where n is called the *modular ratio*. Note that $n > 1$ in Eq. (5.46). However, this choice is arbitrary; the technique applies as well for $n < 1$.

5.9.2 Equation of Neutral Axis

Referring to the cross section (Figs. 5.15a and c), the *equilibrium equations* $\Sigma F_x = 0$ and $\Sigma M_z = 0$ lead to

$$\int_A \sigma_x dA = \int_{A_1} \sigma_{x1} dA + \int_{A_2} \sigma_{x2} dA = 0 \quad (a)$$

$$-\int_A y \sigma_x dA = -\int_{A_1} y \sigma_{x1} dA - \int_{A_2} y \sigma_{x2} dA = M \quad (b)$$

where A_1 and A_2 denote the cross-sectional areas for materials 1 and 2, respectively. Substituting σ_{x1} , σ_{x2} and n , as given by Eqs. (5.45) and (5.46), into Eq. (a) results in

$$\int_{A_1} y dA + n \int_{A_2} y dA = 0 \quad (5.47)$$

Using the top of the section as a reference (Fig. 5.15a), from Eq. (5.47) with

$$\int_{A_1} (Y - \bar{y}) dA + n \int_{A_2} (Y - \bar{y}) dA = 0$$

or, setting

$$\int_{A_1} Y dA = \bar{y}_1 A_1 \quad \text{and} \quad \int_{A_2} Y dA = \bar{y}_2 A_2$$

we have

$$A_1 \bar{y}_1 - A_1 \bar{y} + n A_2 \bar{y}_2 - n A_2 \bar{y} = 0$$

This expression yields an alternative form of Eq. (5.47):

$$\bar{y} = \frac{A_1\bar{y}_1 + nA_2\bar{y}_2}{A_1 + nA_2} \quad (5.47')$$

Equations (5.47) and (5.47') can be used to locate the *neutral axis* for a beam of two materials. These equations show that the transformed section will have the same neutral axis as the original beam, provided the width of area 2 is changed by a factor n and area 1 remains the same (Fig. 5.15d). Clearly, this widening must be effected in a direction *parallel* to the neutral axis, since the distance \bar{y}_2 to the centroid of area 2 remains unchanged. The new section constructed in this way represents the cross section of a beam made of a homogeneous material with a modulus of elasticity E_1 and with a neutral axis that passes through its *centroid*, as shown in Fig. 5.15d.

5.9.3 Stresses in the Transformed Beam

Similarly, condition (b) together with Eqs. (5.45) and (5.46) leads to

$$M = -kE_1 \left(\int_{A_1} y^2 dA + n \int_{A_2} y^2 dA \right)$$

or

$$M = -kE_1(I_1 + nI_2) = -kE_1I_t \quad (5.48)$$

where I_1 and I_2 are the moments of inertia about the neutral axis of the cross-sectional areas 1 and 2, respectively. Note that

$$I_t = I_1 + nI_2 \quad (5.49)$$

is the moment of inertia of the *entire* transformed area about the neutral axis. From Eq. (5.48), we have

$$k = -\frac{M}{E_1I_t}$$

The *flexure formulas* for a composite beam are obtained by introducing this relation into Eqs. (5.45):

$$\sigma_{x1} = -\frac{My}{I_t}, \quad \sigma_{x2} = -\frac{nMy}{I_t} \quad (5.50)$$

where σ_{x1} and σ_{x2} are the stresses in materials 1 and 2, respectively. Note that when $E_1 = E_2 = E$, Eqs. (5.50) reduce to the flexure formula for a beam of homogeneous material, as expected.

5.9.4 Composite Beams of Multi Materials

The preceding discussion may be extended to include composite beams consisting of *more than* two materials. It is readily shown that for m different materials, Eqs. (5.47'), (5.49), and (5.50) take the forms

$$\bar{y} = \frac{A_1\bar{y}_1 + \sum n_i A_i \bar{y}_i}{A_1 + \sum n_i A_i}, \quad n_i = \frac{E_i}{E_1} \quad (5.51)$$

$$I_t = I_1 + \sum n_i I_i \quad (5.52)$$

$$\sigma_{x1} = -\frac{My}{I_t}, \quad \sigma_{xi} = -\frac{n_i My}{I_t} \quad (5.53)$$

where $i = 2, 3, \dots, m$ denotes the i th material.

The use of the formulas developed in this section is demonstrated in the solutions of the numerical problems in Examples 5.7 and 5.8.

EXAMPLE 5.7 Aluminum-Reinforced Wood Beam

A wood beam with $E_w = 8.75$ GPa, 100 mm wide by 220 mm deep, has an aluminum plate $E_a = 70$ GPa with a net section 80 mm by 20 mm securely fastened to its bottom face, as shown in Fig. 5.16a. Dimensions are given in millimeters. The beam is subjected to a bending moment of $20 \text{ kN} \cdot \text{m}$ around a horizontal axis. Calculate the maximum stresses in both materials (a) using a transformed section of wood and (b) using a transformed section of aluminum.

Solution

- a. The modular ratio is $n = E_a/E_w = 8$. The centroid and the moment of inertia about the neutral axis of the transformed section (Fig. 5.16b) are

$$\bar{y} = \frac{100(220)(110) + 20(640)(230)}{100(220) + 20(640)} = 154.1 \text{ mm}$$

$$I_t = \frac{1}{12}(100)(220)^3 + 100(220)(44.1)^2 + \frac{1}{12}(640)(20)^3 + 640(20)(75.9)^2 \\ = 205.6 \times 10^6 \text{ mm}^4$$

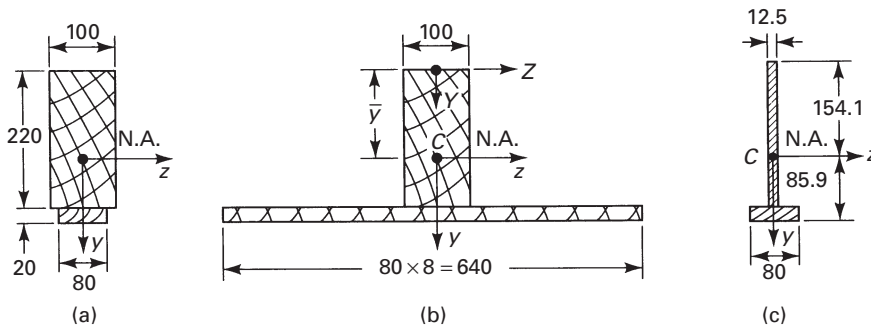


FIGURE 5.16. Example 5.7. (a) Composite cross section; (b) equivalent wood cross section; (c) equivalent aluminum cross section.

In turn, the maximum stresses in the wood and aluminum portions are

$$\sigma_{w,\max} = \frac{Mc}{I_t} = \frac{20 \times 10^3(0.1541)}{2056(10^{-6})} = 15 \text{ MPa}$$

$$\sigma_{a,\max} = \frac{nMc}{I_t} = \frac{8(20 \times 10^3)(0.0859)}{205.6(10^{-6})} = 66.8 \text{ MPa}$$

At the juncture of the two parts,

$$\sigma_{w,\min} = \frac{Mc}{I_t} = \frac{20 \times 10^3(0.0659)}{2056(10^{-6})} = 6.4 \text{ MPa}$$

$$\sigma_{a,\min} = n(\sigma_{w,\min}) = 8(6.4) = 51.2 \text{ MPa}$$

- b. For this case, the modular ratio is $n = E_w/E_a = 1/8$ and the transformed area is shown in Fig. 5.16c. We now have

$$\begin{aligned} I_t &= \frac{1}{12}(12.5)(220)^3 + 12.5(220)(44.1)^2 + \frac{1}{12}(80)(20)^3 + 80(20)(75.9)^2 \\ &= 25.7 \times 10^6 \text{ mm}^4 \end{aligned}$$

Then

$$\sigma_{a,\max} = \frac{Mc}{I_t} = \frac{20 \times 10^3(0.0859)}{25.7(10^{-6})} = 66.8 \text{ MPa}$$

$$\sigma_{w,\max} = \frac{nMc}{I_t} = \frac{20 \times 10^3(0.1541)}{8(25.7 \times 10^{-6})} = 15 \text{ MPa}$$

as have already been found in part (a).

EXAMPLE 5.8 Steel-Reinforced-Concrete Beam

A concrete beam of width $b = 250$ mm and *effective depth* $d = 400$ mm is reinforced with three steel bars, providing a total cross-sectional area $A_s = 1000 \text{ mm}^2$ (Fig. 5.17a). Dimensions are given in millimeters. Note that it is usual for an approximate *allowance* $a = 50$ mm to be used to protect the steel from corrosion and fire. Let $n = E_s/E_c = 10$. Calculate the maximum stresses in the materials produced by a *negative* bending moment of $M = 60 \text{ kN} \cdot \text{m}$.

Solution Concrete is very weak in tension but strong in compression. Thus, only the portion of the cross section located a distance kd above the neutral axis is used in the transformed section (Fig. 5.17b); the concrete is assumed to take no tension. The transformed area of the steel nA_s is identified by a single dimension from the neutral axis to its centroid. The compressive stress in the concrete is assumed to vary linearly from the neutral axis, and the steel is assumed to be uniformly stressed.

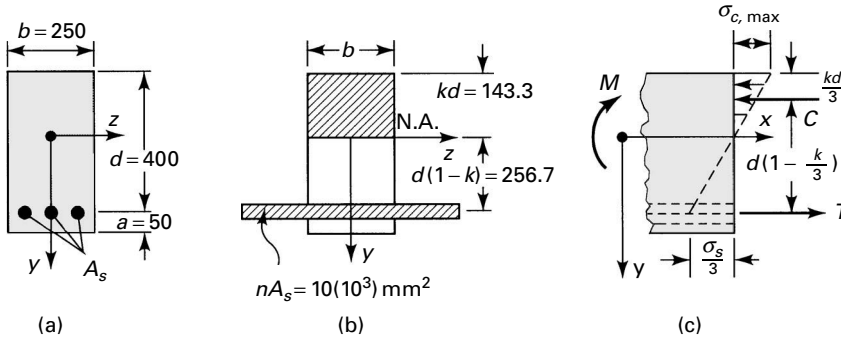


FIGURE 5.17. Example 5.8. (a) Reinforced-concrete cross section; (b) equivalent concrete cross section; (c) compressive force C in concrete and tensile force T in the steel rods.

The condition that the first moment of the transformed section with respect to the neutral axis be zero is satisfied by

$$b(kd)\frac{kd}{2} - nA_s(d - kd) = 0$$

or

$$(kd)^2 + (kd)\frac{2n}{b}A_s - \frac{2n}{b}dA_s = 0 \quad (5.54)$$

By solving this quadratic expression for kd , we can obtain the position of the neutral axis.

Introducing the data given, Eq. (5.54) reduces to

$$(kd)^2 + 80(kd) - 32 \times 10^3 = 0$$

from which

$$kd = 143.3 \text{ mm} \quad \text{and hence} \quad k = 0.358 \quad (c)$$

The moment of inertia of the transformed cross section about the neutral axis is

$$\begin{aligned} I_t &= \frac{1}{12}(0.25) + (0.1433)^3 + 0.25(0.1433)(0.0717)^2 + 0 + 10 \times 10^{-3}(0.2567)^2 \\ &= 904.4 \times 10^{-6} \text{ m}^4 \end{aligned}$$

Thus, the *peak compressive* stress in the concrete and the *tensile* stress in the steel are

$$\begin{aligned} \sigma_{c, \max} &= \frac{Mc}{I_t} = \frac{60 \times 10^3(0.1433)}{904.4 \times 10^{-6}} = 9.5 \text{ MPa} \\ \sigma_s &= \frac{nMc}{I_t} = \frac{10(60 \times 10^3)(0.2567)}{904.4 \times 10^{-6}} = 170 \text{ MPa} \end{aligned}$$

These stresses act as shown in Fig. 5.15c.

An *alternative method* of solution is to obtain $\sigma_{c,\max}$ and σ_s from a free-body diagram of the portion of the beam (Fig. 5.17c) without computing I_t . The first equilibrium condition, $\Sigma F_x = 0$, gives $C = T$, where

$$C = \frac{1}{2}\sigma_{c,\max}(b \cdot kd), \quad T = \sigma_s(A_s) \quad (d)$$

are the compressive and tensile stress resultants, respectively. From the second requirement of statics, $\Sigma M_z = 0$, we have

$$M = Cd(1 - kl/3) = Td(1 - kl/3) \quad (e)$$

Equations (d) and (e) result in

$$\sigma_{c,\max} = \frac{2M}{bd^2k(1 - k/3)}, \quad \sigma_s = \frac{M}{A_s d(1 - k/3)} \quad (5.55)$$

Substituting the data given and Eq. (c) into Eq. (5.55) yields

$$\sigma_{c,\max} = \frac{2(60 \times 10^3)}{0.25(0.4^2)(0.358)(1 - 0.358/3)} = 9.5 \text{ MPa}$$

$$\sigma_s = \frac{60 \times 10^3}{1000 \times 10^{-6}(0.4)(1 - 0.358/3)} = 170 \text{ MPa}$$

as before.

5.10 SHEAR CENTER

Given any cross-sectional configuration, one point may be found in the plane of the cross section through which the resultant of the transverse shearing stresses passes. A transverse load applied on the beam must act through this point, called the *shear center* or *flexural center*, if no twisting is to occur [Ref. 5.3]. The center of shear is sometimes defined as the point in the end section of a cantilever beam at which an applied load results in bending only. When the load does not act through the shear center, in addition to bending, a twisting action results (Section 6.1).

The location of the shear center is independent of the direction and magnitude of the transverse forces. For singly symmetrical sections, the shear center lies on the axis of symmetry, while for a beam with two axes of symmetry, the shear center coincides with their point of intersection (also the centroid). It is not necessary, in general, for the shear center to lie on a principal axis, and it may be located outside the cross section of the beam.

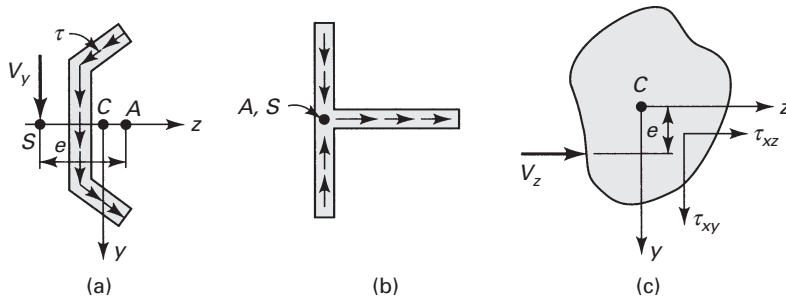


FIGURE 5.18. *Shear centers.*

5.10.1 Thin-Walled Open Cross Sections

For thin-walled sections, the shearing stresses are taken to be distributed uniformly over the thickness of the wall and directed so as to parallel the boundary of the cross section. If the shear center S for the typical section of Fig. 5.18a is required, we begin by calculating the shear stresses by means of Eq. (5.39). The moment M_x of these stresses about arbitrary point A is then obtained. Since the external moment attributable to V_y about A is $V_y e$, the distance between A and the shear center is given by

$$e = \frac{M_x}{V_y} \quad (5.56)$$

If the force is parallel to the z axis rather than the y axis, the position of the line of action may be established in the manner discussed previously. If both V_y and V_z exist, the shear center is located at the intersection of the two lines of action.

The determination of M_x is simplified by propitious selection of point A , such as in Fig. 5.18b. There, the moment M_x of the shear forces about A is zero; point A is also the shear center. For all sections consisting of two intersecting rectangular elements, the same situation exists.

For thin-walled *box beams* (with boxlike cross section), the point or points in the wall where the shear flow $q = 0$ (or $\tau_{xy} = 0$) is unknown. Here, shear flow is represented by the superposition of transverse and torsional flow (see Section 6.8). Hence, the unit angle of twist equation, Eq. (6.23), along with $q = VQ/I$, is required to find the shear flow for a cross section of a box beam. The analysis procedure is as follows: First, introduce a free edge by *cutting* the section *open*; second, close it again by obtaining the shear flow that makes the angle of twist in the beam zero [Refs. 5.4 through 5.6].

In the following examples, the shear center of an open, thin-walled section is determined for two typical situations. In the first, the section has only one axis of symmetry; in the second, there is an asymmetrical section.

EXAMPLE 5.9 Shearing Stress Distribution in a Channel Section

Locate the shear center of the channel section loaded as a cantilever (Fig. 5.19a). Assume that the flange thicknesses are small when compared with the depth and width of the section.

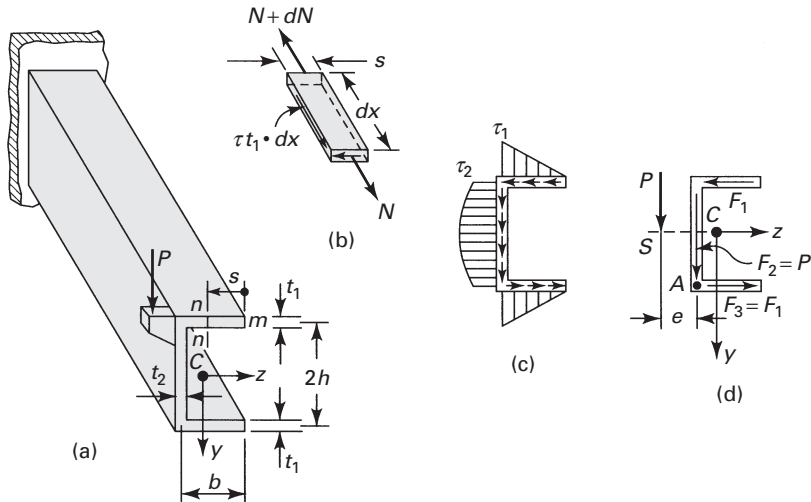


FIGURE 5.19. Example 5.9. (a) Cantilever beam with a concentrated load at the free end; (b) an element of the upper flange; (c) shear distribution; (d) location of the shear center S .

Solution The shearing stress in the upper flange at any section nn will be found first. This section is located a distance s from the free edge m , as shown in the figure. At m , the shearing stress is zero. The first moment of area st_1 about the z axis is $Q_z = st_1h$. The shear stress at nn , from Eq. (5.39), is thus

$$\tau_{xz} = \frac{V_y Q_z}{I_z b} = P \frac{sh}{I_z} \quad (\text{a})$$

The direction of τ along the flange can be determined from the equilibrium of the forces acting on an element of length dx and width s (Fig. 5.19b). Here the normal force $N = t_1 s \sigma_x$, owing to the bending of the beam, increases with dx by dN . Hence, the x equilibrium of the element requires that $\tau t_1 \cdot dx$ must be directed as shown in the figure. This flange force is directed to the left, because the shear forces must intersect at the corner of the element.

The distribution of the shear stress τ_{xz} on the flange, as Eq. (a) indicates, is linear with s . Its maximum value occurs at

$$\tau_1 = P \frac{bh}{I_z} \quad (\text{b})$$

Similarly, the value of stress τ_{xy} at the top of the web is

$$\tau_2 = P \frac{bt_1 h}{t_2 I_z} \quad (\text{c})$$

The stress varies parabolically over the web, and its maximum value is found at the neutral axis. Figure 5.19c sketches the shear stress distribution in the

channel. As the shear stress is linearly distributed across the flange length, from Eq. (b), the flange force is expressed by

$$F_1 = \frac{1}{2} \tau_1 b t_1 = P \frac{b^2 h t_1}{2I_z} \quad (\text{d})$$

Symmetry of the section dictates that $F_1 = F_3$ (Fig. 5.19d). We will assume that the web force $F_2 = P$, since the vertical shearing force transmitted by the flange is negligibly small, as shown in Example 5.3. The shearing force components acting in the section must be statically equivalent to the resultant shear load P . Thus, the principle of the moments for the system of forces in Fig. 5.19d or Eq. (5.56), applied at A , yields $M_x = Pe = 2F_1 h$. Substituting F_1 from Eq. (d) into this expression, we obtain

$$e = \frac{b^2 h^2 t_1}{I_z}$$

Since for the usual channel section t_1 is small in comparison to b or h , the simplified moment of inertia has the following form:

$$I_z = \frac{2}{3} t_2 h^3 + 2b t_1 h^2$$

The shear center is, in turn, located by the expression

$$e = \frac{3}{2} \frac{b^2 t_1}{h t_2 + 3b t_1} \quad (\text{e})$$

Comments Note that e depends on only the section dimensions. Examination reveals that e may vary from a minimum of zero to a maximum of $b/2$. A zero or near-zero value of e corresponds to either a flangeless beam ($b = 0, e = 0$) or an especially deep beam ($h \gg b$). The extreme case, $e = b/2$, is obtained for an infinitely wide beam.

EXAMPLE 5.10 Shear Flow in an Asymmetrical Channel Section

Locate the shear center S for the asymmetrical channel section shown in Fig. 5.20a. All dimensions are in millimeters. Assume that the beam thickness $t = 125$ mm is constant.

Solution The centroid C of the section is located by \bar{y} and \bar{z} with respect to nonprincipal axes z and y . By performing the procedure given in Example 5.1, we obtain $\bar{y} = 15.63$ mm, $\bar{z} = 5.21$ mm, $I_y = 4765.62$ mm⁴, $I_z = 21,054.69$ mm⁴, and $I_{yz} = 3984.37$ mm⁴. Equation (5.18) then yields the direction of the principal axis x', y' as $\theta_p = 13.05^\circ$, and Eq. (5.19) gives the principal moments of inertia as $I_{y'} = 3828.12$ mm⁴, $I_{z'} = 21,953.12$ mm⁴ (Fig. 5.20a).

Let us now assume that a shear load $V_{y'}$ is applied in the y', z' plane (Fig. 5.20b). This force may be considered the resultant of force components $F_1, F_2,$

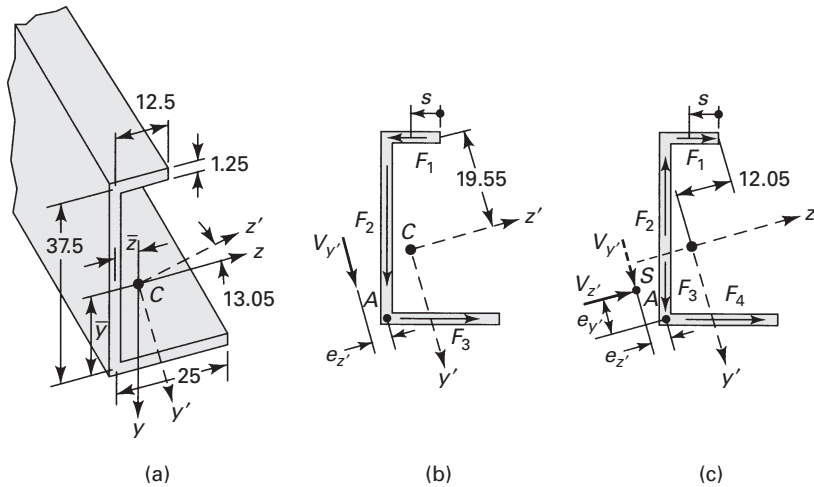


FIGURE 5.20. Example 5.10. (a) Portion of a beam with a channel cross section; (b) shear flow; (c) location of the shear center S .

and F_3 acting in the flanges and web in the directions indicated in the figure. The algebra will be minimized if we choose point A , where F_2 and F_3 intersect, in finding the line of action of $V_{y'}$ by applying the principle of moments. To do so, we need to determine the value of F_1 acting in the upper flange. The shear stress τ_{xz} in this flange, from Eq. (5.39), is

$$\tau_{xz} = \frac{V_{y'} Q_{z'}}{I_z b} = \frac{V_{y'}}{I_z t} \left[st \left(19.55 + \frac{1}{2} s \sin 13.05^\circ \right) \right] \quad (\text{f})$$

where s is measured from right to left along the flange. Note that $Q_{z'}$, the bracketed expression, is the first moment of the shaded flange element area with respect to the z' axis. The constant 19.55 is obtained from the geometry of the section. After substituting the numerical values and integrating Eq. (f), the total shear force in the upper flange is found to be

$$F_1 = \int_0^s \tau_{xz} t ds = \frac{V_{y'} t}{I_z} \int_0^{12.5} s \left(19.55 + \frac{1}{2} s \sin 13.05^\circ \right) ds = 0.0912 V_{y'} \quad (\text{g})$$

Application of the principle of moments at A gives $V_{y'} e_{z'} = 37.5 F_1$. Introducing F_1 from Eq. (g) into this equation, the distance $e_{z'}$, which locates the line of action of $V_{y'}$ from A , is

$$e_{z'} = 3.42 \text{ mm} \quad (\text{h})$$

Next, assume that the shear loading V_z acts on the beam (Fig. 5.20c). The distance $e_{y'}$ may be obtained as in the situation just described. Because of V_z ,

the force components F_1 to F_4 will be produced in the section. The shear stress in the upper flange is given by

$$\tau_{xz} = \frac{V_z Q_{y'}}{I_{y'} b} = \frac{V_z}{I_{y'} t} [st(12.05 - \frac{1}{2}s \cos 13.05^\circ)] \quad (\text{i})$$

The quantity $Q_{y'}$ represents the first moment of the flange segment area with respect to the y' axis, and 12.05 is found from the geometry of the section. The total force F_1 in the flange is

$$F_1 = \frac{V_z}{I_{y'}} \int_0^{12.5} st(12.05 - \frac{1}{2}s \cos 13.05^\circ) ds = 0.204 V_z$$

The principle of moments applied at A , $V_z e_{y'} = 37.5 F_1 = 7.65 V_z$ leads to

$$e_{y'} = 7.65 \text{ mm} \quad (\text{j})$$

Thus, the intersection of the lines of action of $V_{y'}$ and $V_{z'}$, and $e_{z'}$ and $e_{y'}$, locates the shear center S of the asymmetrical channel section.

5.10.2 Arbitrary Solid Cross Sections

The preceding considerations can be extended to beams of arbitrary solid cross section, in which the shearing stress varies with both cross-sectional coordinates y and z . For these sections, the exact theory can, in some cases, be successfully applied to locate the shear center. Examine the section of Fig. 5.18c subjected to the shear force V_z , which produces the stresses indicated. Denote y and z as the principal directions. The moment about the x axis is then

$$M_x = \iint (\tau_{xy} z - \tau_{xz} y) dz dy \quad (\text{5.57})$$

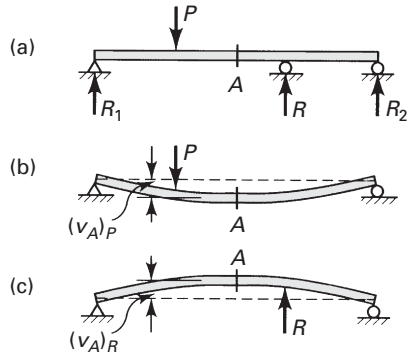
V_z must be located a distance e from the z axis, where $e = M_x/V_z$.

5.11 STATICALLY INDETERMINATE SYSTEMS

A large class of problems of considerable practical interest relate to structural systems for which the equations of statics are not sufficient (but are necessary) for determination of the reactions or other unknown forces. Such systems are called *statically indeterminate*, and they require supplementary information for their solution. Additional equations usually describe certain geometric conditions associated with displacement or strain. These *equations of compatibility* state that the strain owing to deflection or rotation must preserve continuity.

With this additional information, the solution proceeds in essentially the same manner as for statically determinate systems. The number of reactions in excess of the number

FIGURE 5.21. *Superposition of displacements in a continuous beam.*



of equilibrium equations is called the *degree of static indeterminacy*. Any reaction in excess of that which can be obtained by statics alone is said to be *redundant*. Thus, the number of redundants is the same as the degree of indeterminacy.

Several methods are available to analyze statically indeterminate structures. The principle of superposition, briefly discussed next, is an effective approach for many cases. In Section 5.6 and in Chapters 7 and 10, a number of commonly employed methods are discussed for the solution of the indeterminate beam, frame, and truss problems.

5.11.1 The Method of Superposition

In the event of complicated load configurations, the method of *superposition* may be used to good advantage to simplify the analysis. Consider, for example, the continuous beam shown in Fig. 5.21a, which is then replaced by the beams shown in Fig. 5.21b and c. At point A , the beam now experiences the deflections $(v_A)_P$ and $(v_A)_R$ due to P and R , respectively. Subject to the restrictions imposed by small deformation theory and a material obeying Hooke's law, the deflections and stresses are linear functions of transverse loadings, and superposition is valid:

$$\begin{aligned} v_A &= (v_A)_P + (v_A)_R \\ \sigma_A &= (\sigma_A)_P + (\sigma_A)_R \end{aligned}$$

This procedure may, in principle, be extended to situations involving any degree of indeterminacy.

EXAMPLE 5.11 Displacements of a Propped Cantilever Beam

Figure 5.22 shows a propped cantilever beam AB subject to a uniform load of intensity p . Determine (a) the reactions, (b) the equation of the deflection curve, and (c) the slope at A .

Solution Reactions R_A , R_B and M_B are statically indeterminate because there are only two equilibrium conditions ($\Sigma F_y = 0, \Sigma M_z = 0$); thus, the beam

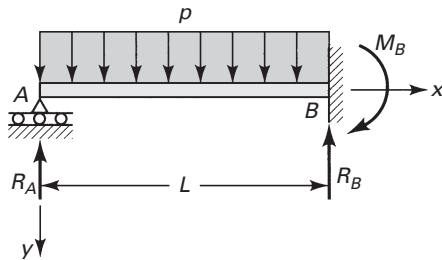


FIGURE 5.22. Example 5.11. A propped beam under uniform load.

is statically indeterminate to the first degree. With the origin of coordinates taken at the left support, the equation for the beam moment is

$$M = -R_A x + \frac{1}{2} p x^2$$

The third of Eqs. (5.32) then becomes

$$EI v'' = -R_A x + \frac{1}{2} p x^2$$

and successive integrations yield

$$EI v' = -\frac{1}{2} R_A x^2 + \frac{1}{6} p x^3 + c_1 \quad (\text{a})$$

$$EI v = -\frac{1}{6} R_A x^3 + \frac{1}{24} p x^4 + c_1 x + c_2$$

There are three unknown quantities in these equations (c_1 , c_2 , and R_A) and three boundary conditions:

$$v(0) = 0, \quad v'(L) = 0, \quad v(L) = 0 \quad (\text{b})$$

a. Introducing Eqs. (b) into the preceding expressions, we obtain $c_2 = 0$, $c_1 = pL^3/48$ and

$$R_A = \frac{3}{8} pL \quad (\text{5.58a})$$

We can now determine the remaining reactions from the equations of equilibrium:

$$R_B = \frac{5}{8} pL, \quad M_B = \frac{1}{8} pL^2 \quad (\text{5.58b, c})$$

b. By substituting for R_A , c_1 and c_2 in Eq. (a), we obtain the equation of the deflection curve:

$$v = \frac{P}{48EI} (2x^4 - 3Lx^3 + L^3x) \quad (\text{5.59})$$

c. Differentiating Eq. (5.59) with respect to x , we obtain the equation of the angle of rotation:

$$\theta = \frac{P}{48EI} (8x^3 - 9Lx^2 + L^3) \quad (\text{5.60})$$

Setting $x = 0$, we have the slope at A :

$$\theta_A = \frac{pL^3}{48EI} \quad (\text{5.61})$$

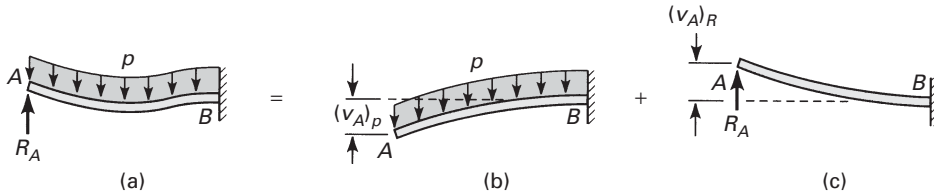


FIGURE 5.23. Example 5.12. Method of superposition: (a) reaction R_A is selected as redundant; (b) deflection at end A due to load P ; (c) deflection at end A due to reaction R_A .

EXAMPLE 5.12 Reactions of a Propped Cantilever Beam

Consider again the statically indeterminate beam shown in Fig. 5.22. Determine the reactions using the method of superposition.

Solution Reaction R_A is selected as redundant; it becomes an unknown load when we eliminate the support at A (Fig. 5.23a). The loading is resolved into those shown in Figs. 5.23b and 5.23c. The solution for each case is (see Table D.4)

$$(v_A)_P = \frac{pL^4}{8EI}, \quad (v_A)_R = -\frac{R_AL^3}{3EI}$$

The compatibility condition for the original beam requires that

$$v_A = \frac{pL^4}{8EI} - \frac{R_AL^3}{3EI} = 0$$

from which $R_A = 3pL/8$. Reaction R_B and moment M_B can now be found from the equilibrium requirements. The results correspond to those of Example 5.11.

5.12 ENERGY METHOD FOR DEFLECTIONS

Strain energy methods are frequently employed to analyze the deflections of beams and other structural elements. Of the many approaches available, *Castigliano's second theorem* is one of the most widely used. To apply this theory, the strain energy must be represented as a function of loading. Detailed discussions of energy techniques are found in Chapter 10. In this section, we limit ourselves to a simple example to illustrate how the strain energy in a beam is evaluated and how the deflection is obtained by the use of Castigliano's theorem (Section 10.4).

The strain energy stored in a beam under bending stress σ_x only, substituting $M = EI(d^2v/dx^2)$ into Eq. (2.63), is expressed in the form

$$U_b = \int \frac{M^2 dx}{2EI} = \int \frac{EI}{2} \left(\frac{d^2v}{dx^2} \right)^2 dx \quad (5.62)$$

where the integrations are carried out over the beam length. We next determine the strain energy stored in a beam that is *only* due to the *shear* loading V . As described in Section 5.7, this force produces shear stress τ_{xy} at every point in the beam. The strain energy density is, from Eq. (2.50), $U_o = \tau_{xy}/2G$. Substituting τ_{xy} as expressed by Eq. (5.39), we have $U_o = V^2 Q^2 / 2GI^2 b^2$. Integrating this expression over the volume of the beam of cross-sectional area A , we obtain

$$U_s = \int \frac{V^2}{2GI^2} \left[\int \frac{Q^2}{b^2} dA \right] dx \quad (\mathbf{a})$$

5.12.1 Form Factor for Shear

Let us denote

$$\alpha = \frac{A}{I^2} \int \frac{Q^2}{b^2} dA \quad (\mathbf{5.63})$$

This value is termed the *shape* or *form factor for shear*. When it is substituted in Eq. (a), we obtain

$$U_s = \int \frac{\alpha V^2 dx}{2AG} \quad (\mathbf{5.64})$$

where the integration is carried over the beam length. The form factor is a dimensionless quantity specific to a given cross-section geometry.

For example, for a *rectangular* cross section of width b and height $2h$, the first moment Q , from Eq. (5.41), is $Q = (b/2)(h^2 - y_1^2)$. Because $A/I^2 = 9/2bh^5$, Eq. (5.63) provides the following result:

$$\alpha = \frac{9}{2bh^5} \int_{-h}^h \frac{1}{4}(h^2 - y_1^2)^2 b dy_1 = \frac{6}{5} \quad (\mathbf{b})$$

In a like manner, the form factor for other cross sections can be determined. Table 5.2 lists several typical cases. Following the determination of α , the strain energy is evaluated by applying Eq. (5.64).

TABLE 5.2. *Form Factor for Shear for Various Beam Cross Sections*

<i>Cross Section</i>	<i>Form Factor α</i>
A. Rectangle	6/5
B. I-section, box section, or channels ^a	A/A_{web}
C. Circle	10/9
D. Thin-walled circular	2

^a A = area of the entire section, A_{web} = area of the web ht , where h is the beam depth and t is the web thickness.

For a linearly elastic beam, Castigliano's theorem, from Eq. (10.3), is expressed by

$$\delta = \frac{\partial U}{\partial P} \quad (\text{c})$$

where P is a load acting on the beam and δ is the displacement of the point of application in the direction of P . Note that the strain energy $U = U_b + U_s$ is expressed as a function of the externally applied forces (or moments).

As an illustration, consider the bending of a cantilever beam of rectangular cross section and length L , subjected to a concentrated force P at the free end (Fig. 5.5). The bending moment at any section is $M = Px$ and the shear force V is equal in magnitude to P . Substituting these together with $\alpha = \frac{6}{5}$ into Eqs. (5.62) and (5.64) and integrating, we find the strain energy stored in the cantilever to be

$$U = \frac{P^2 L^3}{6EI} + \frac{3P^2 L}{5AG}$$

The displacement of the free end owing to bending and shear is, by application of Castigliano's theorem, therefore

$$\delta = v = \frac{PL^3}{3EI} + \frac{6PL}{5AG}$$

The exact solution is given by Eq. (5.24).

Part C: Curved Beams

5.13 ELASTICITY THEORY

Our treatment of stresses and deflections caused by the bending has been restricted so far to straight members. In real-world applications, many members—such as crane hooks, chain links, C -lamps, and punch-press frames—are curved and loaded as beams. Part C deals with the stresses caused by the bending of bars that are initially curved.

A curved bar or beam is a structural element for which the locus of the centroids of the cross sections is a curved line. This section focuses on an application of the theory of elasticity to a bar characterized by a constant narrow rectangular cross section and a circular axis. The axis of symmetry of the cross section lies in a single plane throughout the length of the member.

5.13.1 Equations of Equilibrium and Compatibility

Consider a beam subjected to equal end couples M such that bending takes place in the plane of curvature, as shown in Fig. 5.24a. Given that the bending moment remains constant along the length of the bar, the stress distribution should be identical in any radial

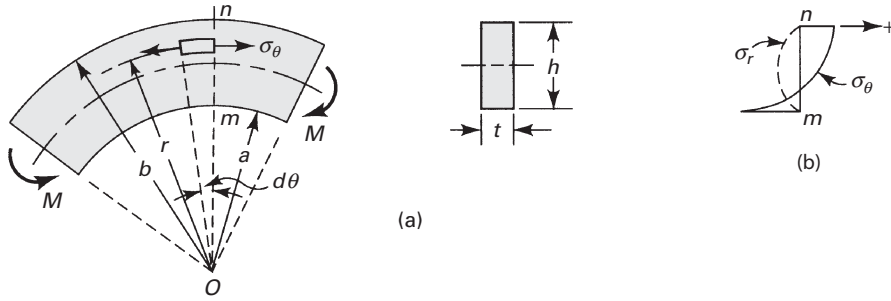


FIGURE 5.24. Pure bending of a curved beam of rectangular cross section.

cross section. Stated differently, we seek a distribution of stress displaying θ independence. It is clear that the appropriate expression of equilibrium is Eq. (8.2):

$$\frac{d\sigma_r}{dr} + \frac{\sigma_r - \sigma_\theta}{r} = 0 \quad (\text{a})$$

and that the condition of compatibility for plane stress, Eq. (3.41),

$$\frac{d^2(\sigma_r + \sigma_\theta)}{dr^2} + \frac{1}{r} \frac{d(\sigma_r + \sigma_\theta)}{dr} = 0$$

must also be satisfied. The latter is an equidimensional equation, which can be reduced to a second-order equation with constant coefficients by substituting $r = e^t$ or $t = \ln r$. Direct integration then leads to $\sigma_r + \sigma_\theta = c'' + c' \ln r$, which may be written in the form $\sigma_r + \sigma_\theta = c''' + c' \ln(r/a)$. Solving this expression together with Eq. (a) results in the following equations for the radial and tangential stress:

$$\begin{aligned} \sigma_r &= c_1 + c_2 \ln \frac{r}{a} + \frac{c_3}{r^2} \\ \sigma_\theta &= c_1 + c_2 \left(1 + \ln \frac{r}{a} \right) - \frac{c_3}{r^2} \end{aligned} \quad (\text{5.65})$$

5.13.2 Boundary Conditions

To evaluate the constants of integration, the boundary conditions are applied as follows:

1. No normal forces act along the curved boundaries at $r = a$ and $r = b$, so that

$$(\sigma_r)_{r=a} = (\sigma_r)_{r=b} = 0 \quad (\text{b})$$

2. Because there is no force acting at the ends, the normal stresses acting at the straight edges of the bar must be distributed to yield a zero resultant:

$$t \int_a^b \sigma_\theta dr = 0 \quad (\text{c})$$

where t represents the beam thickness.

3. The normal stresses at the ends must produce a couple M :

$$t \int_a^b r \sigma_\theta dr = M \quad (\text{d})$$

The conditions (c) and (d) apply not just at the ends; that is, because of σ_θ independence, they apply at any θ . In addition, shearing stresses are assumed to be zero throughout the beam, so $\tau_{r,\theta} = 0$ is satisfied at the boundaries, where no tangential forces exist.

Combining the first equation of Eqs. (5.65) with the condition (b), we find that

$$c_3 = -a^2 c_1, \quad c_1 \left(\frac{a^2}{b^2} - 1 \right) = c_2 \ln \frac{b}{a}$$

These constants together with the second of Eqs. (5.65) satisfy condition (c). Thus, we have

$$c_1 = \frac{b^2 \ln(b/a)}{a^2 - b^2} c_2, \quad c_3 = \frac{a^2 b^2 \ln(b/a)}{b^2 - a^2} c_2 \quad (\text{e})$$

Finally, substitution of the second of Eqs. (5.65) and (e) into (d) provides

$$c_2 = \frac{M}{N} \frac{4(b^2 - a^2)}{tb^4} \quad (\text{f})$$

where

$$N = \left(1 - \frac{a^2}{b^2} \right)^2 - 4 \frac{a^2}{b^2} \ln^2 \frac{b}{a} \quad (\text{5.66})$$

5.13.3 Stress Distribution

When the expressions for constants c_1 , c_2 , and c_3 are inserted into Eq. (5.65), the following equations are obtained for the radial stress and tangential stress:

$$\begin{aligned} \sigma_r &= \frac{4M}{tb^2 N} \left[\left(1 - \frac{a^2}{b^2} \right) \ln \frac{r}{a} - \left(1 - \frac{a^2}{r^2} \right) \ln \frac{b}{a} \right] \\ \sigma_\theta &= \frac{4M}{tb^2 N} \left[\left(1 - \frac{a^2}{b^2} \right) \left(1 + \ln \frac{r}{a} \right) - \left(1 + \frac{a^2}{r^2} \right) \ln \frac{b}{a} \right] \end{aligned} \quad (\text{5.67})$$

If the end moments are applied so that the force couples producing them are distributed in the manner indicated by Eq. (5.67), then these equations are applicable throughout the bar. If the distribution of applied stress (to produce M) differs from Eq. (5.67), the results may be regarded as valid in regions away from the ends, in accordance with Saint-Venant's principle.

These results, when applied to a beam with radius a , large relative to its depth h , yield an interesting comparison between straight and curved beam theory. For *slender beams* with $h \ll a$, the radial stress σ_r in Eq. (5.67) becomes negligible, and the tangential stress σ_θ is approximately the same as that obtained from My/I . Note that the radial stresses developed in *nonslender* curved beams made of isotropic materials are small enough that they can be neglected in analysis and design.

The bending moment is taken as positive when it tends to decrease the radius of curvature of the beam, as in Fig. 5.24a. Employing this sign convention, σ_r as determined from Eq. (5.67) is always negative, indicating that this stress is compressive. Similarly, when σ_θ is positive, the stress is tensile; otherwise, it is compressive. Figure 5.24b plots the stresses at section mn . Note that the maximum stress magnitude is found at the extreme fiber of the concave side.

5.13.4 Deflections

Substitution of σ_r and σ_θ from Eq. (5.67) into Hooke's law provides expressions for the strains ϵ_θ , ϵ_r , and $\gamma_{r\theta}$. The displacements u and v then follow, upon integration, from the strain-displacement relationships, described by Eqs. (3.33). The resulting displacements indicate that plane sections of the curved beam subjected to pure bending remain plane subsequent to bending. Castigliano's theorem (Section 5.12) is a particularly attractive method for determining the deflection of curved members.

For beams in which the *depth of the member is small relative to the radius of curvature* or, as is usually assumed, $\bar{r}/c > 4$, the initial curvature may be neglected in evaluating the strain energy. In such a case, \bar{r} represents the radius to the centroid, and c is the distance from the centroid to the extreme fiber on the concave side. Thus, the strain energy due to the bending of a straight beam [Eq. (5.62)] is also a good approximation for curved, slender beams.

5.14 CURVED BEAM FORMULA

The approach to curved beams explored in this section was developed by E. Winkler (1835–1888). As an extension of the elementary theory of straight beams, *Winkler's theory* assumes that all conditions required to make the straight-beam formula applicable are satisfied except that the beam is initially curved.

Consider the pure bending of a curved beam as illustrated in Fig. 5.25a. The distance from the center of curvature to the centroidal axis is \bar{r} . The *positive* y coordinate is measured *toward* the center of curvature O from the neutral axis (Fig. 5.25b). The outer and inner fibers are at distances of r_o and r_i from the center of curvature, respectively.

5.14.1 Basic Assumptions

Derivation of the stress in the beam is again based on the three principles of solid mechanics and the familiar presuppositions:

1. All cross sections possess a vertical axis of symmetry lying in the plane of the centroidal axis passing through C .
2. The beam is subjected to end couples M . The bending moment vector is everywhere normal to the plane of symmetry of the beam.
3. Sections originally plane and perpendicular to the centroidal beam axis remain so subsequent to bending. (The influence of transverse shear on beam deformation is not taken into account.)

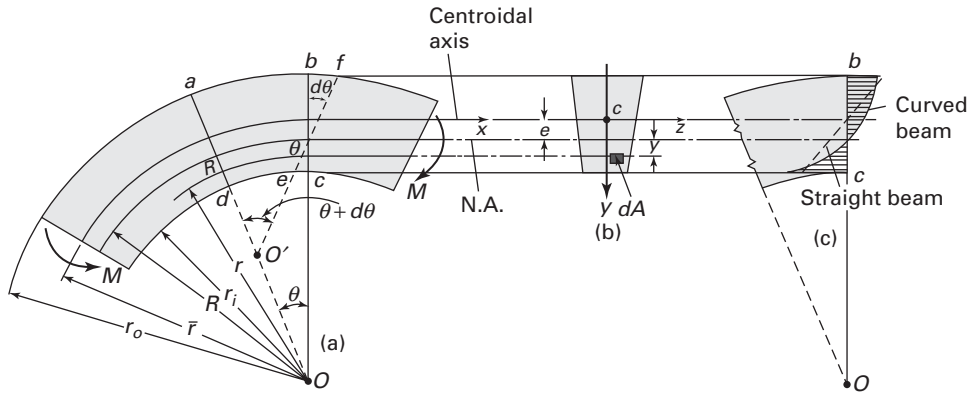


FIGURE 5.25. (a) Curved beam in pure bending with a cross-sectional vertical (y) axis of symmetry; (b) cross section; (c) stress distributions over the cross section.

Referring to assumption (3), note the relationship in Fig. 5.25a between lines bc and ef representing the plane sections before and after the bending of an initially curved beam. Note also that the initial length of a beam fiber such as gh depends on the distance r from the center of curvature O . On the basis of plane sections remaining plane, we can state that the total deformation of a beam fiber obeys a linear law, as the beam element rotates through small angle.

5.14.2 Location of the Neutral Axis

In Fig. 5.25a, it is clear that the initial length of any arbitrary fiber gh of the beam depends on the distance r from the center of curvature O . Thus, the total deformation of a beam fiber obeys a linear law, as the beam element rotates through a small angle $d\theta$. Conversely, the normal or tangential strain ϵ_θ does *not* follow a linear relationship. The contraction of fiber gh equals $-(R-r)d\theta$, where R is the distance from O to the neutral axis (yet to be determined) and its initial length is $r\theta$. So, the normal strain of this fiber is given by $\epsilon_\theta = -(R-r)d\theta/r\theta$. For convenience, we denote $\lambda = d\theta/\theta$, which is constant for any element.

The tangential normal stress, acting on an area dA of the cross section, can now be obtained through the use of *Hooke's law*, $\sigma_\theta = E\epsilon_\theta$. It follows that

$$\sigma_\theta = -E\lambda \frac{R-r}{r} \quad (\text{a})$$

The *equations of equilibrium*, $\sum F_x = 0$ and $\sum M_z = 0$ are, respectively,

$$\int \sigma_\theta dA = 0 \quad (\text{b})$$

$$\int \sigma_\theta (R-r) dA = M \quad (\text{c})$$

When the tangential stress of Eq. (a) is inserted into Eq. (b), we obtain

$$\int_A -E\lambda \left(\frac{R-r}{r} \right) dA = 0 \quad (d)$$

Since $E\lambda$ and R are constants, they may be moved outside the integral sign, as follows:

$$E\lambda \left(R \int_A \frac{dA}{r} - \int_A dA \right) = 0$$

The *radius of the neutral axis* R is then written in the form

$$R = \frac{A}{\int_A \frac{dA}{r}} \quad (5.68)$$

where A is the cross-sectional area of the beam. The integral in Eq. (5.68) may be evaluated for various cross-sectional shapes (see Example 5.13 and Probs. 5.46 through 5.48). For reference, Table 5.3 lists explicit formulas for R and A for some commonly used cases.

The *distance* e between the *centroidal axis* and the *neutral axis* ($y = 0$) of the cross section of a curved beam (Fig. 5.25b) is equal to

$$e = \bar{r} - R \quad (5.69)$$

Thus, in a curved member, the *neutral axis does not coincide with the centroidal axis*. This differs from the case involving straight elastic beams.

5.14.3 Tangential Stress

Once we know the location of the neutral axis, we can obtain the equation for the stress distribution by introducing Eq. (a) into Eq. (c). Therefore,

$$M = E\lambda \int_A \frac{(R-r)^2}{r} dA$$

Expanding this equation, we have

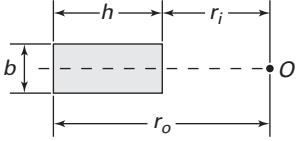
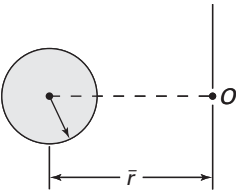
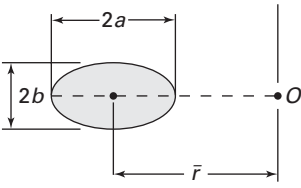
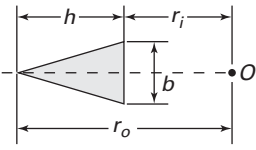
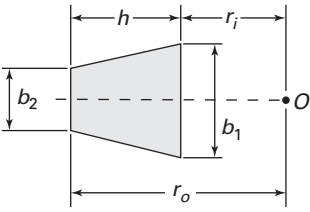
$$M = E\lambda \left(R^2 \int_A \frac{dA}{r} - 2R \int_A dA + \int_A r dA \right)$$

Here, the first integral is equivalent to A/R , as determined by Eq. (5.68), and the second integral equals the cross-sectional area A . The third integral, by definition, represents $\bar{r}A$, where \bar{r} is the radius of the centroidal axis. Therefore, $M = E\lambda A(\bar{r} - R) = E\lambda Ae$.

We now introduce E from Eq. (a) into the discussion and solve for σ_θ from the resulting expression. Then, the *tangential stress* in a curved beam, subject to pure bending at a distance r from the center of curvature, is expressed in the following form:

$$\sigma_\theta = \frac{M(R-r)}{Aer} \quad (5.70)$$

TABLE 5.3. *Properties for Various Cross-Sectional Shapes*

Cross Section	Radius of Neutral Surface R
A. Rectangle	$R = \frac{h}{\ln \frac{r_o}{r_i}}$ $A = bh$
	
B. Circle	$R = \frac{A}{2\pi(\bar{r} + \sqrt{\bar{r}^2 - c^2})}$ $A = \pi c^2$
	
C. Ellipse	$R = \frac{A}{\frac{2\pi b}{a}(\bar{r} - \sqrt{\bar{r}^2 - a^2})}$ $A = \pi ab$
	
D. Triangle	$R = \frac{A}{\frac{br_o}{h} \left(\ln \frac{r_o}{r_i} \right) - b}$ $A = \frac{1}{2}bh$
	
E. Trapezoid	$R = \frac{A}{\frac{1}{h}[(b_1 r_o - b_2 r_i) \ln \frac{r_o}{r_i} - h(b_1 - b_2)]}$ $A = \frac{1}{2}(b_1 + b_2)h$
	

where e is defined by Eq. (5.69). Alternatively, substituting $y = R - r$ or $r = R - y$ (Fig. 5.25a) into Eq. (5.70) yields

$$\sigma_{\theta} = -\frac{My}{Ae(R-y)} \quad (5.71)$$

5.14.4 Winkler's Formula

Equations (5.70) and (5.71) represent two forms of the *curved-beam formula*. Another alternative form of these equations is often referred to as *Winkler's formula*. The variation of stress over the cross section is *hyperbolic*, as sketched in Fig. 5.25c. The *sign convention* applied to bending moment is the same as that used in Section 5.13—namely, the bending moment is positive when directed toward the concave side of the beam, as shown in the figure. If Eq. (5.70) or Eq. (5.71) results in a positive value, a tensile stress is present.

5.15 COMPARISON OF THE RESULTS OF VARIOUS THEORIES

We now examine the solutions obtained in Sections 5.13 and 5.14 with results determined using the flexure formula for straight beams. To do so, we consider a curved beam of rectangular cross section and unit thickness experiencing pure bending. The tangential stress predicted by the elementary theory (based on a linear distribution of stress) is My/I . The Winkler approach, which leads to a hyperbolic distribution, is given by Eq. (5.70) or Eq. (5.71), while the exact theory results in Eqs. (5.67). In each case, the maximum and minimum values of stress are expressed by

$$\sigma_{\theta} = m \frac{M}{a^2} \quad (5.72)$$

Table 5.4 lists values of m as a function of b/a for the four cases cited [Ref. 5.1], in which $b = r_o$ and $a = r_j$ (see Figs. 5.24 and 5.25). As can be seen, there is good agreement between the exact and Winkler results. On this basis, as well as from more extensive comparisons, we may conclude that the Winkler approach is adequate for practical applications. Its advantage lies in the relative ease with which it may be applied to *any* symmetric section.

TABLE 5.4. *The Values of m for Typical Ratios of Outer Radius b to Inner Radius a*

b/a	Flexure Formula	Curved Beam Formula		Elasticity Theory	
		$r = a$	$r = b$	$r = a$	$r = b$
1.3	± 66.67	-72.980	61.270	-73.050	61.350
1.5	± 24.00	-26.971	20.647	-27.858	21.275
2.0	± 6.00	-7.725	4.863	-7.755	4.917
3.0	± 1.50	-2.285	1.095	-2.292	1.130

The agreement between the Winkler approach and the exact analyses is not as good in situations involved combined loading as it is for the case of pure bending. As might be expected, for beams of only slight curvature, the simple flexure formula provides good results while requiring only simple computation. The *linear and hyperbolic stress distributions are approximately the same for $b/a = 1.1$* . As the curvature of the beam increases ($b/a > 1.3$), the stress on the concave side rapidly increases over the one given by the flexure formula.

5.15.1 Correction of σ_θ for Beams with Thin-Walled Cross Sections

Where I-beams, T-beams, or thin-walled tubular curved beams are involved, the approaches developed in this chapter will not accurately predict the stresses in the system. The error in such cases is attributable to the high stresses existing in certain sections such as the flanges, which cause significant beam distortion. A modified Winkler's equation can be applied in such situations if more accurate results are required [Ref. 5.6]. The distortion, and thus the error in σ_θ , is reduced when the flange thickness is increased. Given that material yielding is highly localized, its effect is not of concern unless the curved beam is under fatigue loading.

EXAMPLE 5.13 Maximum Stress in a Curved Rectangular Bar

A rectangular aluminum bar having mean radius \bar{r} carries end moments M , as illustrated in Fig. 5.26. Calculate the stresses in the member using (a) the flexure formula and (b) the curved beam formula.

Given: $M = 1.2 \text{ kN} \cdot \text{m}$, $b = 30 \text{ mm}$, $h = 50 \text{ mm}$, and $\bar{r} = 125 \text{ mm}$.

Solution The subscripts i and o refer to the quantities of the inside and outside fibers, respectively.

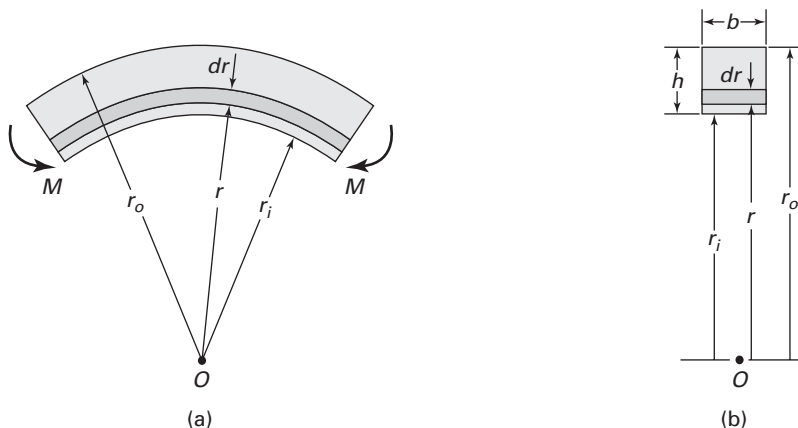


FIGURE 5.26. Example 5.13. (a) Rectangular curved beam in pure bending; (b) cross section.

a. Applying the flexure formula, Eq. (5.38) with $y = h/2$, we obtain

$$\sigma_o = -\sigma_i = \frac{My}{I} = \frac{1200(0.025)}{\frac{1}{12}(0.03)(0.05)^3} = 96 \text{ MPa}$$

This is the result we would get for a straight beam.

b. We first derive the expression for the radius R of the neutral axis. From Fig. 5.26, $A = bh$ and $dA = bdr$. Integration of Eq. (5.68) between the limits r_i and r_o results in

$$R = \frac{A}{\int_A \frac{dA}{r}} = \frac{bh}{\int_{r_i}^{r_o} \frac{bdr}{r}} = \frac{h}{\int_{r_i}^{r_o} \frac{dr}{r}}$$

or

$$R = \frac{h}{\ln \frac{r_o}{r_i}} \quad (5.73)$$

The given data lead to

$$A = bh = (30)(50) = 1500 \text{ mm}^2$$

$$r_i = \bar{r} - \frac{1}{2}h = 125 - 25 = 100 \text{ mm}$$

$$r_o = \bar{r} + \frac{1}{2}h = 125 + 25 = 150 \text{ mm}$$

Then, Eqs. (5.73) and (5.69) yield, respectively,

$$R = \frac{h}{\ln \frac{r_o}{r_i}} = \frac{50}{\ln \frac{3}{2}} = 123.3152 \text{ mm}$$

$$e = \bar{r} - R = 125 - 123.3152 = 1.6848 \text{ mm}$$

Note that the radius of the neutral axis R must be calculated with *five significant* figures.

The maximum compressive and tensile stresses are calculated by using Eq. (5.70) as follows:

$$\begin{aligned} \sigma_i &= \frac{M(R - r_i)}{Aer_i} = \frac{1.2(123.3152 - 100)}{1.5(10^{-3})(1.6848(10^{-3})(0.1))} \\ &= -110.7 \text{ MPa} \\ \sigma_o &= \frac{M(R - r_o)}{Aer_o} = -\frac{1.2(123.3152 - 150)}{1.5(10^{-3})(1.6848(10^{-3})(0.15))} \\ &= 84.5 \text{ MPa} \end{aligned}$$

The negative sign means a compressive stress.

Comment The maximum stress 96 MPa obtained in part (a) by the flexure formula represents an error of about 13% from the more accurate value for the maximum stress (110.7 MPa) found in part (b).

5.16 COMBINED TANGENTIAL AND NORMAL STRESSES

Curved beams are often loaded so that there is both an axial force and a moment on the cross section. The tangential stress given by Eq. (5.70) may then be algebraically added to the stress due to an axial force P acting through the centroid of cross-sectional area A . For this simple case of *superposition*, the total stress at a point located at distance r from the center of curvature O may be expressed as follows:

$$\sigma_{\theta} = \frac{P}{A} - \frac{M(R-r)}{Aer} \quad (5.74)$$

As before, a negative sign would be associated with a compressive load P .

Of course, the theory developed in this section applies only to the elastic stress distribution in curved beams. Stresses in straight members under various combined loads are discussed in detail throughout this text.

The following problems illustrate the application of the formulas developed to statically determinate and statically indeterminate beams under combined loadings. In the latter case, the energy method (Section 10.4) facilitates the determination of the unknown, redundant moment in the member.

CASE STUDY 5.1 Stresses in a Steel Crane Hook by Various Methods

A load P is applied to the simple steel hook having a rectangular cross section, as illustrated in Fig. 5.27a. Find the tangential stresses at points A and B , using (a) the curved beam formula, (b) the flexure formula, and (c) elasticity theory.

Given: $P = 6$ kN, $\bar{r} = 50$ mm, $b = 25$ mm, and $h = 32$ mm.

Solution

a. Curved Beam Formula. For the given numerical values, we obtain (Fig. 5.27b):

$$A = bh = (25)(32) = 800 \text{ mm}^2$$

$$r_i = \bar{r} - \frac{1}{2}h = 50 - 16 = 34 \text{ mm}$$

$$r_o = \bar{r} + \frac{1}{2}h = 50 + 16 = 66 \text{ mm}$$

Then, Eqs. (5.73) and (5.69) result in

$$R = \frac{h}{\ln \frac{r_o}{r_i}} = \frac{32}{\ln \frac{66}{34}} = 48.2441 \text{ mm}$$

$$e = \bar{r} - R = 50 - 48.2441 = 1.7559 \text{ mm}$$

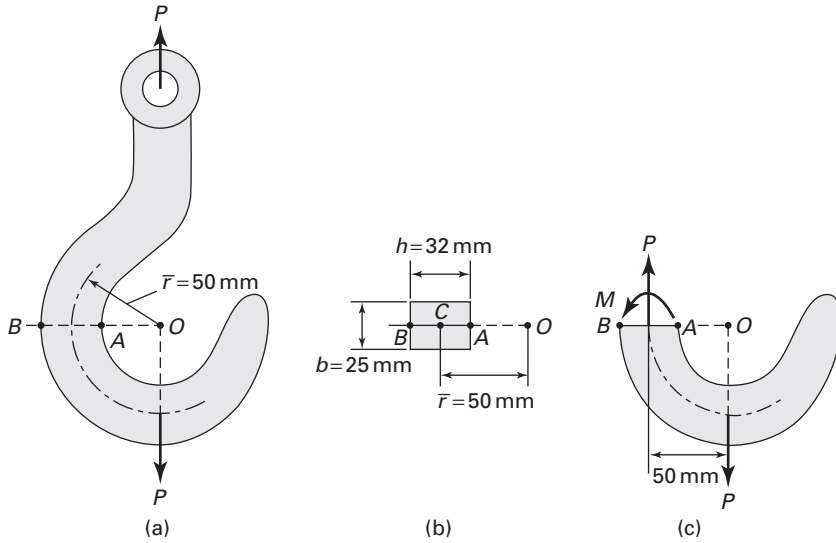


FIGURE 5.27. Case Study 5.1. A crane hook of rectangular cross section.

To maintain applied force P in equilibrium, there must be an axial tensile force P and a moment $M = -P\bar{r}$ at the centroid of the section (Fig. 5.27c). Then, by Eq. (5.74), the stress at the inner edge ($r = r_i$) of the section A – B is

$$\begin{aligned}
 (\sigma_\theta)_A &= \frac{P}{A} - \frac{(-P\bar{r})(R - r_i)}{Aer_i} = \frac{P}{A} \left[1 + \frac{\bar{r}(R - r_i)}{er_i} \right] & (5.75a) \\
 &= \frac{6000}{0.0008} \left[1 + \frac{50(48.2441 - 34)}{(1.7559)(34)} \right] = 97 \text{ MPa}
 \end{aligned}$$

Likewise, the stress at the outer edge ($r = r_o$) is

$$\begin{aligned}
 (\sigma_\theta)_B &= \frac{P}{A} - \frac{(-P\bar{r})(R - r_o)}{Aer_o} = \frac{P}{A} \left[1 + \frac{\bar{r}(R - r_o)}{er_o} \right] & (5.75b) \\
 &= \frac{6000}{0.0008} \left[1 + \frac{50(48.2441 - 66)}{(1.7559)(66)} \right] = -50 \text{ MPa}
 \end{aligned}$$

The negative sign of $(\sigma_\theta)_B$ means a compressive stress is present. The maximum tensile stress is at A and equals 97 MPa.

Comment The stress due to the axial force,

$$\frac{P}{A} = \frac{6000}{0.0008} = 7.5 \text{ MPa}$$

is negligibly small compared to the combined stresses at points A and B of the cross section.

b. Flexure Formula. Equation (5.5), with $M = P\bar{r} = 6(50) = 300 \text{ N} \cdot \text{m}$, gives

$$(\sigma_\theta)_B = -(\sigma_\theta)_A = \frac{My}{I} = \frac{3.00(0.01.6)}{\frac{1}{12}(0.025)(0.032)^3} = 70.3 \text{ MPa}$$

c. Elasticity Theory. Using Eq. (5.66) with $a = r_i = 34 \text{ mm}$ and $b = r_o = 66 \text{ mm}$, we find

$$N = \left[1 - \left(\frac{34}{66} \right)^2 \right]^2 - 4 \left(\frac{34}{66} \right)^2 \ln^2 \left(\frac{66}{34} \right) = 0.0726$$

Superposition of $-P/A$ and the second of Eqs. (5.67) with $t = 25 \text{ mm}$ at $r = a$ leads to

$$\begin{aligned} (\sigma_\theta)_A &= -\frac{6000}{0.0008} + \frac{4(300)}{(0.025)(0.066)^2(0.0726)} \left[\left(1 - \frac{34^2}{66^2} \right) (1+0) - (1+1) \ln \frac{66}{34} \right] \\ &= -7.5 - 89.85 = -97.4 \text{ MPa} \end{aligned}$$

Similarly, at $r = b$, we find $(\sigma_\theta)_B = -7.5 + 58.1 = 50.6 \text{ MPa}$.

Comments The results obtained with the curved-beam formula and with elasticity theory are in good agreement. In contrast, the flexure formula provides a result with *unacceptable* accuracy for the tangential stress in this non-slender curved beam.

EXAMPLE 5.14 Ring with a Diametral Bar

A steel ring of 350-mm mean diameter and of uniform rectangular section 60 mm wide and 12 mm thick is shown in Fig. 5.28a. A rigid bar is fitted across diameter AB , and a tensile force P is applied to the ring as shown. Assuming an allowable stress of 140 MPa, determine the maximum tensile force that can be carried by the ring.

Solution Let the thrust induced in bar AB be denoted by $2F$. The moment at any section $a-a$ (Fig. 5.28b) is then

$$M_\theta = -F\bar{r} \sin \theta + M_B + \frac{P\bar{r}}{2}(1 - \cos \theta) \quad (\mathbf{a})$$

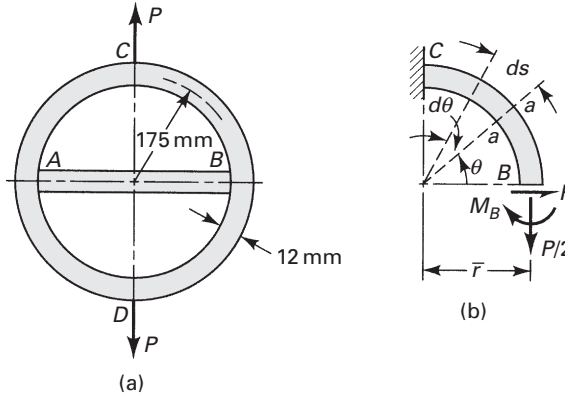


FIGURE 5.28. Example 5.14. (a) Ring with a bar AB is subjected to a concentrated load P ; (b) moment at a section.

Note that before and after deformation, the relative slope between B and C remains unchanged. Therefore, the relative angular rotation between B and C is zero. Applying Eq. (5.32), we obtain

$$EI\theta = 0 = \int_B^C M_\theta dx = \bar{r} \int_0^{\pi/2} M_\theta d\theta$$

where $dx = ds = \bar{r}d\theta$ is the length of beam segment corresponding to $d\theta$. Substituting in Eq. (a), this becomes, after integrating,

$$\frac{1}{2}\pi M_B + \frac{1}{2}P\bar{r}\left(\frac{\pi}{2} - 1\right) - F\bar{r} = 0 \quad (b)$$

This expression involves two unknowns, M_B and F . Another expression in terms of M_B and F is found by recognizing that the deflection at B is zero. By applying Castiglino's theorem,

$$\delta_B = \frac{\partial U}{\partial F} = \frac{1}{EI} \int_0^{\pi/2} M_\theta \frac{\partial M_\theta}{\partial F} (\bar{r} d\theta) = 0$$

where U is the strain energy of the segment. This expression, upon introduction of Eq. (a), takes the form

$$\int_0^{\pi/2} \left\{ -F\bar{r} \sin\theta + M_B + \frac{P\bar{r}}{2}(1 - \cos\theta) \right\} \sin\theta d\theta = 0$$

After integration,

$$-\frac{1}{4}\pi F\bar{r} + \frac{1}{4}P\bar{r} + M_B = 0 \quad (c)$$

Solution of Eqs. (b) and (c) yields

$$M_B = 0.1106P\bar{r}$$

and $FR = 0.4591P\bar{r}$. Substituting Eq. (a) gives

$$M_C = -F\bar{r} + M_B + \frac{1}{2}P\bar{r} = 0.1515P\bar{r}$$

Thus, $M_C > M_B$.

Since $\bar{r}/c = 0.175/0.006 = 29$, the simple flexure formula offers the most efficient means of computation. The maximum stress is found at points A and B :

$$(\sigma_\theta)_{A,B} = \frac{P/2}{A} + \frac{M_{Bc}}{I} = 694P + 13,441P = 14,135P$$

Similarly, at C and D ,

$$(\sigma_\theta)_{C,D} = \frac{M_{Cc}}{I} = 18,411P$$

Hence $\sigma_{\theta C} > \sigma_{\theta B}$, and we have $\sigma_{\max} = 140 \times 10^6 = 18,411P$. The maximum tensile load is therefore $P = 7.604$ kN.

REFERENCES

- 5.1. TIMOSHENKO, S. P., and GOODIER, J. N. *Theory of Elasticity*, 3rd ed. New York: McGraw-Hill, 1970.
- 5.2. UGURAL, A. C. *Mechanics of Materials*. Hoboken, NJ: Wiley, 2008, Chapter 8.
- 5.3. SOKOLNIKOFF, I. S. *Mathematical Theory of Elasticity*, 2nd ed. Melbourne, FL: Krieger, 1986.
- 5.4. COOK, R. D., and YOUNG, W. C. *Advanced Mechanics of Materials*. New York: Macmillan, 1985.
- 5.5. BUDYNAS, R. G. *Advanced Strength and Applied Stress Analysis*, 2nd ed. New York: McGraw-Hill, 1999.
- 5.6. BORESI, A. P., and SCHMIDT, R. J. *Advanced Mechanics of Materials*, 6th ed. Hoboken, NJ: Wiley, 2003.

PROBLEMS

Sections 5.1 through 5.5

- 5.1. A simply supported beam constructed of a 0.15×0.015 m angle is loaded by concentrated force $P = 22.5$ kN at its midspan (Fig. P5.1). Calculate stress σ_x at A and the orientation of the neutral axis. Neglect the effect of shear in bending and assume that beam twisting is prevented.
- 5.2. A wood cantilever beam with cross section as shown in Fig. P5.2 is subjected to an inclined load P at its free end. Determine (a) the orientation of the neutral axis and (b) the maximum bending stress. *Given:* $P = 1$ kN, $\alpha = 30^\circ$, $b = 80$ mm, $h = 150$ mm, and length $L = 1.2$ m.

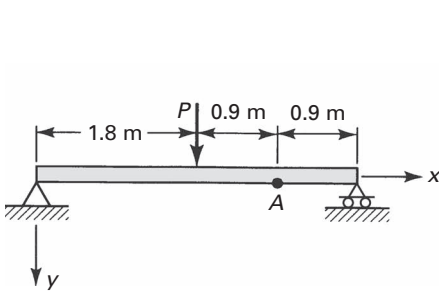


FIGURE P5.1.

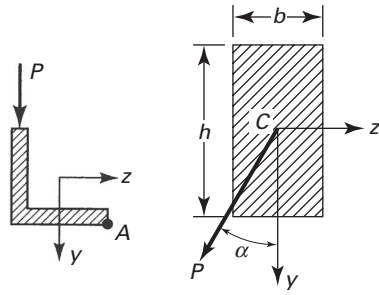


FIGURE P5.2.

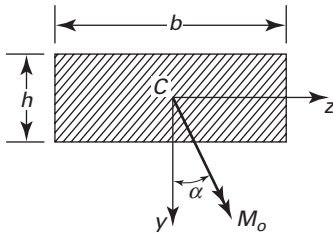


FIGURE P5.3.

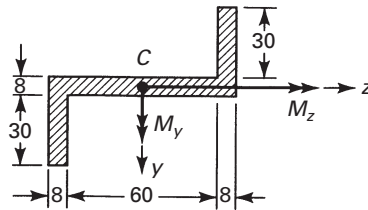


FIGURE P5.4.

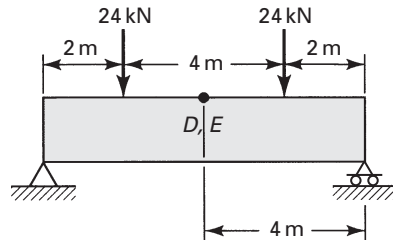
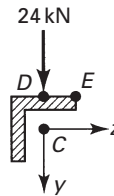


FIGURE P5.5.



- 5.3. A moment M_o is applied to a beam of the cross section shown in Fig. P5.3 with its vector forming an angle α . Use $b = 100 \text{ mm}$, $h = 40 \text{ mm}$, $M_o = 800 \text{ N} \cdot \text{m}$, and $\alpha = 25^\circ$. Calculate (a) the orientation of the neutral axis and (b) the maximum bending stress.
- 5.4. Couples $M_y = M_o$ and $M_z = 1.5M_o$ are applied to a beam of cross section shown in Fig. P5.4. Determine the largest allowable value of M_o for the maximum stress not to exceed 80 MPa. All dimensions are in millimeters.
- 5.5. For the simply supported beam shown in Fig. P5.5, determine the bending stress at points D and E . The cross section is a $0.15 \times 0.15 \times 0.02 \text{ m}$ angle (Fig. 5.4).
- 5.6. A concentrated load P acts on a cantilever, as shown in Fig. P5.6. The beam is constructed of a 2024-T4 aluminum alloy having a yield strength

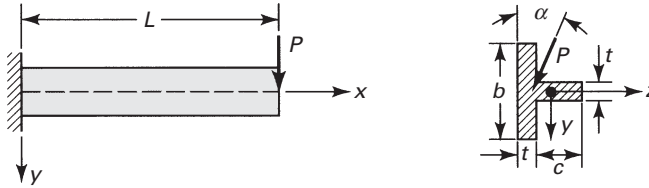


FIGURE P5.6.

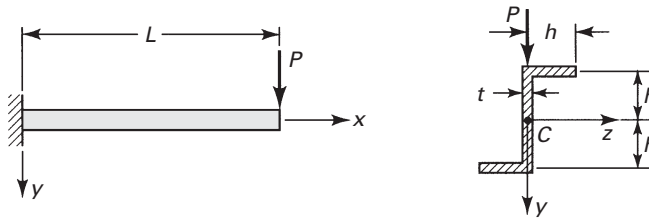


FIGURE P5.8.

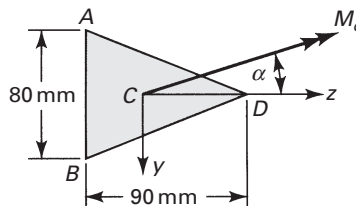


FIGURE P5.9.

$\sigma_{yp} = 290 \text{ MPa}$, $L = 1.5 \text{ m}$, $t = 20 \text{ mm}$, $c = 60 \text{ mm}$, and $b = 80 \text{ mm}$. Based on a factor of safety $n = 1.2$ against initiation of yielding, calculate the magnitude of P for (a) $\alpha = 0^\circ$ and (b) $\alpha = 15^\circ$. Neglect the effect of shear in bending and assume that beam twisting is prevented.

- 5.7. Re-solve Prob. 5.6 for $\alpha = 30^\circ$. Assume the remaining data are unchanged.
- 5.8. A cantilever beam has a Z section of uniform thickness for which $I_y = \frac{2}{3}th^3$, $I_z = \frac{8}{3}th^3$ and $I_{yz} = -th^3$. Determine the maximum bending stress in the beam subjected to a load P at its free end (Fig. P5.8).
- 5.9. A beam with cross section as shown in Fig. P5.9 is acted on by a moment $M_o = 3 \text{ kN} \cdot \text{m}$, with its vector forming an angle $\alpha = 20^\circ$. Determine (a) the orientation of the neutral axis and (b) the maximum bending stress.
- 5.10 and 5.11. As shown in the cross section in Figs. P5.10 and P5.11, a beam carries a moment M , with its vector forming an angle α with the horizontal axis. Find the stresses at points A , B , and D .

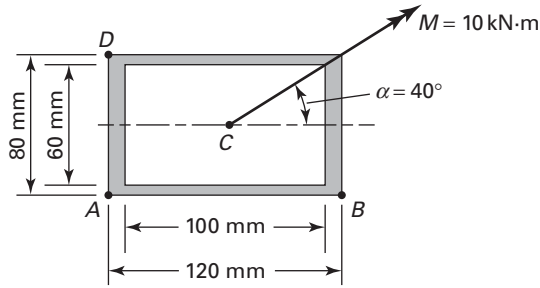


FIGURE P5.10.

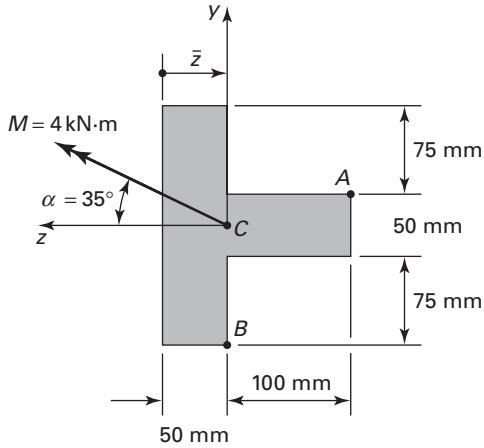


FIGURE P5.11.

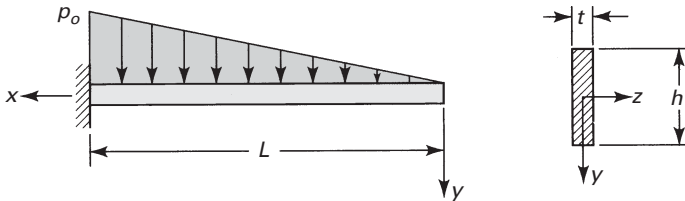


FIGURE P5.12.

5.12. For the thin cantilever shown in Fig. P5.12, the stress function is given by

$$\Phi = -c_1 xy + c_2 \frac{x^3}{6} - c_3 \frac{x^3 y}{6} - c_4 \frac{xy^3}{6} - c_5 \frac{x^3 y^3}{9} - c_6 \frac{xy^5}{20}$$

- Determine the stresses σ_x , σ_y , and τ_{xy} by using the elasticity method.
- Determine the stress σ_x by using the elementary method.
- Compare the values of maximum stress obtained by the preceding approaches for $L = 10h$.

5.13. Consider a cantilever beam of constant unit thickness subjected to a uniform load of $p = 2000$ kN per unit length (Fig. P5.13). Determine the maximum stress in the beam:

a. Based on a stress function

$$\Phi = \frac{p}{0.43} \left[-x^2 + xy + (x^2 + y^2) \left(0.78 - \tan^{-1} \frac{y}{x} \right) \right]$$

b. Based on the elementary theory. Compare the results of (a) and (b).

Sections 5.6 through 5.11

5.14. A bending moment acting about the z axis is applied to a T-beam, as shown in Fig. P5.14. Take the thickness $t = 15$ mm and depth $h = 90$ mm. Determine the width b of the flange needed so that the stresses at the bottom and top of the beam will be in the ratio 3:1, respectively.

5.15. A wooden, simply supported beam of length L is subjected to a uniform load p . Determine the beam length and the loading necessary to develop simultaneously $\sigma_{\max} = 8.4$ MPa and $\tau_{\max} = 0.7$ MPa. Take thickness $t = 0.05$ m and depth $h = 0.15$ m.

5.16. A box beam supports the loading shown in Fig. P5.16. Determine the maximum value of P such that a flexural stress $\sigma = 7$ MPa or a shearing stress $\tau = 0.7$ will not be exceeded.

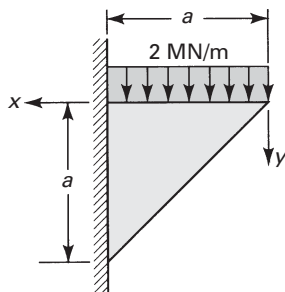


FIGURE P5.13.

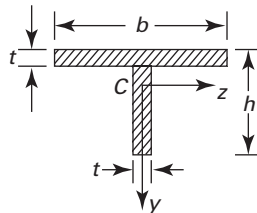


FIGURE P5.14.

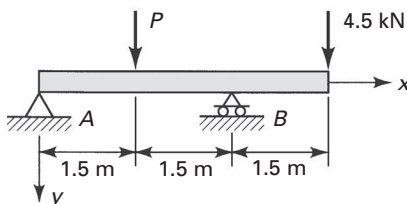
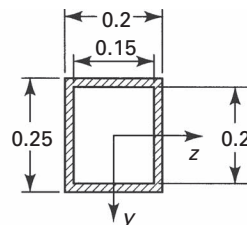


FIGURE P5.16.



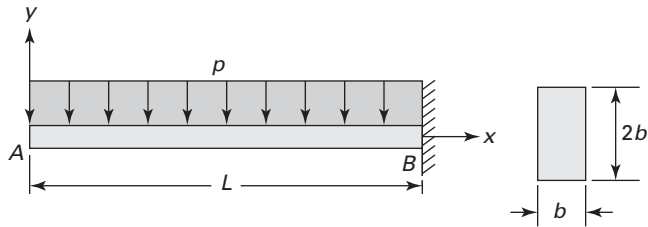


FIGURE P5.17.

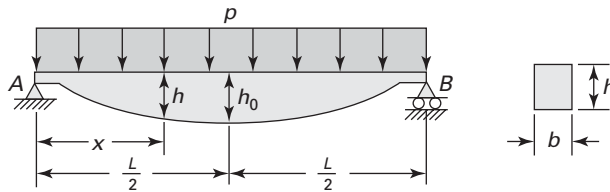


FIGURE P5.18.

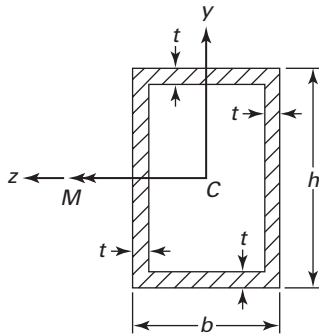


FIGURE P5.19.

- 5.17.** Design a rectangular cantilever beam of constant strength and width b , to carry a uniformly distributed load of intensity w (Fig. P5.17). *Assumption:* Only the normal stresses due to the bending need be taken into account; the permissible stress equals σ_{all} .
- 5.18.** Design a simply supported rectangular beam of constant strength and width b , supporting a uniformly distributed load of intensity w (Fig. P5.18). *Assumption:* Only the normal stresses due to the bending need be taken into account; the allowable stress is σ_{all} .
- 5.19.** A steel beam of the tubular cross section seen in Fig. P5.19 is subjected to the bending moment M about the z axis. Determine (a) the bending moment M and (b) the radius of curvature r_x of the beam. *Given:* $\sigma_{\text{all}} = 150 \text{ MPa}$, $E = 70 \text{ GPa}$, $b = 120 \text{ mm}$, $h = 170 \text{ mm}$, and $t = 10 \text{ mm}$.

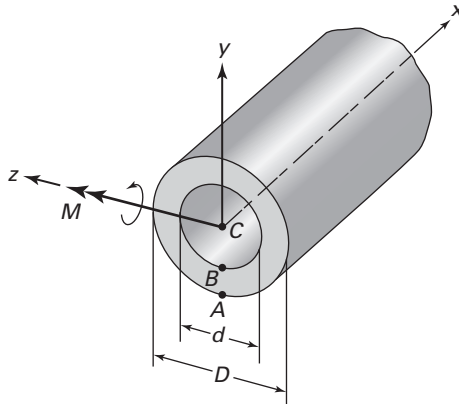


FIGURE P5.20.

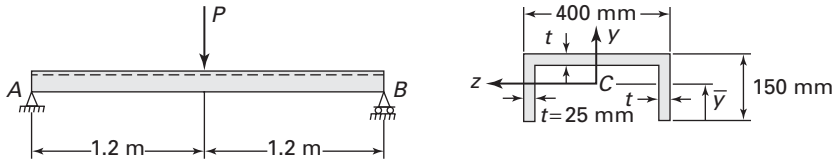


FIGURE P5.21.

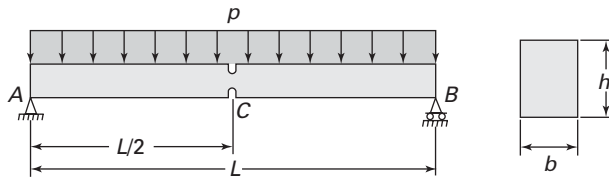


FIGURE P5.22.

- 5.20.** An aluminum alloy beam of hollow circular cross section is subjected to a bending moment M about the z axis (Fig. P5.20). Determine (a) the normal stress at point A , (b) the normal stress at point B , and (c) the radius of curvature r_x of the beam of a transverse cross section. *Given:* $M = 600 \text{ N} \cdot \text{m}$, $D = 60 \text{ mm}$, $d = 40 \text{ mm}$, $E = 70 \text{ GPa}$, and $\nu = 0.29$.
- 5.21.** A simply supported beam AB of the channel cross section carries a concentrated load P at midpoint (Fig. P5.21). Find the maximum allowable load P based on an allowable normal stress of $\sigma_{\text{al1}} = 60 \text{ MPa}$ in the beam.
- 5.22.** A uniformly loaded, simply supported rectangular beam has two 15-mm deep vertical grooves opposite each other on the edges at midspan, as illustrated in Fig. P5.22. Find the smallest permissible radius of the grooves for the case in which the normal stress is limited to $\sigma_{\text{max}} = 95 \text{ MPa}$. *Given:* $p = 12 \text{ kN/m}$, $L = 3 \text{ m}$, $b = 80 \text{ mm}$, and $h = 120 \text{ mm}$.

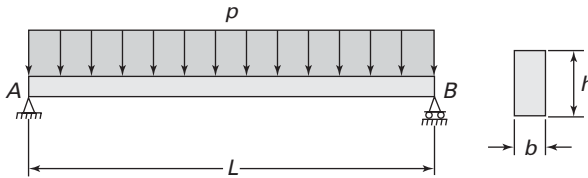


FIGURE P5.23.

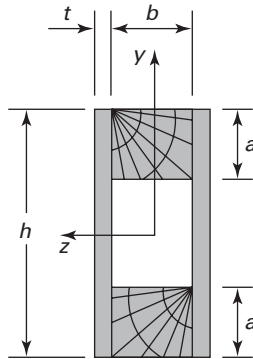


FIGURE P5.25.

- 5.23. A simple wooden beam is under a uniform load of intensity p , as illustrated in Fig. P5.23. (a) Find the ratio of the maximum shearing stress to the largest bending stress in terms of the depth h and length L of the beam. (b) Using $\sigma_{a11} = 9 \text{ MPa}$, $\tau_{a11} = 1.4 \text{ MPa}$, $b = 50 \text{ mm}$, and $h = 160 \text{ mm}$, calculate the maximum permissible length L and the largest permissible distributed load of intensity p .
- 5.24. A composite cantilever beam 140 mm wide, 300 mm deep, and 3 m long is fabricated by fastening two timber planks, 60 mm \times 300 mm, to the sides of a steel plate ($E_s = 200 \text{ GPa}$), 20 mm wide by 300 mm deep. Note that the 300-mm dimension is vertical. The allowable stresses in bending for timber and steel are 7 and 120 MPa, respectively. Calculate the maximum vertical load P that the beam can carry at its free end.
- 5.25. A simple beam pan length 3 m supports a uniformly distributed load of 40 kN/m. Find the required thickness t of the steel plates. *Given:* The cross section of the beam is a hollow box with wood flanges ($E_w = 10.5 \text{ GPa}$) and steel ($E_s = 210 \text{ GPa}$), as seen in Fig. P5.25. Let $a = 62.5 \text{ mm}$, $b = 75 \text{ mm}$, and $h = 225 \text{ mm}$. *Assumptions:* The permissible stresses are 140 MPa for the steel and 10 MPa for the wood.
- 5.26. A 180-mm-wide by 300-mm-deep wood beam ($E_w = 10 \text{ GPa}$), 4 m long, is reinforced with 180-mm-wide and 10-mm-deep aluminum plates ($E_a = 70 \text{ GPa}$) on the top and bottom faces. The beam is simply supported and subject to a uniform load of intensity 25 kN/m over its entire length. Calculate the maximum stresses in each material.

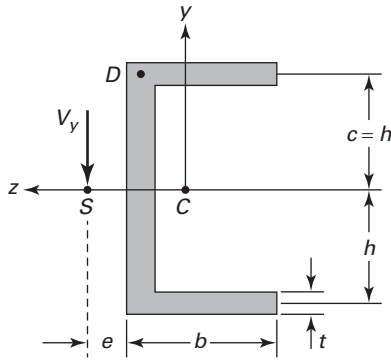


FIGURE P5.29.

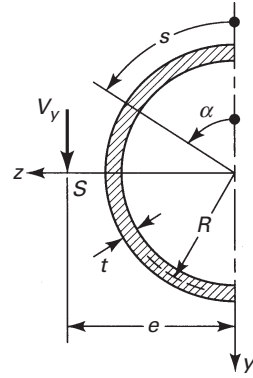


FIGURE P5.30.

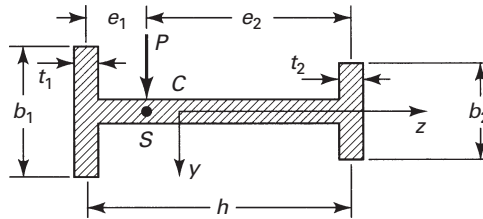


FIGURE P5.31.

- 5.27. Referring to the reinforced concrete beam of Fig. 5.17a, assume $b = 300$, $d = 450$ mm, $A_s = 1200$ mm², and $n = 10$. Given allowable stresses in steel and concrete of 150 and 12 MPa, respectively, calculate the maximum bending moment that the section can carry.
- 5.28. Referring to the reinforced concrete beam of Fig. 5.17a, assume $b = 300$ mm, $d = 500$ mm, and $n = 8$. Given the actual maximum stresses developed to be $\sigma_s = 80$ MPa and $\sigma_c = 5$ MPa, calculate the applied bending moment and the steel area required.
- 5.29. A channel section of uniform thickness is loaded as shown in Fig. P5.29. Find (a) the distance e to the shear center, (b) the shearing stress at D , and (c) the maximum shearing stress. *Given:* $b = 100$ mm, $h = 90$ mm, $t = 4$ mm, $V_y = 5$ kN.
- 5.30. A beam is constructed of half a hollow tube of mean radius R and wall thickness t (Fig. P5.30). Assuming $t \ll R$, locate the shear center S . The moment of inertia of the section about the z axis is $I_z = \pi R^3 t / 2$.
- 5.31. An H-section beam with unequal flanges is subjected to a vertical load P (Fig. P5.31). The following assumptions are applicable:
1. The total resisting shear occurs in the flanges.
 2. The rotation of a plane section during bending occurs about the symmetry axis so that the of curvature of both flanges are equal.
- Find the location of the shear center S .

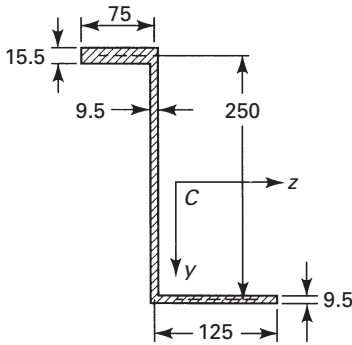


FIGURE P5.32.

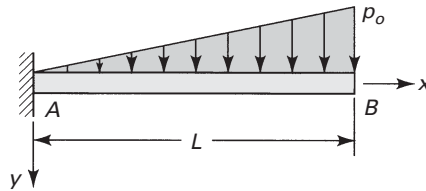


FIGURE P5.33.

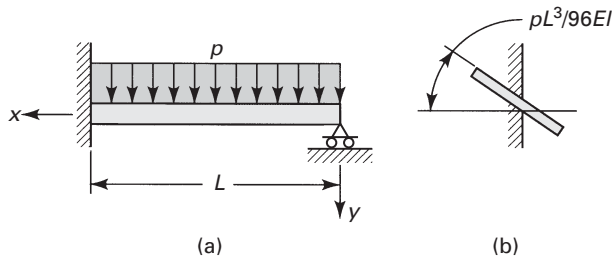


FIGURE P5.34.

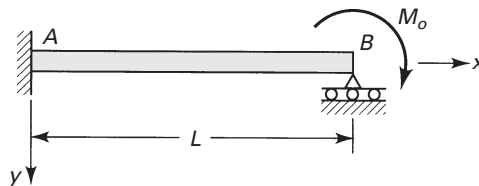


FIGURE P5.36.

- 5.32. Determine the shear center S of the section shown in Fig. P5.32. All dimensions are in millimeters.
- 5.33. A cantilever beam AB supports a triangularly distributed load of maximum intensity p_0 (Fig. P5.33). Determine (a) the equation of the deflection curve, (b) the deflection at the free end, and (c) the slope at the free end.
- 5.34. The slope at the wall of a built-in beam (Fig. P5.34a) is as shown in Fig. P5.34b and is given by $pL^3/96EI$. Determine the force acting at the simple support, expressed in terms of p and L .
- 5.35. A fixed-ended beam of length L is subjected to a concentrated force P at a distance c away from the left end. Derive the equations of the elastic curve.
- 5.36. A propped cantilever beam AB is subjected to a couple M_0 acting at support B , as shown in Fig. P5.36. Derive the equation of the deflection curve and determine the reaction at the roller support.

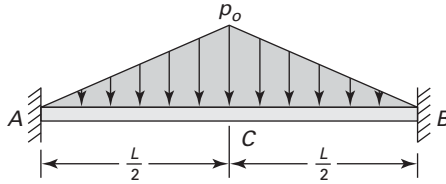


FIGURE P5.37.

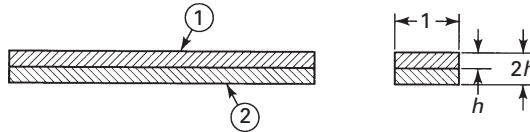


FIGURE P5.38.

- 5.37.** A clamped-ended beam AB carries a symmetric triangular load of maximum intensity p_0 (Fig. P5.37). Find all reactions, the equation of the elastic curve, and the maximum deflection, using the second-order differential equation of the deflection.
- 5.38.** A welded bimetallic strip (Fig. P5.38) is initially straight. A temperature increment ΔT causes the element to curve. The coefficients of thermal expansion of the constituent metals are α_1 and α_2 . Assuming elastic deformation and $\alpha_2 > \alpha_1$, determine (a) the radius of curvature to which the strip bends, (b) the maximum stress occurring at the interface, and (c) the temperature increase that would result in the simultaneous yielding of both elements.

Sections 5.12 through 5.16

- 5.39.** Verify the values of α for cases B, C, and D of Table 5.2.
- 5.40.** Consider a curved bar subjected to pure bending (Fig. 5.24). Assume the stress function

$$\Phi = A \ln r + Br^2 \ln r + Cr^2 + D$$

Re-derive the stress field in the bar given by Eqs. (5.67).

- 5.41.** The allowable stress in tension and compression for the clamp body shown in Fig. P5.41 is 80 MPa. Calculate the maximum permissible load that the member can resist. Dimensions are in millimeters.

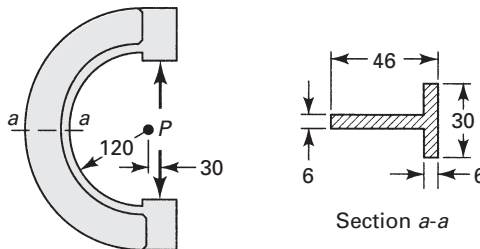


FIGURE P5.41.

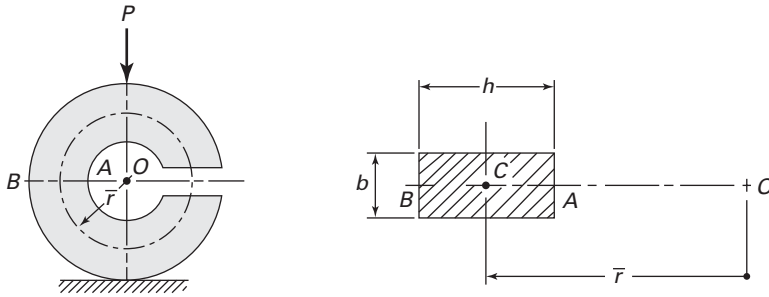


FIGURE P5.42.

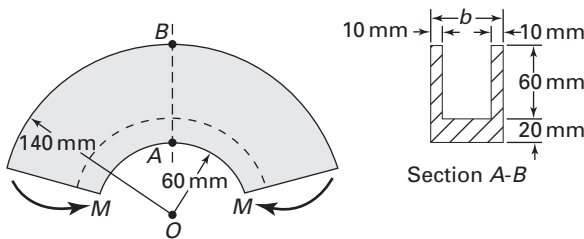


FIGURE P5.43.

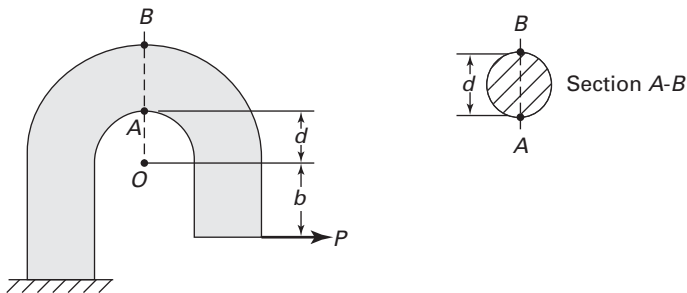


FIGURE P5.44.

- 5.42.** A curved frame of rectangular cross section is loaded as shown in Fig. P5.42. Determine the maximum tangential stress (a) by using the second of Eqs. (5.67) together with the method of superposition and (b) by applying Eq. (5.73). *Given:* $h = 100$ mm, $\bar{r} = 150$ mm, and $P = 70$ kN.
- 5.43.** A curved frame having a channel-shaped cross section is subjected to bending by end moments M , as illustrated in Fig. P5.43. Determine the dimension b required if the tangential stresses at points A and B of the beam are equal in magnitude.
- 5.44.** A curved beam of a circular cross section of diameter d is fixed at one end and subjected to a concentrated load P at the free end (Fig. P5.44). Calculate (a) the tangential stress at point A and (b) the tangential stress at point B . *Given:* $P = 800$ N, $d = 20$ mm, $a = 25$ mm, and $b = 15$ mm.

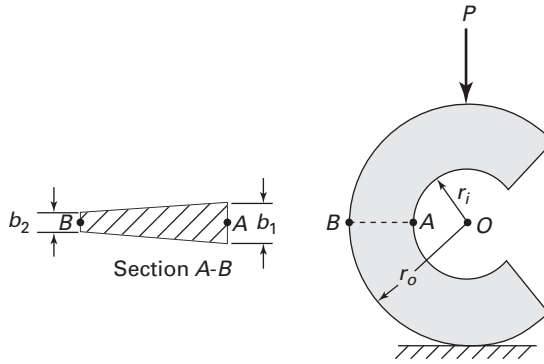


FIGURE P5.45.

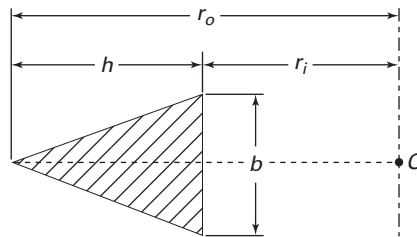


FIGURE P5.46.

- 5.45.** A circular steel frame has a cross section approximated by the trapezoidal form shown in Fig. P5.45. Calculate (a) the tangential stress at point *A* and (b) the tangential stress at point *B*. Given: $r_i = 100$ mm, $b = 75$ mm, $b = 50$ mm, and $P = 50$ kN.
- 5.46.** The triangular cross section of a curved beam is shown in Fig. P5.46. Derive the expression for the radius R along the neutral axis. Compare the result with that given for Fig. D in Table 5.3.
- 5.47.** The circular cross section of a curved beam is illustrated in Fig. P5.47. Derive the expression for the radius R along the neutral axis. Compare the result with that given for Fig. B in Table 5.3.
- 5.48.** The trapezoidal cross section of a curved beam is depicted in Fig. P5.48. Derive the expression for the radius R along the neutral axis. Compare the result with that given for Fig. E in Table 5.3.
- 5.49.** A machine component of channel cross-sectional area is loaded as shown in Fig. P5.49. Calculate the tangential stress at points *A* and *B*. All dimensions are in millimeters.
- 5.50.** A load P is applied to an *eye bar with rigid insert* for the purpose of pulling (Fig. P5.50). Determine the tangential stress at points *A* and *B* (a) by the elasticity theory, (b) by Winkler's theory, and (c) by the elementary theory. Compare the results obtained in each case.

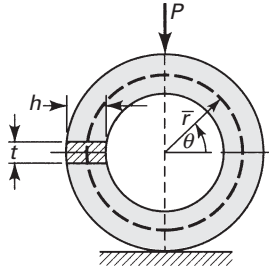


FIGURE P5.51.

where

$$M_{\theta} = 0.182P\bar{r} - \frac{1}{2}P\bar{r}(1 - \cos\theta)$$

Use Castigliano's theorem.

- 5.52.** The ring shown in Fig. P5.51 has the following dimensions: $\bar{r} = 150$ mm, $t = 50$ mm, and $h = 100$ mm. Taking $E = \frac{5}{2}G$, determine (a) the tangential stress on the inner fiber at $\theta = \pi/4$ and (b) the deflection along the line of action of the load P , considering the effects of the normal and shear forces, as well as bending moment (Section 10.4).

Index

A

Absolute maximum shear stress, 46
Adhesion, JKR theory, 170–171
Advanced material, 85
Airy's stress function, elasticity problems, 141–143
Allowable stress, 7
Almroth, B.O., 569
Aluminium, 85
Angle of twist, 317, 324, 335–337, 348–349
Angular speed, rotating disks, 446
Anisotropy, 84, 96
Annular disk, rotating, 447, 459
Antiplane strain, 142–143
Antiplastic surfaces, 246
Asymmetrical cross section, beams, 246–251
Autofrettage, 623
Avallone, E. A., 117, 711
Axial
 biaxial tension, 621
 loading, 227
 rigidity, 94
 triaxial stress, 12–13, 42, 45, 98, 200
 uniaxial stress, 13, 92–93, 218–221
 uniaxial tension, 108
Axially loaded bars, 111–112, 387–389
Axis of symmetry, 689, 692
Axisymmetric elements
 finite element solution for, 464–465
 stresses in circular plates, 648–650
Azar, J. J., 568

B

Bar elements
 Castigliano's theorem for, 500
 numerical method for, 379–383

Bar springs, 348–351
Bars, torsion. *see* Torsion, prismatic bars
Bathe, K.I., 423, 673
Baumeister III, T., 117, 711
Beam column, 554, 556
Beams, bending
 analysis of perfectly plastic, 590–600
 applying Castigliano's theorem to, 500, 510–511
 asymmetrical section of, 246–251
 cantilever, 145–146, 251–254, 269, 278
 composite, 270–276
 of constant strength, 267–268
 curvature of, 245
 curved, 286–299
 elasticity theory applied to, 286–289
 kinematic relations of, 244–246
 normal and shear stresses on, 260–268
 numerical methods for, 393–399
 plastic deflection, 588–590
 pure bending, 289
 shear center and, 276–281
 strain energy in, 113, 284–286
 stresses in sandwich, 653–654
 table of deflections and, 705–706
 tangential and normal stresses on, 296–300
 Timoshenko beam theory, 246
 under torsion, 348–349, 373–377
 transverse normal stress on, 268–270
Beams, elastic foundations
 classification of, 484–485
 finite, 483–484

 general theory for, 473–474
 grid configurations for, 490–492
 infinite, 475–480
 semi-infinite, 480–483
 solution by finite differences, 488–490
 solutions for relatively stiff, 486–488
 supported by elastic elements, 485–486
Becker, S. J., 466
Bending
 beams. *see* Beams, bending
 charts of bars/shafts in, 707–710
 elementary bending theory. *see* Elementary bending theory
 impact, failure criteria, 227–230
 pure bending. *see* Pure bending of thin plates, 636, 640
Bernoulli-Euler law, 246
Betti, E., 499
Bifurcation point, 535
Biharmonic equation, 141
Body forces, 2
Boley, B. A., 181
Bonded gages, foil and wire, 103–104
Boresi, A. P., 51, 117, 181, 300, 423
Boundary conditions
 applied to plates, 642–644
 elasticity theory and, 287–288
 numerical methods for, 373–377
 three-dimensional problems and, 49–50
 in torsion problems, 326–327, 348
 in two-dimensional problems, 136, 138
Boundary value problem, elasticity, 133
Bradley, G. S., 117

- Bredt's formulas, 341
 Bridget, F. J., 569
 Brittle material, 86, 88
 Broek, D., 232
 Brush, D. O., 569
 Buckling
 of columns, 549–550, 552
 energy methods applied to, 554–562
 by finite differences, 562–567
 intermediate columns and inelastic, 544
 load, 535
 modes of, 538–539
 of pin-ended columns, 536–538
 Buckling formula, Euler's, 538
 Budynas, R. G., 181, 300, 354, 711
 Bulk modulus, 98
 Burr, A. H., 524
- C**
- CAD (computer-aided design) software, 423
 CAE (computer-aided engineering), 423
 Calculations, engineering, 680
 Cantilever beams
 bending of, 251–254, 259, 278
 Castigliano's theorem for, 510–511
 plane stress in, 414–418
 solving deflection problems, 373–374, 519–522
 Cartesian representations, plane stress, 25–26
 Case studies
 in plane stress, 414–422
 in analysis, 7–8
 Cast irons, 84–85
 Castigliano's theorem
 applied to bars, beams and trusses, 500–501
 applied to strain energy, 284–286
 fictitious loads and, 501–506
 Central differences, numerical methods, 366–368
 Ceramics, 85
 Cheatham, J. B., 524
 Chong, K. P., 51
 Chou, P. C., 51, 117
 Circular
 axisymmetrically loaded plates, 648–650
 bars in torsion, 112–113, 316–321, 351–354
 contact, 171
 cylinders and thermal stresses, 460–464
 Classification, of columns, 543–544
 Clauser, H. R., 117
 Cold working, 92, 194
 Collapse load, plastic, 600–605
 Columns
 buckling of pin-ended, 536–539
 critical load of, 534–535
 deflection response of, 539–540
 design formulas for, 548–550
 with different end conditions, 540–543
 eccentrically loaded, 552–554
 energy methods applied to buckling, 554–562
 imperfections in, 550–552
 inelastic behavior and, 540
 Johnson's buckling criterion for, 546–548
 local buckling of, 552
 long, short and intermediate, 543–544
 solution by finite differences, 562–568
 tangent modulus theory and, 544–546
 Combined stress, 17
 Compatibility equations. *see* Equations of compatibility
 Complete yielding, plastic, 614, 624–626
 Composite areas, moments of centroid, 689–691
 inertia, 692–700
 Composite beams
 equation of neutral axis, 271–272
 of multi materials, 272–276
 stresses in transformed, 272
 transformed section method for, 270–271
 Composites, material, 85
 Compound cylinders, 443–446, 668–670
 Computational tools, numerical methods, 423
 Computer-aided design (CAD) software, 423
 Computer-aided engineering (CAE), 423
 Constant strain triangular (CST), 407
 Constantan, 104
 Contact
 general, 178–181
 pressure for compound cylinders, 443
 spherical and cylindrical, 171–174
 stress distribution, 174–178
 stresses and deflections, 169–171
 Conversion, SI Unit/U.S. Unit, 701–704
 Cook, R. D., 300
 Coordinate transformation, bar element, 380–381
 Coulomb, C. A., 198
 Coulomb-Mohr theory, failure criteria, 207–210
 Cozzarelli, F. A., 118
 Crack, fracture mechanics, 210–213
 Creep curve, 194–195
 Critical load, columns, 534–535, 560–562
 Critical stress, classification of columns, 543–544
 Crotti-Engesser theorem, 508–509
 CST (constant strain triangular), 407
 Curvature, radius of, 245
 Curvature of plates, 636–639
 Curved beam formula, 289–293
 Curved boundaries, numerical methods for, 370–373
 Cylinders
 filament-wound, 666–667
 hydraulic, 34–35, 445
 Cylinders, thick walled compound, 443–446
 failure theories for, 442–443
 finite element solution for, 464–466
 maximum tangential stress, 441–442
 under pressure, 435–441
 stresses in perfectly plastic, 623–627
 thermal stress in long circular, 460–464
 Cylindrical contacts, elasticity, 173–174
 Cylindrical shells, 668–673
- D**
- Da Vinci, Leonardo, 2
 Deflection curve, Rayleigh-Ritz method, 522
 Deflections
 of a beam column, 556–557
 of beams, 373–377
 for columns, 539–540
 contact stresses and, 169–171
 elasticity theory and, 289
 energy method for, 284–286
 equations of plate, 640–641
 perfectly plastic simple beam, 599–600
 plastic deflection of beams, 588–590
 of rectangular plates, 650–652

- Deflections (*cont.*)
of a ring, 512
and slopes of beams, 705
of statically indeterminate
beams, 706
by trigonometric series, 517–522
- Deformation
analysis of stress and, 5
beam kinematics and, 244–245
of plastic, 579–580
plastic axial, 585–588
of a plate in bending, 636
torsion problems and, 324–325
work done in, 497
- Deformational theory, 614
- Degree of static indeterminacy,
282. *see also* Statically
indeterminate systems
- Delta rosette, 106–107
- Design, mechanics of solids, 4–8
- Design formulas, columns, 548–550
- Deviator (distortional) stresses,
114, 579
- Differential equations of
equilibrium, 20
- Dilatation, 93, 98
- Dilatational stress tensor, 113
- Direction cosines, 44, 683–686
- Disks, rotating
of constant thickness, 446–449
disk flywheel, 449–453
elastic-plastic stresses in,
612–614
thermal stresses in thin, 458–459
of uniform stress, 456–458
of variable thickness, 453–456
- Dislocation, 579–580
- Displacement
finite element analysis and,
377–378
finite element solution for thin
plates, 655–657
matrix for two-dimensional
elements, 399–400
Rayleigh-Ritz method, 522
transformation for bar element,
383
- Ductile material, 86–87, 89, 193,
230–232
- Dummy load, energy method,
506–508
- Dynamic loading, 225–226
- E**
- Eccentrically loaded columns,
552–554
- Edge dislocation, 579
- Effective stress, 199, 615
- Eigenfunctions, 539
- Elastic/elasticity
Airy's stress function, 141–143
basic relations in polar
coordinates, 152–157
beam foundations. *see* Beams,
elastic foundations
constants, 96
contact stress distribution,
174–178
contact stresses and deflections,
169–171
elements, beams supported by,
485–486
general contact, 178–181
plane strain, 135–137
plane stress, 138–140
versus plastic material, 91–92
solutions for problems in,
143–148
spherical and cylindrical
contacts, 171–174
strain, stress and matrices,
401–402
stress concentration factors,
163–169
stress distribution acting on a
beam, 161–163
stresses due to concentrated
loads, 157–161
thermal stresses and, 149–152
three-dimensional problems, 134
two-dimensional problems,
134–135, 140–141
- Elasticity theory, beams, 286–289
- Elastic-plastic
strain relations, 621
stresses in rotating disks, 612–614
torque, 606
torsion of circular shafts,
605–609
- Element nodal forces, 410–414
- Elementary bending theory
comparison of results, 253–254,
256
conclusions about, 256–257
method of integration, 258–260
- Elementary formulas. *see*
Mechanics of materials
- Elementary theory of torsion,
circular bars, 316–321
- Ellipsoid, stress, 44
- Elliptical bars, under torsion,
328–331, 372–373. *see also*
Torsion, prismatic bars
- Empirical formulas, columns, 548
- Endurance limit, 217
- Energy, strain, 107–110
- Energy methods
applied to buckling columns,
554–562
for the bar element, 379–380
Castigliano's theorem, 499–506
Crotti-Engesser theorem, 508–509
for deflection of beams,
284–286
deflections by trigonometric
series, 517–522
principle of minimum potential
energy, 515–517
principle of virtual work,
514–515
Rayleigh-Ritz method, 522–524
reciprocity theorem, 498–499
stability of columns and, 536
statically indeterminate systems,
510–513
unit-or dummy-load method,
506–508
work done in deformation, 497
- Engesser formula, 545
- Engineering calculations, 680
- Engineering materials, table, 702–703
- Equation of neutral axis, composite
beams, 271–272
- Equations. *see also* Formulas
axial force, 384–386
cubic equation, 39–40, 682–686
for finite differences, 368–370
Hencky's equations, 616–619,
620
stiffness matrix, 383
of thermoelasticity, 149–152
transformation equations,
155–156, 248
- Equations of compatibility
in beams, 286–287
in polar coordinates, 156–157
in solving torsion problem, 325
strain and, 75–76
in thermoelasticity, 149–152
in two-dimensional problems,
137, 141
- Equations of equilibrium
in beams, 286–287
of plate deflection, 640–641
in polar coordinates, 153
Prandtl's membrane analogy,
333–335
of shells, 661–662
in solving torsion problem, 325
in two-dimensional problems,
136, 138
- Equidimensional equation, 455
- Equilateral hyperbola, 454
- Equilateral triangle bar, under
torsion, 331–332
- Equilibrium
conditions of, 8–9
equations. *see* Equations of
equilibrium

- Equilibrium method
 applied to columns, 535
 for the bar element, 379
 Newton's equilibrium method, 514
- Equivalent alternating stress, 221
- Euler, Leonard, 2
- Eulerian coordinates, 73–74
- Euler's buckling formula, 541
- Euler's curve, 544
- Exact theory, beams, 487
- F**
- Faces, sandwich plates, 652
- Factor of safety, 6–7, 213, 546–549
- Failure
 comparison of the yielding theories, 204
 Coulomb-Mohr theory, 207–210
 criteria for metal fatigue, 217–223
 ductile-brittle transition, 230–232
 fatigue life, 223–225
 fatigue: progressive fracture, 216–217
 by fracture, 195–197
 fracture toughness, 213–215
 impact loads, 225–227
 introduction to fracture mechanics, 210–213
 longitude and bending impact, 227–230
 maximum distortion energy theory, 199–200
 maximum principal stress theory, 204–206
 maximum shearing stress theory, 198–199
 Mohr's theory, 206–207
 octahedral shearing stress theory, 200–203
 theories. *see* Theories, failure yield and fracture criteria, 197–198
 by yielding, 193–195
- Fatigue
 criterion table, 218
 failure criteria for metal, 217–223
 failure diagram, 219
 life, 223–225
 strength and endurance limits, 217
 tests, 216–217
- Faupel, J. H., 118, 181, 466, 524, 627, 673
- Fictitious loads, Castigliano's theorem, 501–506
- Filament-wound cylinder, 666–667
- Filletted bars, stress concentration charts, 707
- Finite beams, elastic foundations, 483–484
- Finite differences
 for beams on elastic foundations, 488–490
 boundary conditions, 373–377
 central differences, 366–368
 columns and solution by, 562–568
 curved boundaries, 370–373
- Finite element analysis (FEA)
 axial force equation, 384–386
 for the bar element, 379–383
 for a beam element, 393–399
 case studies in plane stress, 414–422
 computational tools, 423
 for plates, 654–657
 for a triangular finite element, 407–414
 for a truss, 386–393
 for two-dimensional elements, 399–402
- Finite element method (FEM), 3, 402–407
- Fisher, F. E., 118, 181, 466, 524, 627, 673
- Flexural
 center, 276–277
 formula, 244
 loading, 227
 rigidity, 244, 541, 639
- Flugge, W., 492
- Flywheel, disks, 449–453
- Foil gage, 103–104
- Force transformation, bar element, 381–382
- Forces. *see also* by individual types
 axial force equation, 384–386
 boundary conditions of surface forces, 49–50
 force transformation in bar element, 381–382
 force-displacement relations, 386–393
 internal force resultants, 13–17
 Kirchhoff's force, 642
 nodal forces, 379, 410–414
- Form factor, for shear, 285–286
- Formulas. *see also* Equations
 Bredt's formulas, 341
 column, 548–550, 554
 curved beam, 289–293
 Engesser formula, 545
 Euler's buckling formula, 538, 541
 finite element method, 402–407
 flexural, 244, 259, 272
 Johnson's buckling criterion, 546
- Newton's interpolation formula, 369
 secant formula, 552–554, 615
 transfer formula, 692–694
 Winkler's formula, 293
- Formulation, problem/solution, 679–681
- Fourier series, 517–518, 644
- Fracture
 criteria, 197–198
 failure by, 195–197
 mechanics, 210–213
 progressive, 216–217
 toughness, 213–215
- Free-body diagram (FBD), 10, 679
- Fundamental principals, of elasticity, 134–135
- G**
- Gages, strain, 103–105
- Galilei, Galileo, 2
- General contact, elasticity, 178–181
- Generalized Hooke's law, 96–100.
see also Hooke's law
- Generalized plane strain, 142
- Generator, shell, 670
- Geometry, of deformation. *see also* Deformation
 analysis of stress and, 5
 beam kinematics and, 244–245
 torsion problems and, 324–325
- Gerber criterion, fatigue failure, 219
- Gere, J. M., 524, 568
- Goodier, J., 118, 181, 300, 354
- Goodman criterion, for uniaxial stress, 219–220
- Grid configuration, beams, 490–492
- Griffith's theory, failure by fracture, 195
- H**
- Helical springs, 352–354
- Hencky, H., 199
- Hencky's equations, 616–619, 620
- Hertz, H., 169, 181
- Hertz Theory, contact stresses, 170–171
- Hetényi, M., 118, 492
- Hinge, plastic, 593–601, 604
- Hodge, P. G., 627
- Hoffman, O., 627
- Hooke, Robert, 2
- Hooke's law
 for beams in bending, 244, 252
 for bending of thin plates, 638
 generalized, 96–100

Hooke's law (*cont.*)
for orthotropic material,
102–103
for plane stress, 139–140
in polar coordinates, 155
for uniaxial stress, 92–93

Huber, T. M., 199

Hydraulic cylinders, 34–35,
445

Hydrodynamic analogy, 344–346

Hydrostatic stress, 44

Hyperbolic disk, 455–456

I

Impact loads. *see also* Load
basic assumptions, 227
bending, freely falling weight,
227–228

bending, horizontally moving
weight, 228–230

strain rate and, 226

Imperfect column, 540

Incremental theory, 620

Indicial notation, analysis of stress,
50

Inelastic behavior, columns, 540

Inelastic buckling, 544

Inertia moments

parallel axis theorem, 692–694

principal moments of inertia,
694–700

Infinite beams, elastic foundations,
475–480

Inglis, C. E., 167

Initial yielding, plastic, 612

Instability phenomenon, plastic,
582–583

Interaction curves, elastic-plastic,
595–597

Interface pressure, compound
cylinders, 443

Intermediate beams, 485

Internal force resultants, 13–17

Internal forces, 2

Internal friction theory, 207–210

International System of Units (SI),
2, 701–704

Inverse method, 143

Iron, cast iron, 84–85

Irwin, G. R., 232

Isotropic

bending of thin plates, 636

engineering materials, 84

materials and generalized

Hooke's law, 97

sandwich plates, 654

two-dimensional problems,
140–141

Iyengar, K. T., 492

J

Johnson, K. L., 181

Johnson-Kendall-Roberts (JKR)
theory, 170–171

Johnson's buckling criterion,
546–548

K

Kelvin, William Thomas, 2

Kendall, K., 181

Kinematic relations. *see* Strain-
displacement relations

Kirchhoff's force, 642

Knite, E., 423

Kotter, T., 118

Kreyzig, E., 423, 524

L

Lagrange, Joseph-Louis, 2

Lagrangian coordinates, 73–74

Lagrangian energy method, 514

Lame constants, 98

Large strain, 74

Lateral shears, 347

Levy-Mises theory, 621–622

Limit design, plastic loads, 600–605

Linear elasticity, 92

Linear strain triangular (LST)
elements, 407

Linearly elastic material

beams, 473

Castigliano's theorem and, 499

deformation and, 69

unit load method and, 506

Load

axially loaded, 111–112, 387–

389, 585–588

axisymmetrically loaded,
648–650

buckling, 535

collapse, 600–605

critically loaded columns,
534–535, 560–562

eccentrically loaded columns,
552–554

fictitious loads and Castigliano's
theorem, 501–506

Mohr's circle for torsional

loading, 322

repeated loading, 216

stiffness matrix for deflection
bar under combined loading,
405–406

symmetrically loaded shells,
660–662

ultimate load, 601

unit-or dummy-load method,
506–508

Loading rate, ductile-brittle
transition, 231

Local buckling, of columns, 552

Logan, D. L., 423

Logarithmic strain, 88

Long beams, 485

Long columns, 544

Longitude impact, failure criteria,
227–230

Love, A. E. H., 2, 51

LST (linear strain triangular)
elements, 407

M

Magnesium alloys, 85

Marin, J., 232

Material

brittle. *see* Brittle material

ductile. *see* Ductile material

elastic versus plastic, 91–92

engineering materials table,
702–703

isotropic, 97

linearly elastic. *see* Linearly
elastic material

mechanics of. *see* Mechanics of
materials

multi materials beams

(composite), 272–276

orthotropic, 101–103, 139–140

plastic behavior. *see* Plastic/
plasticity

MATLAB (Matrix Laboratory),
423, 712–714

Matrices (strain, stress and
elasticity), 655

Matrix methods, finite element
analysis, 377–378

Maugis, D., 181

Maximum

distortion energy theory,
199–200

principal stress theory, 204–206

radial stress, 448

shearing stress, 198–199

tangential stress, 441–442

M-code, MATLAB, 712–713

Mean strain, 114

Mean stress, 218–219

Measurement, strain, 103–107

Mechanics of materials

problems in elasticity and, 133

stress formulas, 15–17

theory of elasticity and, 1–2

Mechanism of collapse, 600–601

Meguid, S. A., 232

Membrane action, shells, 658–660

Membrane analogy. *see* Prandtl's
membrane analogy

- Membrane-roof analogy, 610–611
Mendelsson, A., 627
Meridian curve, shells, 660
Mesh refinement, 378
Messal, E. E., 686
Metal fatigue, failure criteria, 217–223
Metals, 84–85
Method
 energy methods. *see* Energy methods
 equilibrium. *see* Equilibrium method
 inverse and semi-inverse, 143
 numerical methods. *see* Numerical methods
 offset method, 86
 of sections, 9–10, 270–276, 500
 superposition, 69–70, 282–284
Midsurface, shells, 658
Minimum potential energy, principle of, 515–517
Mises, R. von, 199
Mises-Hencky yield criterion, 200–203, 610
Modes of failure, 192
Modes of force transmission, 14
Modulus
 bulk, 98
 of elasticity, 90, 591
 of the foundation, 473
 of plasticity, 615
 of rupture, 244
 tangent modulus theory, 544–545
 of toughness/resilience, 109
Mohr's circle
 for curvature of plates, 638
 for plane strain, 80–83
 three dimensional stress, 45–49
 for torsional loading, 322
 two-dimensional stress, 28–35
Mohr's theory, failure criteria, 206–207
Mollick, L., 466
Moment
 bending, twisting, 14, 642
 force and moment over the ends of a bar, 327–333
 of inertia. *see* Inertia moments
 plane stresses and, 638–639
 plastic, 592
 sign convention for, 243, 639
- N**
Nadai, A., 232, 627
Navier, L., 2, 644
Necking, 86
Neuber, H. P., 167, 181
- Neutral
 axes, 244
 axis equation, composite beams, 271–272
 equilibrium, 535
Newton, Sir Isaac, 2
Newton's equilibrium method, 514
Newton's interpolation formula, 369
Nodal forces, 379, 410–414
Nodes, unevenly spaced, 567–568
Nonlinearly elastic, 91, 499, 508–509
Normal strain, 70
Normal stress
 bending of beams and, 260–268
 on an oblique plane, 42–43
 shear stresses versus, 10
 strain energy density for, 108–109
 tangential stresses combined with, 296–300
 transverse normal, 268–270
 transverse normal stress, 268–270
Numerical accuracy, solving problems, 680
Numerical methods
 for an arbitrarily oriented bar element, 380–383
 axial force equation, 384–386
 for a bar element, 379–380
 for a beam element, 393–399
 for boundary conditions, 373–377
 for case studies in plane stress, 414–422
 central differences, 366–368
 computational tools, 423
 for curved boundaries, 370–373
 finite difference equations, 368–370
 finite differences, 365
 finite element fundamentals, 377–378
 finite element method formula, 402–407
 force-displacement relations, 386–393
 for a triangular finite element, 407–414
 for two-dimensional elements, 399–402
- O**
Oblique plane, stresses on, 42–45
Octahedral shearing stress theory, 200–203
Octahedral stress, 44–45
Offset method, 86
- Orthogonality function, 518–519
Orthotropic materials, strain, 101–103, 139–140
Osgood, W. R., 581, 627
Out-of-plane principal strain, 139
- P**
Paez, T. L., 232
Pagano, N. J., 51, 118
Parallel-axis theorem, 692–694
Park, F. R., 466
Partial yielding, plastic, 612–613, 626–627
Particle mechanics, 514
Pawlik, P. S., 51
Peak compressive stress, 275
Pearson, K., 51, 354
Perfectly plastic
 beams, 590–600
 stresses in a flat disk, 612–614
 stresses in thick-walled cylinder, 623–627
Permanent set/strain, 91
Perry, D. J., 568
Pierro, A. G., 232
Pilkey, W. D., 181, 711
Pin-ended columns, buckling, 536–539, 541
Pivot points, 365
Plane strain
 elasticity, problems in, 135–137
 generalized, 142
 Mohr's circle for, 80–83
 in a plate, 73–74
 transformation of, 23
 two-dimensional, 70–72
Plane stress
 bending of beams and, 257
 in a cantilever beam, 414–418
 elasticity, problems in, 138–140
 finite element applied to, 418–421
 on inclined planes, 321–324
 introduction to, 13
 plane-stress transformation, 23–26
 in a thick walled cylinder, 436
 three-dimensional, 40
 transformation of, 23–26
Planes
 inclined planes, 321–324
 slip planes, 193
 of symmetry, orthotropic materials, 101–103
Plastic/plasticity
 axial deformation, 585–588
 behavior of material, 578–579
 collapse load of structures, 600–605

- Plastic/plasticity (*cont.*)
 deflection of beams, 588–590
 deformation, 84, 579–580
 elastic material versus, 91–92
 elastic-plastic stresses in
 rotating disks, 612–614
 elastic-plastic torsion, 605–609
 hinge, 593–601, 604
 idealized stress-strain diagrams,
 580–582
 instability in simple tension,
 582–584
 perfectly plastic beams,
 590–600
 range, 88
 stresses in perfectly plastic
 cylinders, 623–627
 stress-strain relations, 614–623
 torsion: membrane analogy,
 610–611
 types of materials, 85
- Plate stress
 axisymmetrically loaded
 circular, 648–650
 basic assumption of, 635–636
- Plate stress (*cont.*)
 boundary conditions of,
 642–644
 with circular holes, 165–168
 curvature, and moment relations
 of, 638–639
 deflections of rectangular,
 650–652
 finite element solution for,
 654–657
 governing equations of plate
 deflection, 640–641
 sandwich, 652–654
 simply supported rectangular,
 644–647
 strain-curvature relations of,
 636–638
- Poisson, S. D., 92–93
 Poisson's ratio, 92–93, 579
- Polar coordinates, basic relations
 in, 152–157
- Polar representations, plane stress,
 25
- Polycrystalline structural metals,
 failure, 193, 196
- Polynomial solutions, 144–148
- Potential energy, 515–517
- Power transmission, shafts in,
 323–324
- Prandtl's membrane analogy
 equation of equilibrium,
 333–335
 plastic torsion, 610–611
 shearing stress and angle of
 twist, 335–337
- Prandtl's stress function
 boundary conditions of,
 326–327
 force and moments over the
 ends, 327–333
- Pressure
 contact, 443
 cylinders under, 435–441
- Principal moments of inertia,
 694–700
- Principal of superposition, 69. *see*
also Superposition
- Principal stresses
 maximum in-plane shear stress
 and, 26–28
 Mohr's circle and, 29–30
 solving cubic equations,
 682–686
 in three dimensions, 38–42
- Prismatic bars, torsion. *see*
 Torsion, prismatic bars
- Problem formulation/solution,
 679–681
- Progressive fracture, fatigue,
 216–217
- Proportional limit, 83
- Pure bending
 of asymmetrical section of
 beam, 246–251
 of inelastic beam, 588
 of perfectly plastic beams,
 590–591
 of plates, 638, 650–651
 strain energy for beam in, 113
 of symmetrical section of beam,
 242–246
- Pure shear, 13, 92
- Q**
 Quinney, H., 232
- R**
 Radial interference, 443
 Radial stress, 450
 Radians per second, rotating disks,
 446
- Radius
 of curvature of beams, 245
 of curvature of shells, 658
 of gyration, 542, 692
- Ramberg, W., 627
- Ramu, S. A., 492
- Range stress, 218
- Rankine, W. J. M., 204
- Ranov, T., 466
- Rayleigh, Lord, 499, 522
- Rayleigh-Ritz method, 522–524
- Reciprocity theorem, 498–499
- Rectangular bar, torsion of, 332–
 333, 338–340
- Rectangular plates, stresses in,
 644–647, 650–652
- Rectangular rosette, 106–107
- Reddy, J. N., 524
- Reismann, H., 51
- Repeated loading, 216
- Residual rotation, elastic-plastic,
 608–609
- Residual strain, 91
- Residual stress
 elastic-plastic torsion and,
 608–609
 inelastically bent beam and, 592
 perfectly plastic cylinders and,
 623
 plastic axial deformation and,
 585–588
 in rectangular beam, 598
- Revolution, shells of
 circular cylindrical, 664–667
 conical, 663
 spherical, 662–663
 symmetrically loaded, 660–662
- Right-hand screw rule, 14
- Rigid-plastic material, 580, 588,
 615
- Robert Hooke, 92
- Roberts, A. D., 181
- Rotating disks. *see* Disks, rotating
- Rotational inertia, 246
- Rupture stress, 86
- S**
 Sachs, G., 627
 Sadegh, A. M., 117, 181, 354, 711
 SAE relation, 219
 Saint-Venant's principle, 115–117
 Saint-Venant, semi-inverse method,
 324–325
- Sand hill analogy, 611
- Sandwich plates, stresses in,
 652–654
- Schmidt, R. J., 117, 181, 300, 423
- Screw dislocation, 579
- Secant formula, 552–554, 615
- Semi-infinite beams, elastic
 foundations, 480–483
- Semi-inverse method, 143
- Shaffer, B. W., 492
- Shafts
 stress concentration charts,
 708–710
 transmission of power by,
 323–324
- Shames, I. H., 118
- Shape factor, 593
- Shear, form factor for, 285–286

- Shear, pure, 13, 92
 Shear center, beams, 276–281
 Shear deformation, 109, 246
 Shear flow, 261, 279
 Shear stress
 absolute maximum, 46
 axial shear, 320–321
 bending of beams and, 260–268
 elementary theory of torsion
 and, 317
 equality of, 12
 fluid flow analogy and, 345
 formula for, 261
 lateral, 347
 maximum in-plane, 26–28
 normal stress versus, 10
 oblique plane and, 42–45
 Prandtl's membrane analogy,
 335–337
 sign convention for, 640
 strain energy density for,
 108–109
 torsional, 335–337, 347
 transverse shear, 320–321
- Shells, stress in
 cylindrical, of general shape,
 670–673
 examples of revolution,
 662–667
 simple membrane action of,
 658–660
 symmetrically loaded, 660–662
 theories and behavior of,
 657–658
 thermal stresses in compound
 cylinders, 668–670
- Shock loads, 225–226
 Short beams, 484
 Short columns, 544, 554
 Shrink-fit performance analysis,
 disk flywheel, 451–452
 Shrinking allowance, 443
 SI (International System of Units),
 2, 701–704
 Sign convention, stress, 11, 243
 Slenderness ratio, 542
 Slip action, 579
 Slip planes, failure by yielding,
 193
 Slope, 257
 Small deflection theory
 of bending, 636–637
 of sandwich plates, 653
 of shells, 658
- Sokolnikoff, I. S., 51, 117, 181,
 300, 524
 Solderberg criterion, 219, 222
 Solid disks, rotating, 448–449,
 459
 Solving problems, 679–681
- Spherical contacts, elasticity,
 171–173
 Spring constant, 227
 Spring rate, 94
 Springs
 bar springs, 348–351
 helical springs, 352–354
- Stable equilibrium, 515, 535
 Stainless steels, 85
 Statically indeterminate systems
 applying energy methods to,
 510–513
 axially loaded, 585–588
 bending of beams and, 281–284
 deflections of beams, 706
 infinite beams and, 474
 statically determinate systems
 versus, 9
- Steady-state creep, 195
 Steels, 84–85
 Sternberg, E., 118
 Stiff beams, elastic foundations,
 486–488
- Stiffness matrix
 the assembly process for,
 386–387
 for a beam element, 393–399
 for a cantilever beam, 415–416
 for deflection bar under
 combined loading, 405–406
 equilibrium method and the, 379
 governing equations and the,
 383
 nodal forces of a plate segment,
 412–413
 for a stepped axially loaded
 bar, 388
 for thin plates, 657
 for a three-bar truss, 390–391
 for triangular finite element,
 410
 for a truss bar, 385
- Stiffness method, finite element
 analysis, 377–378
- Strain
 antiplane strain, 142–143
 definition of, 70
 effective strain, 615
 elastic versus plastic behavior,
 91–92
 energy. *see* Strain energy
 equations of compatibility,
 75–76
 Eulerian and Lagrangian
 coordinates, 73–74
 hardening, 92, 194, 580–581
 Hooke's law and Poisson's ratio,
 92–100
 large strain, 74
 LST and CST elements, 407
- material properties and, 68
 matrices, 401–402
 measurement of, 103–107
 Mohr's circle for plane strain,
 80–83
 normal strain, 70
 orthotropic materials, 101–103
 permanent and residual strain,
 91
 plane strain. *see* Plane strain
 rate, 226
 Saint-Venant's principle,
 115–117
 state of strain at a point, 76
 stress-strain diagrams, 83–90,
 580–582
 stress-strain relations, 614–623
 superposition, 69–70
 thermal strain, 149–152
 three-dimensional. *see* Three-
 dimensional strain
 transformation, 76–80
 true and logarithmic strain, 88
 two-dimensional. *see* Two-
 dimensional strain
- Strain energy
 for axially loaded bars, 111–112
 in beams, 284–286
 for beams in bending, 113
 Castigliano's second theorem,
 284–286
 of circular bars in torsion,
 112–113
 in common structural members,
 111
 components of, 113–115
 deflections by strain energy
 method, 650–652
 deflections by trigonometric
 series, 518
 for normal and shear stresses,
 108–109
 for three-dimensional stresses,
 110
 variation in, 514–515
- Strain-displacement relations
 bending of beams and, 244–246
 in large (finite) strains, 74
 in plate bending, 636–638
 in polar coordinates, 154–155
 in three-dimensional problems,
 72, 78–80
 in two-dimensional problems,
 76–78
- Strength coefficient, 581
- Stress
 bending of beams and, 260–268
 boundary conditions of surface
 forces, 49–50
 combined stress, 17

- Stress (*cont.*)
 concentration. *see* Stress concentration
 conditions of equilibrium, 8–9
 contact stresses, 169–171
 critical stress in columns, 543–544
 cubic equation, 39–40
 definitions and components, 9–13
 dilatational stress, 113
 distortional (deviator) stress, 114, 579
 distribution. *see* Stress distribution
 effective, 199, 615
 elastic-plastic stresses in rotating disks, 612–614
 function, Airy's, 141–143
 function, Prandtl's. *see* Prandtl's stress function
 historical development of stress analysis, 2–3
 idealized stress-strain diagrams, 580–582
 on inclined planes, 17–19, 321–324
 indicial notation, 50
 intensity factors, 211–213
 matrices, 401–402
 maximum in-plane shear, 26–28
 maximum shearing stress theory, 198–199
 mean stress, 218–219
- Stress (*cont.*)
 mechanics of materials/theory of elasticity, 1–2
 methods for design and, 4–8
 Mohr's circle for two-dimensional, 28–35
 Mohr's circle in three dimensions, 45–49
 normal stress. *see* Normal stress on an oblique plane, 42–45
 octahedral shearing stress, 200–203
 perfectly plastic thick-walled cylinders, 623–627
 plane stress. *see* Plane stress plates and. *see* Plate stress
 principal stress theory, 204–206
 principal stresses and cubic equations, 682–686
 principal stresses in three dimensions, 38–42
 problems in stress analysis, 315–314
 pure shear, 13
 range stress, 218
 relaxation, stress, 195
 residual stress. *see* Residual stress
 resultants, 13–17, 24, 33
 in rotating disks, 612–614
 shear stress. *see* Shear stress
 shells and. *see* Shells, stress in
 sign convention, 11, 243
 strain energy for normal and shear stresses, 108–109
 strain energy for three-dimensional stresses, 110
 stress-strain diagrams, 83–90, 580–582
 stress-strain relations, 614–623
 tangential stress. *see* Tangential stress
 tensor, 12
 thermal stress. *see* Thermal stress
 three-dimensional transformation, 35–38
 trajectories, 25
 in transformed composite beams, 272
 triaxial stress. *see* Triaxial stress
 uniaxial stress. *see* Uniaxial stress
 variation within a body, 20–22
- Stress concentration
 for disk flywheel, 450
 elasticity problems, 157–169
 fluid flow analogy and, 344–346
- Stress cubic equation, 682–686
- Stress distribution
 charts of bars/shafts and, 707–710
 concentrated load, acting on a beam, 161–163
 contact stress distribution, 174–178
 elasticity theory and, 288–289
 pure bending of beams, asymmetrical, 248
- Stress-strain diagrams, 83–90, 580–582
- Stress-strain relations, 139–140
- Sullivan, J. L., 232
- Sundara, R., 492
- Superposition, 69–70, 282–284, 450
- Surface forces, 2, 49–50
- Symmetrical cross section, beams, 242–246
- Symmetrically loaded shells, 660–662
- Systems of units, 2
- T**
- Tangent modulus theory, columns, 544–546
- Tangential stress
 curved beams and, 291–293
 disk flywheel under, 450–452
 normal stress combined with, 296–300
 thick walled cylinders under, 441–442
- Tangential stress in cylinders, 441–442
- Taylor, G. L., 232
- Taylor, R. I., 423, 466, 673
- Temperature
 ductile-brittle transition and, 230–231
 stress-strain properties and effects of, 90
- Tension, plastic, 582–584
- Theories
 and behavior of shells, 657–658
 elementary theory of torsion, 316–321
 small deflection theory for plates, 636
 theory of elasticity, 1–2, 133
- Theories, bending of beams
 comparison of, 293–296
 elementary bending theory, 246, 253–254, 256
 Timoshenko beam theory, 246
- Theories, columns
 Johnson's buckling criterion, 546–548
 tangent modulus theory, 544–546
- Theories, failure
 comparison of yielding, 204
 Coulomb-Mohr, 207–210
 maximum distortion energy, 199–200, 625
 maximum principal stress, 204–206
 maximum shear stress, 198, 625
 Mohr's, 206–207
 octahedral shearing stress, 200–203
 for thick walled cylinders, 442–443
- Thermal stress
 in compound cylinders, 668–670
 elasticity, problems in, 149–152
 in long circular cylinders, 460–464
 in thin rotating disks, 458–459
- Thermoelasticity, 149–152
- Thermoplastic, 85
- Thermosets, engineering materials, 85
- Thick walled cylinders. *see* Cylinders, thick walled
- Thin disks, thermal stresses, 458–459
- Thin plates, bending of, 636

- Thin-walled (plate and shell) structures, 8
- Thin-walled cylinders, 435–436
- Thin-walled sections
 restrained, in torsion, 346–347
 shear center in, 277–281
 torsion of multiply connected, 340–344
- Thin-walled vessels, 15–16, 32–33
- Three-dimensional strain
 for orthotropic materials, 139–140
 overview of, 72
 transformation of, 78–80
- Three-dimensional stress invariants for, 40–42
 Mohr's circle and, 45–46
 principal stresses in, 38–40
 strain energy density for, 110
 transformation of, 35–38
- Timoshenko, S. P., 3, 51, 118, 181, 232, 300, 354, 524, 568, 673
- Timoshenko beam theory, 246
- Ting, B. Y., 492
- Titanic case study, 231–232
- Todhunter, I., 51, 354
- Torque diagram, 317
- Torque-displacement relations, 320
- Torsion
 charts of bars/shafts in, 707–709
 elementary theory of, 316–321
 formula, 112, 317
 plastic behavior of materials, 605–611
 torsional rigidity, 317, 330
 torsional shear, 347
- Torsion, prismatic bars
 bar springs, 350–351
 of bar with square cross-section, 368–370
 basic formulas for stress, 15–16
 of circular bars, 316–321
 of curved circular bars, 351–354
 of elliptical bar, 328–331, 372–373
 of equilateral triangle bar, 331–332
 fluid flow analogy, 344–346
 general solution to, 324–326
 introduction to, 315–316
 of narrow rectangular section, 338–340
 Prandtl's membrane analogy, 333–337
 Prandtl's stress function, 326–333
 of a rectangular bar, 332–333
 of a rectangular tube, 342–343
 of a stepped bar, 336–337
- strain energy for axially loaded bars, 111–112
 of stresses on inclined planes, 321–324
 of thin-walled sections, 340–344, 346–349
 of a three-cell tube, 343–344
- Total strain theory, 614
- Transfer formula, 692–694
- Transformation equations, 155–156, 248
- Transformed section method, composite beams, 270–276
- Transition, ductile-brittle, 230–232
- Transverse stress
 normal, 268–270
 shear, 320–321
- Tresca yield criterion, 198, 612
- Triangular element, numerical method for, 407–414
- Triaxial stress, 12–13, 42, 45, 98, 200, 231
- Triaxiality, ductile-brittle transition, 231
- Trigonometric functions, 680
- Trigonometric series, 483, 517–522
- True factor of safety, 6–7
- True stress-strain, 88, 580–583, 616, 623
- Turbine application, 454
- Twisting moments, 14
- Two-dimensional elements, numerical method, 399–402
- Two-dimensional strain
 elasticity problems, 134–135, 140–141
 matrix, 401–402
 transformation of, 76–78
- U**
- Ugural, A. C., 51, 117, 181, 232, 300, 354, 423, 466, 492, 524, 569, 627, 673, 681, 711
- Ultimate
 load, 601
 moment, 592
 tensile stress, 86
 torque, 607
- Uniaxial stress, 13, 92–93, 218–221
- Uniaxial tension, 108
- Uniform stress, rotating disks, 456–458
- Unit load, energy methods, 506–508
- Units, System of, 701–704
- Unstable equilibrium, 535
- U.S. Customary System of Units (USCS), 701–704
- V**
- Van Vlack, L. H., 232
- Variational method, 496
- Virtual displacement, 514
- Virtual work, 514–515, 518–522
- Viscoelastic material, 83–84
- Volume change, 93, 98–100
- Von Mises stress, 615
- Von Mises theory, 199
- W**
- Wahl, A. M., 354
- Warping deformation, 315
- Wedge, concentrated loads, 157–160
- Weight
 freely falling, 227–228
 horizontally moving, 228–230
- Weiner, J. H., 181
- Wheatstone bridge, 104
- Winkler model, 473
- Winkler's Formula, 293
- Winkler's theory, pure bending, 289
- Wire gage, 103–104
- Woinowsky-Krieger, S., 673
- Work hardening material, 580
- Work-strain energy, 497
- Wriggers, P., 181
- Y**
- Yang, T.Y., 423, 466, 673
- Yield/yielding
 comparison of theories, 204
 complete yielding in plastic, 614, 624–626
 criteria of, 197–198
 initial yielding in plastic, 612
 Mises-Hencky yield criterion, 200–203, 610
 moment, 593
 partial yielding in plastic, 612–613, 626–627
 slip plane failure, 193–195
 surfaces for triaxial stress, 200
 torque, 606
 Tresca yield criterion, 612
- Young, Thomas, 2, 92
- Young, W. C., 181, 300, 354, 700, 711
- Young's modulus, 90, 92
- Z**
- Zhang, S., 673
- Zhao, D., 673
- Zienkiewicz, O. C., 423, 466, 673